GENETIC PORE TYPES AND THEIR RELATIONSHIP TO RESERVOIR QUALITY: CANYON FORMATION (PENNSYLVANIAN), DIAMOND M FIELD, SCURRY COUNTY, TEXAS

A Thesis

by

TRAVIS JAMES BARRY

Submitted to the Office of Graduate Studies of
Texas A&M University
in partial fulfillment of the requirements for the degree of

MASTER OF SCIENCE

December 2011

Major Subject: Geology

GENETIC PORE TYPES AND THEIR RELATIONSHIP TO RESERVOIR QUALITY: CANYON FORMATION (PENNSYLVANIAN), DIAMOND M FIELD, SCURRY COUNTY, TEXAS

A Thesis

by

TRAVIS JAMES BARRY

Submitted to the Office of Graduate Studies of
Texas A&M University
in partial fulfillment of the requirements for the degree of

MASTER OF SCIENCE

Approved by:

Chair of Committee,	Wayne M. Ahr
Committee Members,	Michael Pope
	David S. Schechter
Head of Department,	John R. Giardino

December 2011

Major Subject: Geology

ABSTRACT

Genetic Pore Types and Their Relationship to Reservoir Quality: Canyon Formation (Pennsylvanian), Diamond M Field, Scurry County, Texas. (December 2011)

Travis James Barry, B.S., University of Louisiana Lafayette

Chair of Advisory Committee: Dr. Wayne M. Ahr

Carbonate reservoirs may have a variety of porosity types created by depositional, diagenetic, and fracture processes. This leads to the formation of complex pore systems, and in turn creates heterogeneities in reservoir performance and quality. In carbonate reservoirs affected by diagenesis and fracturing, porosity and peremeability can be independent of depositional facies or formation boundaries; consequently, conventional reservoir characterization methods are unreliable for predicting reservoir flow characteristics.

This thesis provides an integrated petrographic, stratigraphic, and petrophysical study of the 'Canyon Reef' reservoir, a Pennsylvanian phylloid algal mound complex in the Horseshoe atoll. Core descriptions on three full-diameter cores led to the identification of 5 distinct depositional facies based on fundamental rock properties and biota. Fifty-four thin sections taken from the core were described are pores were classified using the Humbolt modification of the Ahr porosity classification.

In order to rank reservoir quality, flow units were established on the basis of combined porosity and permeability values from core analysis. A cut off criterion for

porosity and permeability was established to separate good and poor flow units. Ultimately cross sections were created to show the spatial distribution of flow units in the field.

ACKNOWLEDGEMENTS

I would first like to thank my advisor, Dr. Wayne Ahr, for accepting me as a student and guiding me throughout my journey at Texas A&M University. He sparked my interest in carbonate rocks and has provided me many unique and interesting experiences during my time here. Special thanks also go out to my committee members, Dr. Michael Pope and Dr. David Schechter, for helping me inside and outside of the classroom.

Thanks go out to my fellow office mates Ben, Kelli, Emily, Lora, and Sandra for always being there and making Texas A&M University an enjoyable and wonderful experience. I would also like to express thanks to Alexa Shamshoian, who helped me through the final stretch of graduate school when things were most difficult.

Lastly I would like to thank my amazing family. My mother, father, sister, and brother-in-law have always been there for me, and have supported and motivated me throughout my personal and professional life. I owe much of my success to their continuing patience, understanding, and love. Thank you.

NOMENCLATURE

BBL	Barrels
R1	Reef 1 Facies
R2	Reef 2 Facies
R3	Reef 3 Facies
GS/PS	Grainstone/Packstone Facies
DEB	Debris Facies

TABLE OF CONTENTS

Page

Page

LIST OF TABLES

INTRODUCTION

The Permian Basin of West Texas and New Mexico is one of the major petroleum producing regions of the United States since oil was discovered there in 1921. Seventeen percent of all domestic United States oil production in 2002 came from the Permian Basin, and the region has the greatest potential for production growth in the country with an estimated 29% (17.6 billion bbl) of the United States future oil reserve growth (Dutton et al., 2005). Diamond M field, in Scurry County, Texas, produces from the Horseshoe atoll (Figure H.1), an isolated carbonate platform covering around 6300 square miles in the northern Midland Basin (Waite, 1993). The Horseshoe atoll, commonly called the "Canyon Reef", consists of Late Paleozoic Strawn through Wolfcampian strata, and is one of the largest oil reservoirs in the Midland Basin (Figure H.2).

Seventy-five percent of the total oil production in the Permian Basin is from carbonate reservoirs (Dutton et al., 2005); however, these reservoirs have not been studied in detail or with the most recent techniques for reservoir characterization. Unlike siliciclastic rocks, carbonates are primarily composed of skeletal and chemical grains, which are greatly susceptible to diagenetic alteration. This leads to the formation of complex pore systems, and in turn creates heterogeneities in reservoir performance and quality.

This thesis follows the style of the American Association of Petroleum Geologists Bulletin.

Terrigenous sandstone reservoirs are typically dominated by depositional interparticle porosity that has a relatively consistent relationship with porosity and permeability (Ahr, 2009). Carbonate reservoirs may have a variety of porosity types created by depositional, diagenetic, or fracture processes. These pore types were sub-divided into three end-member genetic categories: depositional, diagenetic, and fracture with hybrids between the end members (Ahr et al., 2005). The scale between depositional and diagenetic end members was expanded to more precisely define hybrid pore types for use in distinguishing petrophysical rock types (Humbolt, 2008).

Because carbonate pore types are formed by depositional, diagenetic, or fracture processes, porosity and permeability may not conform to depositional facies boundaries. Therefore it is crucial to: 1) classify genetic pore types by mode of origin; 2) establish flow units by determining which genetic pore types have high, medium, and low combined values of porosity and permeability; 3) identify bulk-rock properties that can be used as correlatable makers, or proxies, for the genetic pore types; and 4) correlate the pore-proxy rock properties between wells to determine the 3-D spatial distribution of flow units and pore types at a reservoir scale (Humbolt, 2008). Flow units are reservoir zones with high connectivity, meaning high porosity and permeability and low capillary resistance to fluid flow (Ahr, 2008). Baffles are zones with low poroperm values, but are limited in lateral and vertical extent so fluids can still flow around or through them. Barriers are zones that do not allow fluid to flow at reasonable rates, and may be laterally and vertically extensive (Ahr, 2009). Carbonate reservoir performance depends on the distribution and connectivity of flow units, baffles, and barriers.

Definition of Problem

Diamond M field produces from a Pennsylvanian aged phylloid algal mound complex in the Horseshoe atoll. In 2002, Parallel Petroleum drilled four 'Gemstone' wells (Emerald, Garnet, Jade, and Topaz) in search of 'attic' oil locations (Fisher, 2005). The field is undergoing stages of secondary recovery, but the 3-D distribution of porosity and permeability in the field was not thoroughly studied. Also, the geologic origins of porosity and permeability are not fully documented.

Purpose of Study

The primary objective of this study is to determine the 3-D distribution of porosity and permeability in part of the Diamond M field. This study will determine the cause-effect system by which porosity and permeability were created in this field. This knowledge will be the basis for a geologic model that explains the Diamond M reservoir performance characteristics and be used to recommend methods for further enhanced recovery.

REGIONAL GEOLOGIC SETTING

Structural Setting

Tai (2001) presented a brief tectonic history of the Permian Basin. In Early Paleozoic time, the present Permian Basin area was covered by the shallow Tobosa Basin, and thought to be formed by a regional sag in the stable passive margin along the southern side of Laurasia (Galley, 1958; Frenzel et al., 1988). Only minor deformation occurred until the Late Mississippian when the Hercynian orogeny was initiated by the collision of North America and Gondwana Land (South America and Africa). This collision gave rise to the Ouachita - Marathon fold belt and deformed the ancestral Tobosa Basin intensively along high angle basement faults and pre-existing zones of weaknesses (Horak, 1985) in (Alnaji, 2002). The Tobosa Basin began to segment into a series of fault-bounded basement uplifts (e.g., Central Basin Platform and Diablo Platform) and created sub-basins (e.g., Midland and Delaware Basins) in Late Mississippian times (Galley, 1958; Frenzel et al., 1988; Figures H.3, H.4). The Central Basin Platform (Figure H.5), which geographically separates the Midland Basin and Delaware Basin, achieved maximum uplift during the Late Pennsylvanian (middle Wolfcampian) (Frenzel et al., 1988; Yang and Dorobek, 1995a). Both the Midland and Delaware Basins are asymmetrical in east-west profiles, and are deepest near the structural margins of the Central Basin Platform (Yang and Dorobek, 1995a). The Midland Basin is shallower than the Delaware Basin, and has a much gentler basement profile. The asymmetric profiles of both sub-basins suggest that the Central Basin

Platform acted as a topographic load within the Marathon foreland, causing flexural subsidence in the adjacent Midland and Delaware Basins (Yang and Dorobek, 1995b; Ye et al., 1996) in (Tai, 2001, p. 9). This subsidence created deep water which led to the deeper areas of the Midland Basin becoming relatively sediment-starved. The uplifted Central Basin Platform, however, became an area for shallow carbonate platform sedimentation (Frenzel et al., 1988; Hanson et al., 1991; Ewing, 1991; Yang and Dorobek, 1995b). Even though by the early Leonardian most of the deformation associated with the Central Basin Platform was over, the Permian Basin continued to subside at a decreasing rate throughout the Permian (Frenzel et al., 1988; Hanson et al., 1991; Ewing, 1991; Yang and Dorobek, 1995b). The greatest relief from the top of the Central Basin Platform to the adjacent sub-basins was generated during the early Leonardian (Mazzullo and Reid, 1989).

During the Late Permian (Guadalupian), the Midland Basin, as well as the Central Basin Platform, Eastern Shelf, and Northern Shelf ceased to be sites of carbonate platform sedimentation and became areas where cyclical deposition of siliciclastic, evaporite, and mixed carbonate facies dominated (Figure H.6). By the end of the Permian (Figure H.5), the Midland Basin was essentially filled with sediment (Galley, 1958; Ward et al., 1986; Frenzel et al., 1988). Since the Late Permian, the Permian Basin has not experienced significant deformation, and the present structural features are similar to those existing during the Late Paleozoic (Frenzel et al., 1988).

Diamond M field is one of many fields located within the Horseshoe atoll isolated carbonate platform. The aggrading platform margins that formed the distinctive

U-shaped atoll began in the Missourian (mid-late Pennsylvanian) and lasted until the Wolfcampian (early Permian); (Myers et al., 1956; Stafford 1959). During the Late Pennsylvanian the Eastern shelf of the Midland Basin was located within the tropics less than 10 degrees from the equator (Heckel, 1980), and extensive Strawn carbonate sedimentation produced an aggradational isolated carbonate platform measuring roughly 80 miles across with no significant well defined buildups surrounding it (Cleaves, 2000). The highest points of the rim crest were as high as 3,000 feet above the basin floor (Galloway et al., 1983 in Cleaves, 2000).

Late Pennsylvanian Stratigraphy

The Horseshoe atoll is subdivided into major biostratigraphic units (i.e., Strawn, Canyon, Cisco, Wolfcamp units) based on fusulinid foraminiferal biostratigraphy (Waite, 1993). Biostratigraphic correlations are necessary because the massive atoll carbonates are depositionally heterogeneous and lack regionally extensive, internal log markers (Rothrock et al., 1953) in (Waite, 1993). During the Late Pennsylvanian, shallow water carbonate deposition dominated most of the northern Midland Basin, and the area of the present Diamond M field was a quiet water shallow subtidal depositional environment (Schatzinger, 1988).

Diamond M field produces from Late Pennsylvanian (Canyon) rocks (Figure H.2). These rocks are composed of reefal limestones up to 680 ft thick, deposited unconformably over Strawn limestone beds that are up to 760 ft thick (Vest, 1970).

Cisco reef limestone deposits up to 500 ft thick unconformably lie on Canyon rocks (Figure H.7), but in many places the Cisco rocks are not present (Vest, 1970).

The Horseshoe atoll developed on top of 40 to 100 ft of Strawn limestones, and in Scurry County these bedded limestones grade upwards into reefal limestones of the atoll (Stafford, 1959). The top of the Horseshoe atoll is composed of Wolfcampian reef rocks up 1,120 ft thick (Figure H.8), although most of the atoll lacks these reef rocks and is instead covered with Wolfcamp shale and sandstone that form the top seal of the reservoir (Vest, 1970).

Cross sections were made to better understand the stratigraphy in the study area (Appendix G). These cross sections correlate depositional lithofacies outward from the 3 cored wells. Correlation between wells was difficult, however, since carbonate buildups modify the depositional topography causing major variations in thickness and lithological characteristics. Wireline log character varies greatly from well to well as a result.

PREVIOUS WORK

Diamond M Field and Horseshoe Atoll

Diamond M field was discovered in 1948 by Lion Oil Company and 111 wells were drilled between 1948 and 1951, including one water injection well. Secondary recovery by water flooding has been utilized since the beginning of field development (Fisher, 2005). The field has produced over 3.6 million barrels of oil since discovery, and continues to produce today. The field is currently operated by Parallel Petroleum Company, which purchased the field in 2000 from Burlington Resources. In 2002, Parallel Petroleum Company drilled four 'gemstone' wells (Emerald, Garnet, Jade, and Topaz) based on a 1992 3-D seismic shoot (Fisher, 2005). With the exception of the Garnet well, the gemstone wells were cored in the Canyon Formation and the cores were analyzed by Rotary Labs Incorporated.

The stratigraphic architecture, depositional and diagenetic histories, and reservoir characteristics of Diamond M field were delineated by Fisher (2005). His study focused on predicting the spatial distribution and quality of flow units in the field by using a "slice map" technique developed by Hammel (1996). Slice mapping involves averaging porosity and permeability over ten foot thick reservoir slices in the study area. Porosity and permeability values are estimated from logs when core analysis is not available. The spatial distribution of porous and permeable zones can be identified by stacking the slices, and flow units can be constructed based on these superimposed slices (Fisher, 2005).

Earlier papers on the Horseshoe atoll such as Myers et al. (1956), Stafford (1959), Burnside (1959), and Vest (1970) focused mainly on the regional biostratigraphic aspects and "reefal" nature of the buildup (Schatzinger, 1988). The transition of facies and depositional environments in the eastern portion of the Horseshoe atoll was studied by Schatzinger (1988). More recent studies involve using 2-D and 3-D seismic to define seismic sequences and improve the accuracy of reservoir modeling. 2-D seismic was used to sub-divide Late Pennsylvanian carbonates in the eastern and southern Horseshoe atoll into four, biostratigraphically contained third order seismic sequences by Waite (1993). 3-D seismic surveys were used to locate and develop smaller Pennsylvanian age pinnacle reefs southeast of the Horseshoe atoll by Jumper and Pardue (1996). Attribute volumes calculated from P and S wave data were investigated to better understand reservoir compartmentalization, define reef edges, and resolve inner reef structure in the Diamond M field by Russian et al. (2010). This thesis builds on previous work by conducting a reservoir characterization study of the "Canyon Reef" reservoir of Diamond M field by integrating genetic porosity classification with reservoir petrophysical properties.

Carbonate Porosity Classification

Several carbonate porosity classification schemes have been developed throughout history. Many group pores according to pore size, (Archie, 1952 and Lucia, 1983), or relationship to depositional fabric (Choquette & Pray, 1970). The problem with these classifications is that they do not illustrate the relationships between pore

origin (genetic pore types) and ways to define 3-D distribution of effective porosity (Ahr, 2008).

One of the first carbonate porosity classifications was proposed by Archie (1952). Archie divided porosity space into *visible* and *matrix* categories, where *matrix* porosity was based on texture (chalky, sucrosic, or compact), and *visible* porosity was described by size (Humbolt, 2008). Archie's classification was significant because it related petrophysical properties such as capillary pressure and permeability to different rock types. Unfortunately he did not relate the pore origin to rock origin, and when mode of origin is not part of the porosity classification, establishing a correspondence between pore types and rock matrix properties is not possible (Ahr, 2008).

Unlike Archie, Choquette and Pray (1970) recognized the importance of including mode of origin in their porosity classification, and organized pores into three groups depending on whether they are *fabric selective, not fabric selective,* or *fabric selective or not* (Ahr, 2008). The main problem with this classification is that no correlation is made between pore type and external geological characteristics with which spatial distribution of pore types and associated poroperm values can be determined.

Lucia (1983) developed a classification emphasizing two pore types: interparticle and vuggy. He divided pores into *vuggy* (separate or touching) and *interparticle* (between grains or crystals) categories (Ahr, 2008). The major difficulty in using Lucia's classification is that even though it relates pore type petrophysical characteristics (Archie *m* values, porosity, and permeability), it does not offer any way to establish 3-D distribution of poroperm values associated with pore types.

A new genetic porosity classification was developed by Ahr et al. (2005). This classification divides pores based on three end-member processes: *depositional, diagenetic,* or *fracture* (Figure H.9). Depositional pores are closely related to original rock texture and fabric, including interparticle, intraparticle, fenestral, shelter, and reef porosity. Diagenetic pores are formed and either enhanced or reduced through processes like dissolution, replacement, recrystallization, compaction, and cementation. Fracture porosity forms when rocks undergo brittle failure from differential stress (Ahr et al., 2005). Hybrid pore types exist between each of these end members. By linking pore genesis and pore geometry, the Ahr porosity classification can be used for subsurface mapping to establish 3-D distribution of poroperm values, to aid in generating petrophysical rock types, and to establish flow units.

In the Ahr porosity classification, depositional pores that were subjected to diagenesis are classified as Hybrid 1 pores. Humbolt (2008) subdivided the hybrid 1 pores into three categories based on the amount of diagenetic alteration: H1-A, H1-B, and H1-C (Figure H.10).

If depositional aspects dominate but diagenesis has affected the pore/ pore throat geometry, then the porosity is classified as Hybrid 1-A. In this instance porosity is still facies selective, so facies maps are reliable proxies for porosity maps. If depositional and diagenetic aspects equally contribute to porosity, then the porosity is classified as Hybrid 1-B. In this case facies maps are still proxies for porosity maps, but they are less reliable than for H1-A pores. When diagenetic aspects dominate, the porosity is

classified as H1-C. Facies maps are no longer reliable proxies for porosity maps, and diagenetic alteration controls flow unit characteristics.

The Ahr classification notes that hybrid pore types can be further classified as enhanced or reduced, depending on the direction of diagenetic change, e.g., changes such as cementation, compaction, replacement and recrystallization can reduce porosity in a rock; while processes such as dissolution and some forms of replacement and recrystallization can enhance porosity. These alterations are denoted by adding either the letter ‘r’ or ‘e’ to the hybrid pore types, so for example, an H1-B pore that was reduced would be denoted H1-Br.

METHODS

Materials for Study

Parallel Petroleum Co. provided approximately 350 feet of full diameter core from three gemstone wells, along with full core and core plug analysis data from Rotary Labs Incorporated. The core analysis included vertical, horizontal, and maximum permeability, porosity, grain density, fluorescence, lithology, water saturation, and oil saturation taken at one foot intervals. The three cored wells had paper logs including gamma ray, resistivity, neutron porosity and density porosity data. Well locations for nearly 400 wells and wireline logs for 147 wells were also provided.

Fifty-four thin sections from the study by Aaron Fisher (Fisher, 2005) were used in this study. These thin sections are representative of major facies and pore type variations in the cores. No additional thin sections were required. Porosity and permeability values at thin section locations were not available, so core analysis poroperm values for the 1 foot interval containing the thin section were used instead.

Lithologic Study of Cores

Three full diameter cores totaling approximately 350 feet were etched in diluted HCl to provide a fresh rock surface and described wet at one inch intervals using a low-zoom stereo microscope. The core descriptions follow the AAPG Sample Examination Manual format. Focus was placed on identifying constituent grains, visible porosity, sedimentary structures, depositional texture, and significant facies changes. Detrital

facies were classified using the Dunham (1962) classification, and reef rocks were classified using the Riding (2002) classification. Core descriptions led to the identification of 5 distinct depositional facies based on fundamental rock properties and biota.

Porosity and permeability values from core analysis data were compared to visual porosity estimates from core description and calculated porosity from wireline logs. Plots were created in Microsoft Excel to compare core poroperm values and depth, facies, and genetic pore type. The combined poroperm values were used to define and rank different reservoir flow units.

Thin Section Petrography

Fifty-four thin sections provided by Aaron Fisher (Fisher, 2005) were examined in this study. The thin sections were described using a petrographic microscope in both plain and polarized light. The main emphasis of the petrographic analysis was to classify the genetic pore types for each thin section using the Humbolt (2008) modification of the Ahr porosity classification (Figure H.10), and to confirm the depositional facies interpretation from core descriptions. Fracturing was not important as a reservoir performance characteristic. All of the thin sections exhibit pore types in the hybrid 1 group.

Borehole Log Interpretation

One hundred forty-seven wells had wireline logs available for this study, but many of these wells only had one or two digital log curves. The gemstone wells had paper logs available. Those logs were scanned and digitized into a software program called Petra. Almost all of the wells had gamma ray log curves, but these were of limited use in the carbonate rocks of Diamond M field, which do not have variations in gamma-ray traces that facilitate stratigraphic correlation (Fisher, 2005). Gamma ray logs may help identify concentrations of insoluable residue at unconformities, but they do not indicate anything about depositional environment, particle characteristics, or pore types (Ahr, 2008). Only 13 wells had density log curves, and many of the wells were not located near the cored gemstone wells. One hundred twenty-six wells had neutron logs, 82 wells had neutron porosity logs, and roughly 50 wells had both.

In order to correlate outward from the gemstone wells, an equation was derived to convert neutron logs to neutron porosity logs and vice versa. In wells that had both sets of logs, the neutron values were plotted against the neutron porosity values in Microsoft Excel and a logarithmic best fit curve was determined for each well. An average equation was created that fit most data sets with 95% accuracy or above.

Eq. 1 Neutron Porosity = -0.1427647 ln (Neutron) + 0.9494235

Using this equation neutron and neutron porosity digital logs were created for most wells, and were used to correlate depositional facies outward from the cored wells (Appendix G).

RESULTS

Depositional Lithofacies

Unlike modern reefs which have a rigid framework composed of aragonitic scleractinian corals, Pennsylvanian reefs were often constructed by small calcareous phylloid algae (*Eugonophyllum)* and to a lesser extent sponges and problematica (*Tubiphytes* and *Archaeolithoparella)* (Forsythe, 2003). It was originally thought that *Eugonophyllum* constructed reefs by passive baffling and trapping, but Forsythe (2003) suggests that *Eugonophyllum* are capable of both initiating reef growth and forming a stable substrate. This new substrate, known as the 'pioneer community', is commonly later stabilized by secondary encrusters (problematica and sponges), microbialites, and early marine cements. The study area is interpreted to be part of a phylloid algal pioneer community, because it lacks *Archaeolithoporella*, *Tubiphytes*, and other encrusters. Subsequent encrustation most likely occurred, because without encrustation by both calcareous organisms and microbialites many communities of phylloid algae may have grown, died, and been rapidly fragmented (Forsythe, 2003).

Core description revealed five lithofacies: three of which are reef facies, one is a detrital grainstone/packstone facies, and the remaining one is a debris facies. The three reef facies are mainly phylloid algal dominated automicrite. "Automicrite", short for autocthonous micrite, refers to carbonate mud that has formed in place (Riding, 2002). The grainstone/packstone facies is dominated by moderate to well sorted forams and phylloid algal fragments. The debris facies contains similar grains to the

grainstone/packstone facies, but also includes large angular intraclasts. A complete description of these facies can be found in Appendix F.

Grainstone/Packstone Facies

The grainstone/packstone facies varies in color from tan to dark gray, and is typically moderately to well sorted. The color roughly correlates to grain size, with tan areas usually being finer grained, brown areas medium to coarse grained, and grey areas composed of large phylloid algae grains. The facies generally has indistinct bedding, but parallel layering can be seen in some areas, usually near the bottom erosional surface (Figure C.1). Forams and phylloid algae make up a majority of the rock, but bivalves, brachiopods, bryozoans, crinoids, fusulinids, gastropods, peloids, and sponge spicules are also present.

Stylolites, dissolution seams, calcite filled veins, geopetal structures, pyrite, silica, and saddle dolomite are all present in this facies. Pockets of automicritic reef rock usually around 4 feet thick are present in the Emerald and Jade wells. Solution enhanced interparticle porosity dominates, but moldic, vuggy, solution enhanced intercrystalline and solution enhanced intraparticle are all present.

Reef 1 Facies

The reef 1 facies ranges from light brown to dark gray in color, and is typically moderately to poorly sorted. The majority of the section is composed of heavily mottled automicrite (Figure C.2), but some parallel layers can be identified in well sorted

grainstone/packstone areas. Approximately half of this facies is micritic, while the other half is dominated by phylloid algae, brachiopods, and forams. Bryozoans, crinoids, fusulinids, gastropods, micritic clasts, peloids, and trilobite fragments are present as well.

Calcite filled veins, geopetal structures, silica nodules up to 5 cm, and grain replacing silica are common. Stylolites, dissolution seams, pyrite, and saddle dolomite are present. Detrital grainstone/packstone intervals usually less than 3 feet thick occur in the Emerald and Jade wells. These detrital intervals often have parallel bedding and erosional truncation. Vuggy porosity dominates this facies (Figure C.6). Moldic porosity is common, and solution enhanced interparticle and solution enhanced intraparticle are present usually in the grainstone/packstone intervals.

Reef 2 Facies

The reef 2 facies ranges from light to dark gray in color, and is usually moderately to poorly sorted. Most of the facies is automicrite with indistinct bedding, but some areas are slightly mottled. This facies has a higher mud to grain ratio than the reef 1 facies. Approximately 2/3 of this facies is micritic, with the remaining 1/3 dominated by forams and phylloid algae. Large crinoids (5-35 mm) are more common than in reef 1, and brachiopods, bivalves, bryozoans, fusulinids, gastropods, peloids, and sponge spicules are all present.

Stylolites and calcite filled veins are common (Figure C.3) in the reef 2 facies. Dissolution seams, geopetal structures and pyrite are present. Reef 2 has less visible

porosity than reef 1. Moldic porosity dominates, vuggy porosity is common, and solution enhanced interparticle and solution enhanced intraparticle also occur.

Reef 3 Facies

The reef 3 facies varies from light to dark brown in color, and is mostly poorly sorted with some areas being moderately sorted. The upper 2/3 of this facies is a mottled automicrite, whereas the basil 1/3 is automicrite with indistinct bedding. Forams and phylloid algae dominate the facies, but brachiopods, bivalves, crinoids, fusulinids, peloids and sponge spicules are also present.

Blue-gray silica nodules are abundant, replacing about 30% of the facies and often spanning across the entire width of the core (Figure C.4). Stylolites, dissolution seams, and calcite filled veins are common. This facies is only present at the very bottom of the Topaz #1 core and contains almost no visible porosity.

Debris Facies

The debris facies ranges from gray to dark gray in color, and is composed primarily of poorly sorted intraclasts (Figure C.5). Packstones with indistinct bedding are the majority of this facies, but micrite is also common. Similar to the grainstone/packstone facies, forams and phylloid algae dominate, but bivalves, brachiopods, bryozoans, crinoids, fusulinids, gastropods, peloids, and sponge spicules are present as well.

Pyrite and saddle dolomite are abundant in the facies (Figure C.7). Stylolites, dissolution seams, geopetal structures, and silica are present. The facies is only present in the Jade #1 core, and is only 6 feet thick. Moldic porosity dominates and solution enhanced interparticle porosity is common, but overall visible porosity is fairly low.

Diagenesis

Diagenesis is defined as any changes that happen to a sedimentary rock after deposition and before metamorphism (Ahr, 2008). Diagenesis can result from mechanical, biological, or chemical processes, or any combination of these processes. The dominant forms of diagenetic change that affected Diamond M reservoir rocks are discussed below.

Cementation

Cementation is one of the most common forms of diagenesis in Diamond M field, and is seen in all of the cored wells. Cements in the study area are exclusively composed of calcite. The two main forms of cementation seen are small blocky (equant) calcite and large blocky calcite. Small blocky calcite typically ranges from 10 to 30 microns, and large blocky calcite from 40 to 120 microns. Three other types of cement are observed, but they are not volumetrically significant. The first is syntaxial overgrowth cement of crinoid fragments, which occurs when cement grows around a crystal in such a way that they form a single larger crystal, and share the same crystallographic axes (Scholle and Ulmer-Scholle, 2003). The second is drusy cement,

in which crystals line a cavity and crystal sizes increase from the edges to the center of pores (Scholle and Ulmer-Scholle, 2003). The last observed cement is poikilotopic spar, where small grains or crystals are irregularly scattered without common orientation in a larger crystal of another mineral (Scholle and Ulmer-Scholle, 2003).

Recrystallization

Two forms of recrystallization are very common in the study area, micritization and neomorphism. Micritization occurs when sand or silt sized particles are partly or completely converted to calcite micrite, by retrograde diagenesis or by filling of micro-borings by algae or fungi (Bathurst, 1975 in Scholle and Ulmer-Scholle, 2003). Micritization is observed in every thin section; especially affecting, brachiopods, forams, fusulinids, and phylloid algae (Figure E.4).

The term neomorphism includes both mineralogical inversion and true recrystallization (Folk, 1965). True recrystallization occurs when small calcite crystals dissolve and reprecipitate as larger neomorphic spar crystals, while inversion is the process in which metastable minerals change to stable minerals (Ahr, 2008). Neomorphism commonly is observed in the muddier reef facies, but at the Diamond M field also occurs in some of its grainier facies as well.

Replacement

Replacement occurs when a mineral is replaced by a polymorph or mineral of a different composition (Scholle and Ulmer-Scholle, 2003). Replacement in Diamond M

field is restricted to replacement of calcite by pyrite, silica, and saddle dolomite. Pyrite replacement commonly occurs in small amounts throughout the field. It can easily be identified in core description, and in thin section (Figure E.5).

Silica, in the form of chert, is another common replacement mineral in the study area. It usually replaces blocky calcite cement, and grains (typically crinoids and brachiopods) in small amounts irregularly throughout the field. The major exception is the Reef 3 facies, where blue-gray chert has replaced about 30% of the section and often spans the width of the core. Sponge spicules are common biogenic contributors of diagenetic silica (Scholle and Ulmer-Scholle, 2003), and occur commonly in the field.

Saddle dolomite is a variety of dolomite that is characterized by curved crystal faces, curved cleavage, and sweeping extinction (Scholle and Ulmer-Scholle, 2003). The homogenization temperature for saddle dolomite ranges from below 80 to more than 235° C, but usually falls into the 100-180° C range (Davies and Smith, 2006). Saddle dolomite can form in at least three ways: from advection, from local redistribution of older dolomite during stylolization, and as a by-product of thermochemical sulphate reduction in a closed or semi-closed system (Machel, 2004; Radke and Mathis, 1980; Machel, 1987; Machel and Lonnee, 2002). Saddle dolomite occurs in all the lithofacies, but is most common in the Debris facies, often times replacing grains and large crystals of pore filling blocky calcite (Figure E.8).

Dissolution

Dissolution occurs when undersaturated waters dissolve surrounding rock, producing a variety of different pore types that share a common origin, but differ in size, shape, and connectivity (Ahr, 2008). The porosity types seen in this study are listed below in order of abundance.

Vugs

Vugs are large pores that form from either the dissolution enlargement of previous pores or the combination of pores into a much larger pore. A characteristic of vugs is that they are larger than the surrounding grains, and do not conform to the outline of any grain type. In the study area, vugs nearly always have high porosity and permeability, and account for approximately 40% of the total porosity. The fact that the areas dominated by vuggy porosity consistently have higher poroperm values suggests that the vugs in the study area are touching, rather than separate vugs. Vugs occur in all of the facies, but tend to be more prevalent in the muddier reef rocks.

Molds

Moldic porosity is formed when grains are dissolved and the pores conform to the outline of the original grain. Molds are common in every facies in the study area, and make up about 30% of the overall porosity. They occur with vugs or solution enhanced interparticle porosity, and have a wide range of poroperm values from low to high.

Solution Enhanced Interparticle

While interparticle porosity is normally a depositional feature, solution enhanced interparticle porosity occurs when cement or matrix between grains is dissolved. This type of porosity occurs most commonly in the grainstone/packstone facies, but small amounts also occur in the muddier reef facies. Solution enhanced interparticle porosity makes up approximately 20% of the total porosity in the field. Poroperm values are generally better than moldic pores, but not as good as separate vug porosity.

Intercrystalline, Solution Enhanced Intraparticle, and Fracture

The last three observed types of porosity comprise the remaining 10% of porosity in the field. Intercrystalline porosity in the study area occurs in incompletely cemented pores and in neomorphosed micrite. This type of porosity occurs mostly in grainstone/packstone facies and contributes less than 3% of the total porosity.

Solution enhanced intraparticle porosity occurs within larger grains that have been partially dissolved. This type of porosity occurs in every facies, typically in large fusulinids (Figure E.1). Solution enhanced intraparticle porosity contributes about 6% to the total porosity.

Fractures formed throughout the study area, but often they have been healed with calcite cement. The open fractures in the field are uncommon and contribute less than 1% to the total porosity of the study area. The occurrence of fractures does not correspond to higher permeability values in core analysis, because fracture apertures are small, and fracture abundance is commonly low.

Compaction

Mechanical compaction occurs when tectonism or overburden stress during burial deform a rock. When compaction effects are accentuated by dissolution and compaction acting together, then chemical compaction takes place (Ahr, 2008). Mechanical compaction is commonly recognized by identifying brittle grain deformation and fractures in core and thin section. Brittle grain deformation is most common in grain dominated rocks, and large grains such as brachiopods, phylloid algae, and crinoids are the most commonly deformed grains. Fractures result from the brittle failure of a rock under differential stress, and often cut across grains, matrix, and cement (Ahr, 2009). Fractures occur sporadically throughout the study area, are typically small and often healed with calcite cement.

Chemical compaction in Diamond M field occurs as stylolites and dissolution seams (microstylolites), both of which are very common in all three cores. Stylolites are jagged, columnar surfaces in carbonate rocks that form from pressure induced dissolution of carbonate material (Scholle and Ulmer-Scholle, 2003). They are often easily visible due to insoluble carbonate residue left in jagged "teeth" of the stylolites. Typically the larger the amplitude of the stylolite, the more carbonate material was dissolved during its formation. Dissolution seams are similar to stylolites, but have lower amplitude and less insoluble carbonate residue. Stylolites and dissolution seams occur most commonly in the muddier facies.

H1 Genetic Pore Types

Fifty-four thin sections were examined in this study, and the genetic pore types were classified using the Humbolt (2008) modification of the Ahr porosity classification (Appendix D). None of the thin sections displayed purely depositional or diagenetic porosity, so all the sample were classified as hybrid type 1 pore systems (H1). The samples were divided into H1-Ae, H1-Ar, H1-Be, H1-Br, H1-Ce and H1-Cr based on the amount of diagenetic alteration, and whether diagenesis enhanced or reduced porosity (Table 1).

Table 1. Humbolt porosity classification scheme. Hybrid pore types are subdivided based on the ratio of depositional to diagenetic porosity. Source: Humbolt (2008)

H1	Enhanced	Depositional porosity dominate	**Ae**
		Equal ratio of depositional to diagenetic	**Be**
		Diagenetic porosity dominate	**Ce**
	Reduced	Depositional porosity dominate	**Ar**
		Equal ratio of depositional to diagenetic	**Br**
		Diagenetic porosity dominate	**Cr**

H1 Enhanced Pores

The majority of porosity enhancement in this portion of Diamond M field comes from the dissolution of framework grains, cements, and matrix. Recrystallization in the

form of neomorphism of micrite provides some intercrystalline porosity in rare cases, but typically neomorphism reduces porosity in the study area.

H1-Ae pores typically are dominated by solution enhanced interparticle porosity; however moldic porosity also is common. Approximately 50% the H1-Be pores are dominated by vuggy porosity, 35% are dominated by moldic porosity, and the remaining 15% is dominated by solution enhanced interparticle porosity. Vuggy and moldic H1-Be pores are most common in the reef facies, while solution enhanced interparticle porosity is most common in the grainstone/packstone facies. H1-Be pores are the most common genetic pore type in this study, with 29 out of the 54 thin sections being in the H1-Be category. Only one example of the H1-Ce pore type was observed, and it contained primarily vuggy porosity.

H1 Reduced Pores

Porosity reduction is related to three main processes in Diamond M field, cementation, compaction, and recrystallization. The most common form of porosity reduction is cementation. Cement occurs in every thin section and commonly seals pores.

Compaction is another common form of porosity reduction in the study area. Carbonate reservoirs lose much of their original porosity due to chemical and mechanical compaction. Stylolites and dissolution seams identified in thin section and throughout the core suggest that chemical compaction and dissolution of carbonate material were extensive in the study area.

While not as prominent as cementation or compaction, recrystallization is observed as a porosity reducing mechanism in some thin sections. Neomorphism of micrite is common in many of the muddier reef facies, and this often creates a tight mosaic of interlocking calcite crystals that exhibit almost no porosity.

H1-Ar pores have undergone small to moderate amounts of replacement, cementation, recrystallization, and compaction, but the porosity is still strongly controlled by depositional characteristics. H1-Br pores have experienced significant diagenetic alteration, but many depositional attributes are still visible. Only one example of H1-Cr porosity was observed, and the sample was so altered that a relationship between depositional and diagenetic characteristics cannot be established.

Discussion of Results

Data on permeability, porosity, grain density, fluorescence, lithology, water saturation, and oil saturation for the three cored wells was gleaned from routine core analysis. This data was compared to depositional lithofacies, genetic pore type, and porosity type to test for correspondence between data types. Linear regression was done using Microsoft Excel to find out how strong of a relationship exists between the X and Y values in each of the plots. Linear trend lines were added to each plot, using the equation $y = mx + b$, to determine an R^2 value for each plot. The R^2 value is a standard measure of how well the trend line fits the data, with an R^2 value of zero indicating no relationship and an R^2 value of one indicating a perfect relationship.

Porosity and Permeability Data Patterns

Porosity and permeability do not have a strong correlation to one another in any of the cored wells. The strongest correlation is in the Topaz #1 well, where a linear trend line has an R^2 value of 0.3736 (Figures H.11-H.14).

Porosity calculated from wireline log data also does not correlate well with values from core analysis. The strongest correlation is in the Jade #1 well, where a linear trend line has an R^2 value of 0.7674, but the other cored wells have considerably lower R^2 values (Figure H.15-H.17).

Core Analysis Poroperm Values vs. Depth

Porosity and permeability do not correspond well to depth. Typically porosity decreases with depth due to overburden stresses on the rock, but this is not necessarily the case in carbonate rocks, where diagensis can enhance or reduce depositional porosity and permeability. This lack of correspondence suggests that the Diamond M field has undergone significant diagenetic alteration. The strongest correlation is in the Topaz #1 well were the R^2 value on a linear trend line between porosity and depth is 0.5657, but typically R^2 values fall below 0.1 (Figures H.18-H.23).

Oil and water saturation values also typically do not correlate well to depth. This indicates that the reservoir is most likely compartmentalized. Barriers created by depositional or diagenetic processes can isolate oil and water zones. The strongest correlation is in the Topaz #1 well, where a linear trend line for water saturation vs. depth has an R^2 value of 0.7245, but most R^2 values fall below 0.1 (Figures H.24-H.29).

The core analysis data is summarized in Figures H.30-H.32. The porosity ranges from 0.01% to 19.7% and the permeability ranges from 0 md to 282.90 md, although only 5 values exceed 80 md. Water saturation ranges from 11.7 % to 99.7%, and oil saturation ranges from 0.0 % to 44.9 %. In general core analysis data has a very poor relationship with depth. The Topaz #1 well, which had the best relationships, may not be entirely accurate since large gaps exist in the core data.

Poroperm Values and Depositional Facies

Porosity and permeability values seem to correspond to different depositional lithofacies. The reef 1 facies has the best average poroperm values, with the grainstone/packstone facies being the second best (Table 2). The reef 2, reef 3, and debris facies all tend to have lower poroperm values.

Poroperm Values and Genetic Pore Types

Genetic pore types also seem to correlate to an extent with poroperm values. On average, H1 enhanced pores have higher porosity than H1 reduced pores, but they do not always have higher permeability. H1-Be pores typically have the highest porosity and permeability values, while H1-Br has the second highest permeability and H1-Ae has the second highest porosity. Distribution of hybrid pore types in the study area does not seem to be controlled by depositional facies composition. Both mud dominated and grain dominated facies experienced significant porosity enhancement and reduction (Figure H.33).

It is important to remember that the porosity and peremeability values for genetic pore types in Table 2 are not representive of true thin section poroperm values. As stated in the methods portion, thin section poroperm data was not available so core analysis poroperm for the 1 foot interval in which the thin section was taken from was used instead. In some cases the thin section location and surrounding core may have largely different petrophysical properties. For example a thin section may have had large connected vugs and been classified as H1-Be, but the surrounding foot of core could have been heavily cemented, causing the poroperm values to appear lower than expected.

Table 2. Porosity and permeability values for depositional facies, dominant porosity type, and genetic pore type. Data from core analysis. H1-Ce and H1-Cr omitted because only one example of each was observed.

	Average Core Porosity (%)	Average Kmax (md)	Porosity Range (%)	Permeability Range (md)
Facies:				
Debris	3.9	1.7	0.4 - 7.0	0.01 - 4.52
GS/PS	5.8	8.4	0.2 - 17.6	0.00 - 282.90
Reef 1	5.9	13.6	0.1 - 19.7	0.01 - 260.62
Reef 2	2.7	4.7	0.1 - 12.5	0.04 - 70.81
Reef 3	0.7	1.2	0.2 - 1.5	0.01 - 3.52
Dominant Porosity Type:				
Interparticle	6.2	9.3	0.4 - 19.7	0.00 - 70.05
Moldic	5.4	7.3	0.5 - 14.9	0.00 - 260.62
Vuggy	9.1	23.1	0.1 - 16.5	0.66 - 126.05
Genetic Pore Type:				
Ae	6.5	4.2	3.69 - 12.15	0.66 - 15.46
Ar	2.1	3.9	0.28 - 6.54	0.61 - 13.00
Be	8.4	15.5	1.19 - 16.53	0.03 - 126.05
Br	3.4	6.9	0.22 - 12.14	0.21 - 70.05

DISCUSSION

Timing of Diagenesis

Mapping flow units in diagenetically altered pore systems requires understanding the relative timing of different diagenetic events with respect to each other, and also the geologic conditions or events that caused these episodes of diagenesis to occur (Ahr, 2008). This information can be used to find rock properties that act as proxies for porosity when depositional facies boundaries are no longer reliable indicators of flow unit dimensions (Ahr, 2008). Thin section petrography has revealed multiple stages of diagenesis in the Diamond M rocks; these different types of diagenesis include diagenesis in the marine and meteoric phreatic, and burial diagenetic environments. Marine phreatic diagenesis led to the creation of stable micritic envelopes around metastable aragonitic grains such as phylloid algae, forams, and brachiopods. In many cases this micritization (Figure E.7) provides the only traces of the original nature of the sediment (Scholle and Ulmer-Scholle, 2003). Micritization of grains is interpreted to be early diagenesis.

Meteoric phreatic and shallow burial diagenesis are often difficult to distinguish, because similar products are formed during meteoric phreatic and early burial-stage transformations (Scholle and Ulmer-Scholle, 2003). Dissolution porosity commonly forms during burial diagenesis as well at exposure surfaces, and the study area acquired porosity changes from both settings. The Horseshoe atoll experienced at least four periods of subaerial exposure and consequent erosion during Canyon FM time (Reid,

1998 in Fisher, 2005). Most of the effective porosity and permeability in the Horseshoe atoll reef limestones resulted from one or more periods of exposure to meteoric water (Vest, 1970). Vugs constitute nearly half of the total porosity of the field, and Saller et al. (1999) found that intermediate duration (50,000 – 130,000 years) subaerial exposure in West Texas carbonates can create dissolution vugs, fractures, and fissures.

Deeep burial (mesogenetic) diagenesis often plays the most important role in the diagenesis of sediments in terms of porosity changes, because rocks tend to spend the longest amount of time in the burial diagenetic setting (Scholle and Ulmer-Scholle, 2003). Many features commonly associated with mesogentic diagenesis occur in the study area, including brittle grain deformation, stylolites, dissolution seams, blocky calcite, drusy cement, poikilotopic calcite spar, syntaxial overgrowth, saddle dolomite, silica replacement, and pyrite replacement (Mazzullo and Harris, 1992).

Cross cutting relationships give clues to the order in which diagenetic processes occurred. Many of the micritized grains associated with early diagenesis are partially dissolved, and the dissolution pores are filled with cement. This suggests that after micritization there was an episode of dissolution and subsequent cementation of pores by small blocky calcite crystals. This small blocky calcite is often irregularly dissolved creating irregular pores that cut across grains and are filled with large blocky calcite, indicating a second stage of dissolution and cementation. Lastly, saddle dolomite, which indicates a mesogenetic environment, is seen replacing the large blocky calcite in some pores.

Flow Units

In order to rank reservoir quality, flow units were established based on combined porosity and permeability ranges. Nine reservoir quality pairs for Diamond M field were used in slice mapping this area by Fisher (2005), and this study uses similar quality pairs. To designate the ranges for each flow unit porosity and permeability values were taken from core analysis and separated into poroperm brackets. These flow units are ranked from 1 to 9 in sequential order from worst to best. Cooler colors (purple, blue) represent poor reservoir quality while warmer colors (orange, red) represent good reservoir zones (Figure H.34). A cut-off criterion was chosen to designate flow units 1 – 4 as poor reservoirs and flow units 5 – 9 as good reservoirs. Because no zones fall into flow unit 6, the good reservoir zones have porosities greater than 6.67 % and permeabilities above 8 md. Figures H.35-H.40 show core porosity and permeability for the gemstone wells, as well as depths for high ranking flow units.

Petrophysical Relationship with Depositional Facies

Results from this study show that a tenuous relationship exists between facies and reservoir performance characteristics in the study area. On average, the reef 1 facies has the highest poroperm values in the field, and the grainstone/packstone facies has the second highest; however they typically have low poroperm values. The worst reservoir facies (debris, reef 3) always fall into the poorer flow units (1-4), while the best reservoir facies (reef 1, grainstone/packstone) still fall into the poorer flow units at least 70% of

the time (Figure H.41). Therefore no significant correlation occurs between petrophysical characteristics and depositional facies on the reservoir scale.

Petrophysical Relationship with Genetic Pore Types

Results from this study show there is a better relationship between genetic pore type and reservoir performance characteristics than with depositional facies. Typically areas dominated by enhanced pore types fall into better flow units than areas dominated by reduced pores, but this is not always the case. Out of the 54 thin sections, there are two examples where reduced pore types have high poroperm values. One H1-Ar thin section has 6.54 % porosity and a permeability of 13 md, and one H1-Br thin section has 12.14 % porosity and a permeability of 70.05 md (Figure H.42). These are most likely erroneous values, where the core around the thin section had largely different petrophysical properties. As mentioned in the methods section, thin section poroperm data was not available so core analysis poroperm for the surrounding foot of core was used. It is likely that while the thin section showed reduced porosity, the surrounding core had enhanced properties, and elevated poroperm values would show in core analysis.

The H1-Be pore type has the best distribution of high ranking flow units, with 48% of flow units being good reservoir quality (flow units 5-9). The second best is H1-Ae, but this pore type only has 14% of flow units that can be considered of good reservoir quality. Typically, the reduced hybrid pore systems have the lowest reservoir quality, with the exception of the possibly erroneous values mentioned above. One-

hundred perecent of the H1-Ar flow units being ranked poorly, and 92% of the H1-Br flow units being poor (Figure H.43).

The correlation of pore types to flow units is more obvious when considering samples falling in the "good reservoir zone", flow units 5 and above. Looking at core analysis from all 3 wells, 60 feet of the cored zone qualifies for flow unit rank 5 or higher. From this area, 56 feet are H1-Be pore type, while the remaining 4 feet are split between H1-Ae and H1-Br (Figure H.44). It logically follows that H1-Be pore types should comprise the highest quality flow units, because they contain the most vuggy porosity, which typically has the highest poroperm values (Figure H.45). Forty-one percent of H1-Be pores are dominated by vuggy porosity (Figure H.46).

While there is some overlap between poroperm values for enhanced and reduced pore types, it appears that genetic pore types are a more reliable predictor of reservoir flow properties than depositional facies. If thin section poroperm values were acquired and plotted, there is a strong possibility that the grouping of data points would be much better.

Petrophysical Rock Types

Petrophysical rock types are characterized through porosity/permeability ratio analysis on the basis of genetic pore types, and are defined independently of facies. Unfortunately petrophysical rock types could not be established for Diamond M field, because no strong groupings in the porosity/permeability data could be identified. Enhanced and reduced pore types overlap and do not form distinct groupings (Figure

H.42). This lack of grouping can likely be attributed to not having poroperm data for the thin sections intervals, where the genetic pore types were identified. Using core analysis poroperm values as a substitute does not accurately represent true thin section, and therefore genetic pore type, poroperm values. Flow units based on core analysis poroperm values were determined to be the most accurate way to depict the spatial distribution of good reservoir zones.

Spatial Distribution of Flow Units

Flow units in Diamond M field do not conform to facies boundaries, and do not correlate well to depth. Correlating these units between wells was difficult, because they lack distinct gamma ray and neutron log signatures. Even between the cored wells, flow units vary. High ranking flow units typically occur in pockets less than 10 feet thick, and are most often only a few feet thick. Figure G.5 shows the distribution of high ranking flow units in the three cored wells.

Results from this study show that the reef 1facies contains the highest average poroperm values, and the grainstone/packstone facies contains the second highest. This ranking of depositional facies is shown on the cross section (Figure G.5), with the reef 1 facies containing the largest number of high ranking flow units, and the grainstone/packstone facies coming in second. Likewise, the poorer quality depositional facies had the fewest high ranking flow units. The reef 2 facies had a couple zones with high ranking flow units, while the reef 3 and debris facies had none.

CONCLUSIONS

- Diamond M field produces from a diagenetically altered carbonate reservoir.
- Reservoir quality in Diamond M field is related to genetic pore types but not to pore types as defined by Lucia or Choquette and Pray.
- The reef 1 and grainstone/packstone facies contained the largest number of high ranking flow units, which indicate reservoir quality based on combined poroperm values.

REFERENCES

Adams, J. E., 1965, Stratigraphic-tectonic development of Delaware Basin: AAPG Bulletin, v. 49, p. 2140-2148.

Ahr, W. M., 2008, Geology of Carbonate Reservoirs: The Identification, Description, and Characterization of Hydrocarbon Reservoirs in Carbonate Rocks: Hoboken, New Jersey, John Wiley & Sons Inc., 277 p.

Ahr, W. M., 2009, GEOL-624 Carbonate Reservoirs, Course Notes, Texas A&M University.

Ahr, W. M., D. Allen, A. Boyd, H. N. Bachman, T. Smithson, et al., 2005, Confronting the carbonate conundrum: Schlumberger Oilfield Review, Spring 2005, p. 18-29.

Ahr, W. M., E.A. Mancini, W.C. Parcell., 2011, Pore characteristics in microbial carbonate reservoirs: AAPG Annual Convention and Exhibition, Houston, Texas, April 10-13, 2011.

Alnaji, N. S., 2002, Two Carbonate Shelf Margins with Hydrocarbon Potential Compared: Upper Upper Jurassic Formations of Arabian Basin and Guadalupian Formations of Permian Basin of Texas and New Mexico, Master's thesis, University of Arkansas, Little Rock, 292 p.

Archie, G. E., 1952, Classification of carbonate reservoir rocks and petrophysical considerations: AAPG Bulletin, v. 36, p. 278-298.

Bathurst G. C., 1975, Carbonate Sediments and Their Diagenesis: Amsterdam, Elsevier Science B. V., 658 p.

Burnside, R. J., 1959, Geology of part of the Horseshoe atoll in Borden and Howard Counties, Texas: U.S. Geol. Survey, Profesional Paper 315-B, 34 p.

Choquette, P. W., and L. C. Pray, 1970, Geologic nomenclature and classification of porosity in sedimentary carbonates: American Association of Petroleum Geologists Bulletin, v. 54, p. 207-250.

Cleaves, A. W., 2000, Sequence stratigraphy and reciprocal sedimentation in Middle and Late Pennsylvanian carbonate-bank systems, Eastern shelf of the Midland Basin, north-central Texas, *in* K.S. Johnston, ed., Platform carbonates in the southern Midcontinent, 1996 symposium: Oklahoma Geological Survey Circular 101, p. 227-257.

Davies, G. R and L. B. Smith Jr., 2006, Structurally controlled hydrothermal dolomite reservoir facies: An overview: AAPG Bulletin, v. 90, p. 1641-1690.

Dunham, R. J., 1962, Classification of carbonate rocks according to depositional texture, *in* W. E. Ham, ed., Classification of carbonate rocks-a symposium: AAPG Memoir 1, p. 108-121.

Dutton, S. P., E. M. Kim, R. F. Broadhead, W. D. Raatz, C. L. Breton, S. C. Ruppel, and C. Kerans, 2005, Play analysis and leading-edge oil-reservoir development methods in the Permian Basin: Increased recovery through advanced technologies: AAPG Bulletin, v. 89, no. 5, p. 553–576.

Ewing, T. E., 1991, The tectonic framework of Texas: Text to accompany "The Tectonic Map of Texas": University of Texas at Austin, Bureau of Economic Geology, 36 p.

Fisher, A., 2005, Predicting spatial distribution of critical pore types and their influence on reservoir quality, Canyon (Pennsylvanian) Reef reservoir, Diamond M field, Texas, Master's thesis, Texas A&M University 145 p.

Forsythe, G. T. W., 2003, A new synthesis of Permo-Carboniferous phylloid algal reef ecology: SEPM Special Publication, number 78, p. 173-188.

Frenzel, H. N., R. R. Bloomer, R. B. Cline, J. E. Cys, J. E. Galley, W. R. Gibson, J. M. Hills, W. E. King, W. R. Seager, F. E. Kottlowski, S. Thompson III, G. C. Luff, B. T. Pearson, and D. C.Van Siclen, 1988, The Permian Basin region, *in* L. L. Slodd, ed., Sedimentary cover- North American craton: Boulder, Colorado, Geological Society of America, The Geology of North America, v. D-2, p. 261-306.

Galley, J. E., 1958, Oil and geology in the Permian Basin of Texas and New Mexico, *in* L. G. Weeks, ed., Habitat of oil: A symposium: AAPG, p. 395-446.

Galloway, W. E., Ewing, T. E., Garrett, C. M., Jr., Tyler, Noel, and Bebout, D. G., 1983, Atlas of major Texas oil reservoirs: The University of Texas at Austin, Bureau of Economic Geology Special Publication, 139 p.

Garber, R. A., G. A. Grover, and P. M. Harris, 1989, Geology of the Capitan shelf margin - subsurface data from the northern Delaware Basin, in P. M. Harris, and G. A. Grover, eds., Subsurface and outcrop examination of the Capitan shelf margin, northern Delaware Basin: SEPM Core Workshop no. 13, pp. 3-269.

Hammel, B. S., 1996, High resolution characterization of the Permian (Upper Leonardian) Spraberry Formation, Happy Spraberry Field, Garza County, Texas, Master's thesis, Texas A&M University, College Station, Texas, 176 p.

Hanson, B. M., B. K. Powers, C. M. Garrett, Jr., D. E. McGookey, E. H. McGlasson, R. L. Horak, S. J. Mazzullo, A. M. Reid, G. G. Calhoun, J. Clendening, and B. Claxton, 1991, The Permian Basin, *in* H. J. Gluskoter, D. D. Rice, and R. B. Taylor, eds., Economic geology, U.S.: Boulder, Colorado, Geological Society of American, The Geology of North America, v. P-2, p. 339-356.

Heckel, P. H., 1980, Paleogeography of eusatic model for deposition of Midcontinent Upper Pennsylvanian cyclothems, *in* Fouch, T. D., and E. R. Magathan, Rocky Mountain paleogeography of the west-central United States: Soceity of Economic Paleontologists and Mineralogists, Rocky Mountain Section, Denver, p. 197-251.

Horak, R. L., 1985, Tectonic and hydrocarbon maturation history in the Permian Basin: Oil and Gas Journal, v. May 27, p. 124-129.

Humbolt, A., 2008, Genetic Pore Typing as a Means of Characterizing Reservoir Flow Units: San Andres, Sunflower Field, Terry Country, Texas, Master's thesis, Texas A&M University, 187 p.

Jumper, S. C., and H. W. Pardue, 1996, A 3-D case history in the Horseshoe atoll area of Scurry County, Texas, *in* P. Weimer and T. L. Davis, eds. AAPG Studies in Geology No. 42 and SEG Geophysical Developments Series No. 5, AAPG/SEG, Tulsa, p. 155-160

Lucia, F. J., 1983, Petrophysical parameters estimated from visual description of carbonate rocks: a field classification of carbonate pore space: Journal of Petroleum Technology, March, v. 35, p. 626–637.

Machel, H. G., 1987, Saddle dolomite as a by-product of chemical compaction and thermochemical sulfate reduction: Geology, v. 15, p. 936-940.

Machel, H. G., 2004, Concepts and models of dolomitization: a critical reappraisal: *from* Braithwaite, C. J. R., Rizzl, G. and Darke, G. (eds) 2004. The Geometry and Petrogenesis of Dolomite Hydrocarbon Reservoirs. Geological Society, London, Special Publications, 235, 7-63. 0305-8719

Machel, H. G. and J. Lonnee, 2002. Hydrothermal dolomite - a product of poor definition and imagination. Sedimentary Geology, 152, p. 163-171.

Mazzullo, S. J., and P. M. Harris, 1992, Meseogenetic dissolution: its role in porosity development in carbonate reservoirs: AAPG Bullentin, v. 76., no. 5, p. 607-620.

Mazzullo, S. J., and A. M. Reid, 1989, Lower Permian platform and basin depositional systems, northern Midland Basin, Texas, *in* P. D. Crevello, J. L. Wilson, J. F. Sarg, and J. F. Read, eds., Controls on carbonate platform and basin development: SEPM Special Publication 44, p. 305-320.

Myers, D. A., P. T. Stafford, and R. J. Burnside, 1956, Geology of the late Paleozoic Horseshoe atoll in west Texas: University of Texas at Austin Publication 5607, 113 p.

Radke, B. M., and R. L. Mathis, 1980, On the formation and occurrence of saddle dolomite: Journal of Sedimentary Petrology, v. 50, p. 1149-1168.

Reid, S. T., 1998, Diamond M Canyon Unit Study, unpublished from Harold Vance Department of Petroleum Engineering, Texas A&M University.

Riding, R., 2002, Structure and composition of organic reefs and carbonate mud mounds; concepts and categories: Earth Science Reviews 58, p. 163-231.

Rothrock, H. E., R. E. Bergenback, D. A. Myers, P. T. Stafford, and R. T. Terriere, 1953, Preliminary report on the geology of the Scurry reef in Scurry County, Texas: U.S. Geol. Survey Oil and Gas Inv. Map OM 143.

Russian, C., R. Perez, K. Marfurt, O. Davogustto, and H. Alzahrani, 2010, P- and S-wave delineation of the Horseshoe atoll, Diamond-M Field, Texas, USA: The Leading Edge, September 2010, p. 1108-1115.

Saller, A. H., J. A. D. Dickson, and F. Matsuda, 1999, Evolution and distribution of porosity associated with subaerial exposure in Upper Paleozoic platform limestones, West Texas: AAPG Bulletin, v. 83, No. 11, p. 1835-1854.

Schatzinger, R. A., 1988, Changes in facies and depositional environments along and across the trend of the Horseshoe atoll, Scurry and Kent Counties, Texas: PBS-SEPM Research Seminar Number One, p. 79-105.

Scholle, P. A., and D. S. Ulmer-Scholle, 2003, A color guide to the petrography of carbonate rocks: Grains, textures, porosity, diagenesis: AAPG Memoir no. 77, 474 p.

Stafford, P. T., 1959, Geology of part of the Horseshoe atoll in Scurry and Kent Counties, Texas: U.S. Geological Survey Professional Paper 315-A, 18 p.

Tai, P. C., 2001, Late Paleozoic Foreland Deformation in the Southwestern Midland Basin and Adjacent Areas: Implications for Tectonic Evolution of the Permian Basin, West Texas, Ph. D. dissertation, College Station, Texas A&M University, 193 p.

Vest, E. L., 1970, Oil fields of Pennsylvanian-Permian Horseshoe atoll, West Texas: *in* Halbouty, M. T., ed., Geology of Giant Petroleum Fields: AAPG Memoir 14, p. 185-203.

Waite, L. E., 1993, Upper Pennsylvanian Seismic Sequences and Facies of the Eastern and Southern Horseshoe atoll, Midland Basin, West Texas, Loucks, R.G., Sarg, J.F., AAPG Memoir 57, p. 213-240.

Ward, R. F., C. G. S. C. Kendall, and P. M. Harris, 1986, Upper Permian (Guadalupian) facies and their association with hydrocarbons - Permian Basin, west Texas and New Mexico: AAPG Bulletin, v. 70, p. 239-262.

Yang, K. M, and S. L. Dorobek, 1995a, The Permian Basin of west Texas and New Mexico: Tectonic history of a "composite" foreland basin and its effect on stratigraphic development, *in* S. L. Dorobek and G. M. Ross, eds., Stratigraphic evolution in foreland basins: SEPM Special Publication 52, 149-174.

Yang, K. M. and S. L. Dorobek, 1995b, The Permian Basin of west Texas and New Mexico: Flexure modeling and evidence for lithospheric heterogeneity across the Marathon Foreland, *in* S. L. Dorobek and G. M. Ross, eds., Stratigraphic evolution in foreland basins: SEPM Special Publication 52, 37-50.

Ye, H., L. Royden, C. Burchfiel, and M. Schuepbach, 1996, Late Paleozoic deformation of interior North America: The Greater Ancestral Rocky Mountains: AAPG Bulletin, v. 80, p. 1397-1432.

APPENDIX A

CORE DESCRIPTION

Note: 'Intramatrix' porosity refers to intercrystalline porosity in the matrix.

Core Description: Emerald #1
Core Interval: 6613.0' – 6632.2'

Depth (ft)	Thickness (ft)	Dunham/ Riding	Porosity	Grains
6613.0 - 6617.0	4.0	Grainstone	Estimated**:** 10 % Intramatrix Moldic Intraparticle	**Dominant:** skeletal hash **Present:** bivalves, brachiopods, crinoids, forams, fusulinids, phylloid algae (broken), sponge spicules,
Description: Tan limestone, moderate sorting, indistinct bedding, fine grained, abundant broken grains. 6614.7' to 6615' preserved.				

Depth (ft)	Thickness (ft)	Dunham/ Riding	Porosity	Grains
6617.0 – 6625.9	8.9	Automicrite	Estimated:3-5 % Moldic Intraparticle Intramatrix	**Dominant:** fusulinids, skeletal hash **Present:** bivalves, brachiopods, crinoids, forams, phylloid algae (broken), sponge spicules,
Description: Tan to brown limestone, indistinct bedding, moderate sorting below 6620', poor sorting above. Stylolites and saddle dolomite present, calcite filled veins and silica replacement common in certain areas. 6622.7' to 6623' preserved.				

Depth (ft)	Thickness (ft)	Dunham/ Riding	Porosity	Grains
6625.9 – 6630.0	4.1	Automicrite	Estimated: 1-2% Fracture	**Dominant:** phylloid algae (broken) **Present:** bivalves, brachiopods, crinoids, forams, fusulinids, gastropods, micritic clasts, skeletal hash
Description: Brown to gray limestone, mottled texture, poorly sorted abundant dissolution seams, pyrite and blue gray silica replacement. Calcite filled veins, stylolites, and geopetal structures present. Many grains replaced with clear calcite.				

Core Description: Emerald #1 (continued)
Core Interval: 6630.0'– 6639.7'

Depth (ft)	Thickness (ft)	Dunham/ Riding	Porosity	Grains
6630.0 – 6632.2	2.2	Grainstone	Estimated: 0 %	**Dominant:** skeletal hash, crinoids **Present:**bivalves, brachiopods, forams, phylloid algae (broken)
Description: Light gray to dark gray limestone, indistinct bedding, well sorted below 6631', sorting decreased to moderate above 6631'. Pyrite present, abundant cement between grains and silica replacement of grains.				

Depth (ft)	Thickness (ft)	Dunham/ Riding	Porosity	Grains
6632.2 – 6634.5	2.3	Automicrite	Estimated: 1 % Fracture	**Dominant:** phylloid algae (broken) **Present:** bivalves, brachiopods, crinoids, forams, skeletal hash, possible trilobites
Description: Brown to gray limestone, mottled texture, very port sorting, abundant stylolites and dissolution seams. Common blue silica replacement of grains. Phylloid algae are mostly dissolved.				

Depth (ft)	Thickness (ft)	Dunham/ Riding	Porosity	Grains
6634.5 – 6639.7	5.2	Grainstone	Estimated: 10 % Interparticle Intraparticle	**Dominant:** skeletal hash, crinoids **Present:** bivalves, brachiopods, bryozoans, forams, fusulinids, phylloid algae (broken), sponge spicules
Description: Tan to gray limestone, indistinct bedding, moderate sorting that increases to well sorted above the stylolite at 6637.7'. Stylolites and dissolution seams present below 6656.5'. Pyrite and blue silica replacement of grains present. 6635.6' to 6636' preserved.				

Core Description: Emerald #1 (continued)
Core Interval: 6639.7’ – 6647.9’

Depth (ft)	Thickness (ft)	Dunham/ Riding	Porosity	Grains
6639.7 – 6640.4	0.7	Automicrite	Estimated: <1 % Microporosity	**Dominant:** fusulinids **Present:** brachiopods, crinoids, forams, phylloid algae (broken), skeletal hash
Description: Light brown to gray limestone, mottled texture, moderately sorted, abundant stylolites and dissolution seams. Looks similar to area below the absent core (6640.4’- 6643’), but with fewer grains. Some pyrite and blue silica replacement of grains.				

Depth (ft)	Thickness (ft)	Dunham/ Riding	Porosity	Grains
6640.4– 6643.0	2.6	N/A	N/A	N/A
Core Absent				

Depth (ft)	Thickness (ft)	Dunham/ Riding	Porosity	Grains
6643.0 – 6647.9	4.9	Packstone	Estimated: 1-3 % Interparticle Intraparticle Moldic	**Dominant:** fusulinids, phylloid algae **Present:** bivalves, brachiopods, crinoids, forams, skeletal hash
Description: Brown to gray limestone, mostly indistinct bedding, but horizontal grain layers from 6646’ – 6648’, moderate sorting. Large amount of dissolution seams with grey argillaceous material. Pyrite and blue silica replacement of phylloid algae present. Tan fusulinids surrounded by gray argillaceous material in dissolution seams.				

Core Description: Emerald #1 (continued)
Core Interval: 6647.9' – 6671.4'

Depth (ft)	Thickness (ft)	Dunham/ Riding	Porosity	Grains
6647.9– 6655.0	7.1	Packstone	Estimated: 3-10 % Intramatrix Intraparticle Interparticle Fracture	**Dominant:** fusulinids, skeletal hash **Present:** bivalves, brachiopods, crinoids, forams, phylloid algae (broken), sponge spicules
Description: Tan to light gray limestone, indistinct bedding, moderate to poor sorting, sorting decreases up section. Stylolites, dissolution seams, and blue silica replacement of grains present. Some partially healed veins.				

Depth (ft)	Thickness (ft)	Dunham/ Riding	Porosity	Grains
6655.0 – 6671.0	16.0	Automicrite	Estimated: 3-5 % Moldic Intramatrix Vuggy Fracture Intraparticle	**Dominant:** phylloid algae (whole & broken) , fusulinids **Present:** bivalves, brachiopods, crinoids, forams, micritic clasts at 6669.4, sponge spicules.
Description: Tan to dark gray limestone, mottled texture, poor to moderate sorting, stylolites and geopetal features common. Pyrite present in lower section, calcite filled veins common throughout section. Yellow staining near some stylolites, large silica nodule at 6667.5', argillaceous green material at 6655'.				

Depth (ft)	Thickness (ft)	Dunham/ Riding	Porosity	Grains
6671.0 – 6671.4	0.4	N/A	N/A	N/A
Core Preserved				

Core Description: Emerald #1 (continued)
Core Interval: 6671.4' – 6682.9'

Depth (ft)	Thickness (ft)	Dunham/ Riding	Porosity	Grains
6671.4 – 6675.8	4.4	Automicrite	Estimated: 5-10% Moldic Vuggy Intramatrix	**Dominant:** fusulinids, skeletal hash **Present:** bivalves, brachiopods, crinoids, forams, phylloid algae
Description: Light brown to gray limestone, mottled texture, poor sorting near bottoming, moderate sorting near top. Stylolites and geopetal structures common. Abundant pyrite replacement and calcite filled veins. Some vug filling calcite present, large gray silica nodules at 6674.6' and 6672.2'. Porosity varies with 5-10% from 6671' to 6672', and 5% from 6673' to 6674'. Vuggy porosity dominates 6675'.				

Depth (ft)	Thickness (ft)	Dunham/ Riding	Porosity	Grains
6675.8 – 6682.5	6.7	Packstone	Estimated: 3-5% Vuggy, Intramatrix, Fracture Porosity 10-15% at 6680.5', mainly Vuggy and Moldic	**Dominant:** phylloid algae (broken), skeletal hash **Present:** bivalves, brachiopods, forams, fusulinids, gastropods, peloids, sponge spicules
Description: Tan to light gray limestone, indistinct bedding, moderately sorted. Stylolites, geopetal structures, and dissolution seams present. Blue silica replacement of grains common. Large gray silica nodules at 6681.3' and 6678.5'. Phylloid algae replaced with calcite. Abundant microporosity from 6680' – 6682'.				

Depth (ft)	Thickness (ft)	Dunham/ Riding	Porosity	Grains
6682.5 – 6682.9	0.4	N/A	N/A	N/A
Core Preserved				

Core Description: Emerald #1 (continued)
Core Interval: 6682.9’ – 6695.2’

Depth (ft)	Thickness (ft)	Dunham/ Riding	Porosity	Grains
6682.9 – 6690.0	7.1	Automicrite	Estimated: 10-15 % Vuggy Moldic Intramatrix Fracture	**Dominant:** phylloid algae, crinoids, forams **Present:** bivalves, brachiopods, fusulinids, gastropods, sponge spicules
Description: Light brown to gray limestone, mottled texture, moderate to well sorting. Stylolites, dissolution seams, and geopetal structures present. Some pore filling calcite cement and pyrite present. Dark stain at 6686.6’. Porosity higher in vuggy areas.				

Depth (ft)	Thickness (ft)	Dunham/ Riding	Porosity	Grains
6690.0 – 6690.4	0.4	N/A	N/A	N/A
Core Preserved				

Depth (ft)	Thickness (ft)	Dunham/ Riding	Porosity	Grains
6690.4 – 6695.2	4.8	Automicrite	Estimated: 5-10 % Intramatrix Moldic Vuggy Fracture	**Dominant:** phylloid algae (broken), crinoids **Present:** bivalves, brachiopods, forams, skeletal hash, sponge spicules
Description: Tan to gray limestone, mottled texture, moderately sorted. Stylolites, dissolution seams, geopetal structures, and calcite filled veins present. Phylloid algae mostly dissolved. Possible burrowing at 6694’.				

Core Description: Emerald #1 (continued)
Core Interval: 6695.2’ – 6703.0’

Depth (ft)	Thickness (ft)	Dunham/ Riding	Porosity	Grains
6695.2 – 6698.5	3.3	Automicrite	Estimated: 0 %	**Dominant:** skeletal hash, crinoids **Present:** bivalves, forams, phylloid algae (broken), sponge spicules
Description: Brown to gray limestone, mottled texture, moderately sorted. Stylolites, pyrite, and blue silica replacement of grains present. Abundant vein filling calcite. Large area of grey silica replacement at 6695.3’.				

Depth (ft)	Thickness (ft)	Dunham/ Riding	Porosity	Grains
6698.5 – 6700.0	1.5	Grainstone	Estimated: 0 %	**Dominant:** crinoids, phylloid algae (broken) **Present:** brachiopods, forams, fusulinids, peloids, skeletal hash
Description: Tan to gray limestone, fine grained, mostly indistinct bedding but mottled texture near top of section. Well sorted at base but decreases to moderate sorting at the top of the section. Stylolites and dissolution seams sparse, pyrite present. Large vertical calcite vein from 6699.5’ – 6700’.				

Depth (ft)	Thickness (ft)	Dunham/ Riding	Porosity	Grains
6700.0 – 6702.0	2.0	Automicrite	Estimated: 10% Moldic Intramatrix Fracture	**Dominant:** phylloid algae **Present:** bivalves, brachiopods, crinoids, forams, fusulinids
Description: Tan to gray limestone, mottled texture, well sorted. Stylolites and fractures present, calcite filled veins and pyrite replacement common.				

Depth (ft)	Thickness (ft)	Dunham/ Riding	Porosity	Grains
6702.0 – 6703.0	1.0	N/A	N/A	N/A
Core Absent				

Core Description: Emerald #1 (continued)
Core Interval: 6703.0' – 6709.1'

Depth (ft)	Thickness (ft)	Dunham/ Riding	Porosity	Grains
6703.0 – 6704.3	1.3	Automicrite	Estimated: 10 % Moldic Intramatrix Vuggy	**Dominant:** phylloid algae **Present:** bivalves, brachiopods, crinoids, fusulinids, sponge spicules
Description: Tan to gray limestone, mottled texture, poorly sorted. Stylolites, geopetal structures, and calcite filled veins present. Abundant pyrite replacement. Calcite and possible saddle dolomite partially filling some vugs.				

Depth (ft)	Thickness (ft)	Dunham/ Riding	Porosity	Grains
6704.3 – 6706.2	1.9	Automicrite	Estimated: 0 % 1% Vuggy porosity at 6705.3'	**Dominant:** phylloid algae, fusulinids **Present:** bivalves, brachiopods, crinoids, forams
Description: Brown limestone, indistinct bedding, moderately sorted. Stylolites and dissolution seams present. Vein filling calcite common. Grain abundance decreases towards the top of the section.				

Depth (ft)	Thickness (ft)	Dunham/ Riding	Porosity	Grains
6706.2 – 6709.1	2.9	Automicrite Packstone areas from 6707.7' – 6708.7'	Estimated: 0 %	**Dominant:** phylloid algae, fusulinids **Present:** bivalves, brachiopods, bryozoans, crinoids, forams, gastropods, skeletal hash
Description: Light gray to gray limestone, light brown from 6707' – 6707.5', mottled texture, poorly sorted. Stylolites, geopetal structures, and calcite filled veins present. Pyrite present near top of section. Many grains dissolved and replaced with clear calcite.				

Core Description: Emerald #1 (continued)
Core Interval: 6709.1' – 6718.9'

Depth (ft)	Thickness (ft)	Dunham/ Riding	Porosity	Grains
6709.1 – 6711.2	2.1	Automicrite	Estimated: 0 %	**Dominant:** phylloid algae, fusulinids **Present:** bivalves, brachiopods, crinoids, forams, skeletal hash
Description: Brown limestone, indistinct bedding, moderate to poor sorting. Areas with abundant dissolution seams. Calcite filled veins present. Many large whole grains surrounded by fine skeletal hash.				

Depth (ft)	Thickness (ft)	Dunham/ Riding	Porosity	Grains
6711.2 – 6714.7	3.5	Packstone	Estimated: 0 %	**Dominant:** fusulinids, peloids, phylloid algae **Present:** bivalves, crinoids, forams, skeletal hash
Description: Brown limestone, indistinct bedding, moderate to well sorting, medium to coarse grained. Dissolution seams, geopetal structures, and calcite filled veins present. Areas of clear calcite and blue silica replacement of grains.				

Depth (ft)	Thickness (ft)	Dunham/ Riding	Porosity	Grains
6714.7 – 6718.9	4.2	Grainstone 6714.7' – 6718' Packstone 6718'- 6718.9'	Estimated: 5 % Interparticle Moldic Intraparticle	**Dominant:** forams, fusulinids **Present:** bivalves, brachiopods, crinoids, phylloid algae, skeletal hash, sponge spicules
Description: Tan limestone that darkens to brown at the top of section, mainly indistinct bedding but parallel layers from 6716'- 6717'. Well sorted and fine grained at 6718', coarsens upwards and sorting decreases to moderate at 6717' and decreases further to poor at 6715'. Sparse stylolites, fractures, and geopetal structures at 6716'. Trace amounts of pyrite.				

Core Description: Emerald #1 (continued)
Core Interval: 6718.9' – 6737.9'

Depth (ft)	Thickness (ft)	Dunham/ Riding	Porosity	Grains
6718.9 – 6723.1	4.2	Automicrite	Estimated: <1 % Fracture	**Dominant:** phylloid algae (whole & broken) **Present:** bivalves, brachiopods, crinoids, forams, fusulinids
Description: Brown to light gray limestone, patches of both mottled texture and indistinct bedding throughout section, moderate to poor sorting. Areas with abundant dissolution seams. Geopetal structure and calcite filled veins common. Large 3 cm foram at 6719.5'.				

Depth (ft)	Thickness (ft)	Dunham/ Riding	Porosity	Grains
6723.1 – 6736.1	13.0	Automicrite	Estimated: 0 % Small patch of Moldic porosity at 6731.1'	**Dominant:** phylloid algae >70% **Present:** bivalves, brachiopods, crinoids, forams, fusulinids, peloids, skeletal hash, sponge spicules
Description: Light gray to gray limestone, patches of light brown, indistinct bedding, moderate to poor sorting. Stylolites, dissolution seams, and geopetal structures common. Trace amounts of pyrite (6730') and blue silica replacement of brachiopods (6725'). Many grains dissolved and replaced with clear calcite.				

Depth (ft)	Thickness (ft)	Dunham/ Riding	Porosity	Grains
6736.1 – 6737.9	1.8	Automicrite	Estimated: 10-15% Moldic Intraparticle	**Dominant:** fusulinids, skeletal hash **Present:** brachiopods, crinoids, forams, phylloid algae (whole and broken)
Description: Tan to light gray limestone, indistinct bedding, poorly sorted. Dissolution seams, fractures, and vein filling calcite present. Blue silica replacement of crinoids common. Some fractures filled with a green residue. Amount of grain increases towards the top of the section and porosity decreases towards the top of the section.				

Core Description: Emerald #1 (continued)
Core Interval: 6737.9’ – 6740.3’

Depth (ft)	Thickness (ft)	Dunham/ Riding	Porosity	Grains
6737.9 – 6738.5	0.6	N/A	N/A	N/A
Core Preserved				

Depth (ft)	Thickness (ft)	Dunham/ Riding	Porosity	Grains
6738.5 – 6739.1	0.6	Automicrite	Estimated: 5 % Vuggy Moldic Intraparticle	**Dominant:** phylloid algae, skeletal hash **Present:** brachiopods, crinoids, forams, fusulinids, peloids
Description: Tan to light gray limestone, indistinct bedding, moderately sorted. Fractures and vugs commonly filled with calcite. Large vug (15 mm) at 6738.6’. Phylloid algae often dissolved.				

Depth (ft)	Thickness (ft)	Dunham/ Riding	Porosity	Grains
6739.1 – 6739.5	0.4	N/A	N/A	N/A
Core Preserved				

Depth (ft)	Thickness (ft)	Dunham/ Riding	Porosity	Grains
6739.5 – 6740.3	0.8	Automicrite	Estimated: 10-15 % Moldic Intraparticle	**Dominant:** phylloid algae, fusulinids **Present:** bivalves, brachiopods, crinoids, micritic clasts, skeletal hash
Description: Tan to gray limestone, indistinct bedding, moderately sorted. Stylolites and calcite filled veins present. Phylloid algae often dissolved.				

Core Description: Emerald #1 (continued)
Core Interval: 6740.3’ – 6763.0’

Depth (ft)	Thickness (ft)	Dunham/ Riding	Porosity	Grains
6740.3 – 6740.6	0.3	N/A	N/A	N/A
Core Preserved				

Depth (ft)	Thickness (ft)	Dunham/ Riding	Porosity	Grains
6740.6 – 6758.8	18.2	Automicrite	Estimated: 10-15 % Moldic Intramatrix Intraparticle 6743’-6755’ 1-5 %	**Dominant:** phylloid algae, fusulinids **Present:** bivalves, brachiopods, crinoids, forams, gastropods, skeletal hash, sponge spicules
Description: Tan to gray limestone, indistinct bedding, moderate to poor sorting. Stylolites, dissolution seams, geopetal structures, and calcite filled veins present. Blue silica replacement of crinoids at 6747’. Some yellow-orange staining near stylolites, and porosity is usually found closer to stylolites. Grains often dissolved and replaced by clear calcite.				

Depth (ft)	Thickness (ft)	Dunham/ Riding	Porosity	Grains
6758.8 – 6759.0	0.2	N/A	N/A	N/A
Core Preserved				

Depth (ft)	Thickness (ft)	Dunham/ Riding	Porosity	Grains
6759.0 – 6763.0	4.0	Automicrite	Estimated: 10 % Moldic Intramatrix	**Dominant:** phylloid algae, skeletal hash **Present:** bivalves, brachiopods, crinoids, forams, fusulinids
Description: Tan to gray limestone, indistinct bedding, moderately sorted. Stylolites present. Phylloid algae often dissolved and replaced with clear calcite. Core broken into fragments from 6761.2’ to 6763’.				

Core Description: Jade #1
Core Interval: 6745.0’ – 6762.8'

Depth (ft)	Thickness (ft)	Dunham/ Riding	Porosity	Grains
6745.0 – 6750.4	5.4	Automicrite	Estimated: 1-2 % Intramatrix Fracture	**Dominant:** skeletal hash, fusulinids **Present:** bivalves, brachiopods, forams, gastropods, green algae, phylloid algae (whole and broken)
Description: Light tan to gray limestone, mottled texture, poorly sorted. Abundant stylolites and dissolution seams with black argillaceous material in seams. Blue silica replacement of grains and calcite filled veins present. Pyrite at 6745', possible bioturbation from 6749'-6750.4', unusual bright orange deposit at 6746'.				

Depth (ft)	Thickness (ft)	Dunham/ Riding	Porosity	Grains
6750.4 – 6752.4	2.0	Grainstone	Estimated: 0 %	**Dominant:** skeletal hash, fusulinids **Present:** bivalves, brachiopods, forams, phylloid algae (broken)
Description: Brown with grey patches, limestone, indistinct bedding, moderate sorting at base that decreases to poor sorting at the top of the section. Grain size increases from base to top. Yellow rust color on some crinoids, fusulinid layer forms the top boundary.				

Depth (ft)	Thickness (ft)	Dunham/ Riding	Porosity	Grains
6752.4 – 6762.8	10.4	Automicrite	Estimated: 1-2 % Intramatrix Fracture	**Dominant:** phylloid algae (broken), skeletal hash **Present:** bivalves, brachiopods, crinoids, forams, fusulinids, micritic clasts
Description: Brown to gray limestone, mottled texture, moderate to poor sorting. Abundant fractures and dissolution seams. Blue silica replacement of grains and calcite filled veins common throughout the section. Many areas have >75% grains and are borderline packstone.				

Core Description: Jade #1 (continued)
Core Interval: 6762.8' – 6784.7'

Depth (ft)	Thickness (ft)	Dunham/ Riding	Porosity	Grains
6762.8 – 6766.5	3.7	Automicrite	Estimated: 1-2 % Intramatrix Fracture	**Dominant:** skeletal hash, micritic clasts **Present:** brachiopods, crinoids, forams, phylloid algae (broken)
Description: Tan to light brown limestone, mottled texture, fine grained with larger grains near the top of the section, well to moderate sorting. Stylolites, dissolution seams, geopetal structures, and blue silica replacement of grains present. Abundant calcite filled veins. Large angular micritic clasts present.				

Depth (ft)	Thickness (ft)	Dunham/ Riding	Porosity	Grains
6766.5– 6772.0	5.5	PS/GS above 6769.5' Automicrite 6769.5'	Estimated: 5 % In GS/PS Moldic, Intramatrix Estimated: 10-15 % In CCR Intramatrix, Moldic, Vuggy	**Dominant:** phylloid algae (broken), peloids **Present:** bivalves, brachiopods, crinoids, forams, gastropods, sponge spicules
Description: Tan to light brown limestone, indistinct bedding except at 6795.5 which has parallel bedding in fine grainstone. Large poorly sorted grains in automicrite, fine well to moderate sorted grains in packstone/grainstone. Dissolution seams, vertical and horizontal stylolites present. Blue silica replacement of grains and partial vug filling calcite also present.				

Depth (ft)	Thickness (ft)	Dunham/ Riding	Porosity	Grains
6772.0 – 6784.7	12.7	Automicrite Packstone from 6776.5' - 6779.0'	Estimated: 3-8 % Intramatrix Moldic Fracture	**Dominant:** phylloid algae (broken), forams **Present:** bivalves, brachiopods, bryozoans, crinoids, micritic clasts, skeletal hash, sponge spicules
Description: Light tan to light gray limestone, mottled texture, moderate to poor sorting. Poorer sorting in packstone interval. Stylolites, dissolution seams, and calcite filled veins common. Patches of subangular micritic clasts. Grains commonly replaced with clear calcite. Core preserved from 6779.7' - 6780.3'.				

Core Description: Jade #1 (continued)
Core Interval: 6784.7' – 6816.5'

Depth (ft)	Thickness (ft)	Dunham/ Riding	Porosity	Grains
6784.7 – 6798.0	13.3	Packstone	Estimated: 5-12% Intramatrix Moldic Interparticle	**Dominant:** phylloid algae (broken), skeletal hash **Present:** bivalves, brachiopods, forams, peloids
Description: Tan limestone with areas of tan/gray color, indistinct bedding, moderate to well sorted. Fine grained below 6790', and coarsens upward above 6790'. Stylolites, dissolution seams, and calcite filled veins present. Core preserved from 6786.6' - 6787', 6790' - 6790.3', and 6793.7' - 6794.3'.				

Depth (ft)	Thickness (ft)	Dunham/ Riding	Porosity	Grains
6798.0 – 6807.8	9.8	Grainstone	Estimated: 5-10% Interparticle Moldic Intramatrix Vuggy	**Dominant:** phylloid algae (whole & broken) , forams **Present:** bivalves, brachiopods, crinoids, fusulinids, gastropods, micritic clasts
Description: Tan to gray limestone, 6803' - 6807.9' parallel to horizontal beds, 6798' - 6803' indistinct bedding. Mostly well sorted with areas of moderate sorting. Stylolites, dissolution seams, and partial vug filling calcite present. Pyrite from 6800' - 6802'. Forams and phylloid algae more than 80% of grains. Many grains micritized.				

Depth (ft)	Thickness (ft)	Dunham/ Riding	Porosity	Grains
6807.8 – 6816.5	8.7	Grainstone/ Packstone	Estimated: 3-4% above 6812' Moldic Intramatrix Fracture Estimated: 0% below 6812'	**Dominant:** forams, skeletal hash **Present:** bivalves, brachiopods, bryozoans, crinoids, fusulinids, gastropods, micritic clasts, phylloid algae (broken), sponge spicules
Description: Light gray to tan limestone, indistinct bedding, moderate to well sorted. Stylolites, dissolution seams, and geopetal structures present. Calcite filled veins common. Mostly fine forams with some larger grains, many grains have micritic rims. Core broken into fragments from 6812' - 6183'.				

Core Description: Jade #1 (continued)
Core Interval: 6816.5' – 6849.8'

Depth (ft)	Thickness (ft)	Dunham/ Riding	Porosity	Grains
6816.5 – 6821.2	4.7	Automicrite	Estimated: 0 %	**Dominant:** forams, skeletal hash **Present:** bivalves, brachiopods, crinoids, micritic clasts, phylloid algae (broken)
Description: Light to dark gray limestone, mottled texture, moderate to poor sorting. Stylolites and dissolution seams common. Geopetal structures and calcite filled veins present. Many grains have been micritized.				

Depth (ft)	Thickness (ft)	Dunham/ Riding	Porosity	Grains
6821.2 – 6837.8	16.6	Packstone	Estimated: 5-7 % above 6829' Moldic, Vuggy, Intramatrix Estimated: 10-15 % below 6829' Moldic, Intramatrix	**Dominant:** phylloid algae (whole & broken), forams **Present:** bivalves, brachiopods, bryozoans, crinoids, fusulinids, gastropods, micritic clasts, sponge spicules
Description: Light brown to gray limestone, indistinct bedding, moderate sorting below 6829, decreases to poor then very poor upwards as the appearance of very large grains (>20 mm) becomes abundant. Stylolites filled with green and black residue, geopetal structures, and calcite filled veins present. Many grains have been replaced with clear calcite or have been micritized. Some grain replacing saddle dolomite present. Core preserved from 6828.6' - 6829', 6831.7' - 6832', and 6834.7' to 6835'.				

Depth (ft)	Thickness (ft)	Dunham/ Riding	Porosity	Grains
6837.8 – 6849.8	12.0	Automicrite	Estimated: 1-3 % Moldic Fracture	**Dominant:** forams **Present:** bivalves, brachiopods, crinoids, fusulinids, green algae, phylloid algae (broken), sponge spicules
Description: Light gray to gray limestone, slightly mottled texture, well to moderate sorting that decreases to poor at 6848'. Abundant stylolites and calcite filled veins. Fine grained, usually around 40% grains, but increases to 60-70% grains above 6842', possible packstone areas.				

Core Description: Jade #1 (continued)
Core Interval: 6849.8' – 6871.7'

Depth (ft)	Thickness (ft)	Dunham/ Riding	Porosity	Grains
6849.8 – 6864.9	15.1	Automicrite	Estimated: 1 % Fracture	**Dominant:** crinoids, forams **Present:** bivalves, brachiopods, bryozoans, fusulinids, green algae, phylloid algae (broken), skeletal hash
Description: Light brown to dark gray limestone, mottled texture, moderate to poor sorting. Stylolites, dissolution seams, and pyrite present. Abundant calcite filled veins. Large crinoids fragments throughout section, many grains dissolved and replaced with clear calcite.				

Depth (ft)	Thickness (ft)	Dunham/ Riding	Porosity	Grains
6864.9 – 6871.7	6.8	Packstone	Estimated: 1-5 % Intramatrix Fracture Moldic	**Dominant:** phylloid algae (whole & broken), forams **Present:** bivalves, brachiopods, bryozoans, crinoids, fusulinids, green algae, micritic clasts
Description: Brown to gray limestone, debrite, poorly sorted angular clasts. Stylolites, dissolution seams, geopetal structures, and blue silica replacement of grains present. Abundant pyrite. Large patches of yellow/white saddle dolomite 6864.8' - 6870.5'.				

Core Description: Topaz #1
Core Interval: 6706.0' – 6721.2'

Depth (ft)	Thickness (ft)	Dunham/ Riding	Porosity	Grains
6706.0 – 6709.0	3.0	Grainstone	Estimated: 10-15 % Intramatrix Moldic	**Dominant:** forams, skeletal hash **Present:** brachiopods, crinoids, fusulinids, phylloid algae (broken)
Description: Light gray to dark brown limestone, parallel alternating layers of brown micrite and lighter calcite cement, fine grained. Stylolites and dissolution seams common. Blue silica replacement of grains, mainly crinoids, present. Core preserved from 6706.8' - 6707'.				

Depth (ft)	Thickness (ft)	Dunham/ Riding	Porosity	Grains
6709.0 – 6713.2	4.2	Packstone Grainstone from 6710.0' to 6711.0'	Estimated: 20 % Intramatrix Moldic	**Dominant:** fusulinids **Present:** bivalves, brachiopods, crinoids, forams, phylloid algae (broken), skeletal hash, sponge spicules
Description: Light gray limestone, indistinct bedding, poorly sorted, medium to coarse grained. Stylolites present, porosity decreases towards the top of the section. Core preserved from 6710.8' to 6711'.				

Depth (ft)	Thickness (ft)	Dunham/ Riding	Porosity	Grains
6713.2 – 6721.2	8.0	Automicrite	Estimated: 10-15 % Moldic Intramatrix Vuggy Intraparticle	**Dominant:** phylloid algae (broken), fusulinids **Present:** bivalves, brachiopods, crinoids, forams, skeletal hash
Description: Light gray to light brown limestone, mottled texture, moderately sorted. Stylolites, dissolution seams, and calcite filled veins present. Grain abundance increases up section. Porosity in the bottom of the section is mainly near stylolites.				

Core Description: Topaz #1 (continued)
Core Interval: 6721.2’ – 6753.2'

Depth (ft)	Thickness (ft)	Dunham/ Riding	Porosity	Grains
6721.2 – 6722.0	0.8	N/A	N/A	N/A
Core Absent				

Depth (ft)	Thickness (ft)	Dunham/ Riding	Porosity	Grains
6722.0 – 6726.0	4.0	Automicrite	Estimated: 3-5 % Moldic Intramatrix Vuggy at 6722.0'	**Dominant:** phylloid algae (whole & broken) **Present:** brachiopods, crinoids, forams, fusulinids
Description: Light brown to light gray limestone, mottled texture, moderately sorted. Stylolites and dissolution seams present. Phylloid algae often dissolved.				

Depth (ft)	Thickness (ft)	Dunham/ Riding	Porosity	Grains
6726.0 – 6750.0	24.0	N/A	N/A	N/A
Core Not Recovered				

Depth (ft)	Thickness (ft)	Dunham/ Riding	Porosity	Grains
6750.0 – 6753.2	3.2	Automicrite	Estimated: 10 % Moldic Vuggy Intramatrix Intraparticle	**Dominant:** phylloid algae (whole), fusulinids **Present:** bivalves, brachiopods, crinoids, forams, sponge spicules, possible trilobites
Description: Light gray to light brown limestone, mottled texture, moderately sorted. Stylolites, dissolution seams, and geopetal structures present. Phylloid algae often dissolved into molds. Fusulinids often have intraparticle porosity.				

Core Description: Topaz #1 (continued)
Core Interval: 6753.2' – 6831.5'

Depth (ft)	Thickness (ft)	Dunham/ Riding	Porosity	Grains
6753.2 – 6761.5	8.3	Automicrite	Estimated: 5-15 % above 6759.0' and 5% below 6759.0' Intramatrix Moldic Intraparticle	**Dominant:** forams, fusulinids **Present:** brachiopods, crinoids, phylloid algae (broken), skeletal hash, sponge spicules
Description: Light brown to gray limestone, mainly indistinct bedding, but slightly mottled above 6758'. Well sorted below 6757', but above 6757' grains get large and sorting decreases to moderate. Stylolites, dissolution seams, and pyrite present. Patches of blue/gray silica replacement from 6758' - 6760'. Core preserved from 6754.4' - 6754.7', and 6756.8' - 6757.1'.				

Depth (ft)	Thickness (ft)	Dunham/ Riding	Porosity	Grains
6761.5 – 6820.0	58.5	N/A	N/A	N/A
Core Not Recovered				

Depth (ft)	Thickness (ft)	Dunham/ Riding	Porosity	Grains
6820.0 – 6831.5	11.5	Automicrite	Estimated: 1-2 % Fracture	**Dominant:** fusulinids, phylloid algae (broken) **Present:** bivalves, brachiopods, bryozoans, crinoids, forams, skeletal hash, sponge spicules
Description: Light brown to gray limestone, mottled texture, poor sorting below 6828' and moderate sorting above 6828'. Stylolites and dissolution seams common. Calcite filled veins and blue silica replacement of grains present. Grains are often dissolved and replaced with clear calcite. Above 6826' areas of >60% grains common, possible oil stains from 6821' - 6823'.				

Core Description: Topaz #1 (continued)
Core Interval: 6831.5' – 6836.5'

Depth (ft)	Thickness (ft)	Dunham/ Riding	Porosity	Grains
6831.5 – 6836.5	5.0	Automicrite	Estimated: <1 % Fracture	**Dominant:** fusulinids, phylloid algae (whole & broken) **Present:** bivalves, brachiopods, crinoids, forams, skeletal hash
Description: Brown limestone, indistinct bedding, poorly sorted. Around 30% of section replaced with blue/gray silica. Dissolution seams, calcite filled veins, and blue silica replacement of grains common. Phylloid algae, fusulinids, and crinoids much larger than other grains.				

APPENDIX B

GRAPHICAL CORE DESCRIPTION

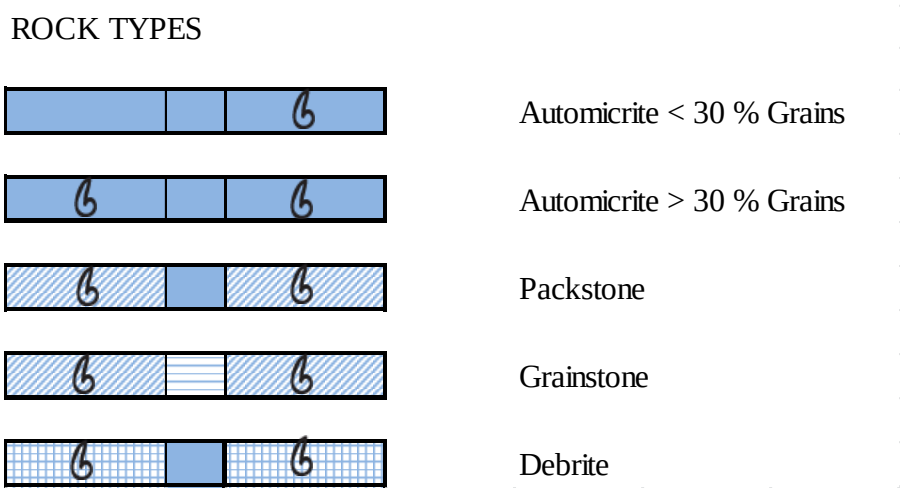

Figure B.1: Rock type key for core description.

Bedding

Indistinct		Irregular	
Mottled		Graded	
Paralell		Cross	

Structures

Stylolites		Bioturbation	
Dissolution Seams		Geopetal	
Fractures		Oil Stains	

Sorting

Extremely Well	XW	Well	W	Poorly	P
Very Well	VW	Moderately	M	Very Poorly	VP

Roundness

Angular		Subrounded	C
Sub Angular		Rounded	O

Grains

Bivalves		Fusulinids		Macro Fossils	
Brachiopods		Phylloid Algae		Intraclasts	
Bryozoans		Sponge Spicules		Gastropods	
Crinoids		Micritic Clasts		Trilobites	
Forams		Peloids			

Porosity

Interparticle		Intraparticle		Microporosity	
Moldic		Intramatrix			
Vuggy		Fracture			

Accessory Minerals

Pyrite	#	Vug Filling Calcite		Silica Nodule	
Saddle Dolomite		Vein Filling Calcite		Silica Replacing Grains	

Figure B.2: Core description key modeled after the Shell Sample Examination Manual.

Well : Emerald #1

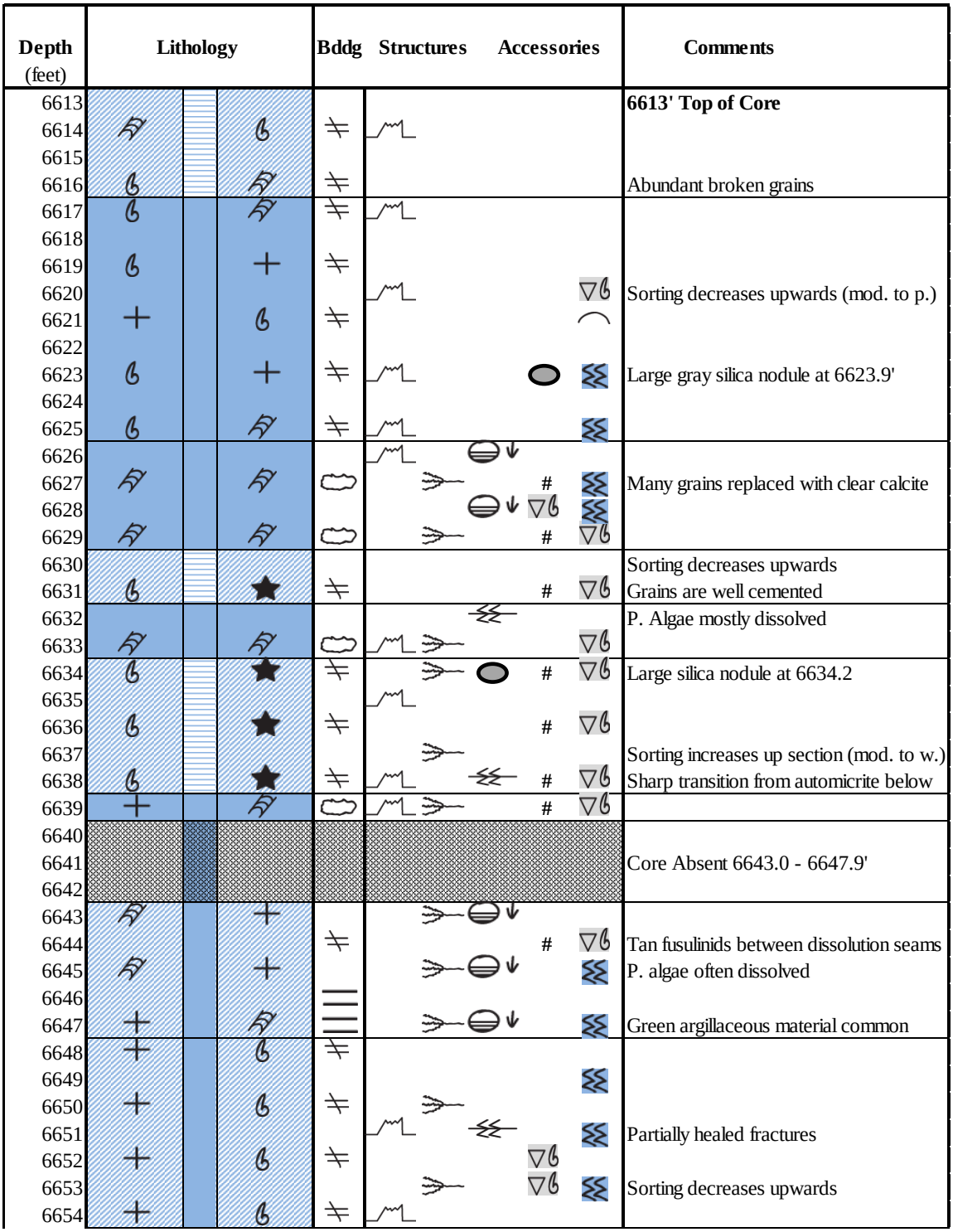

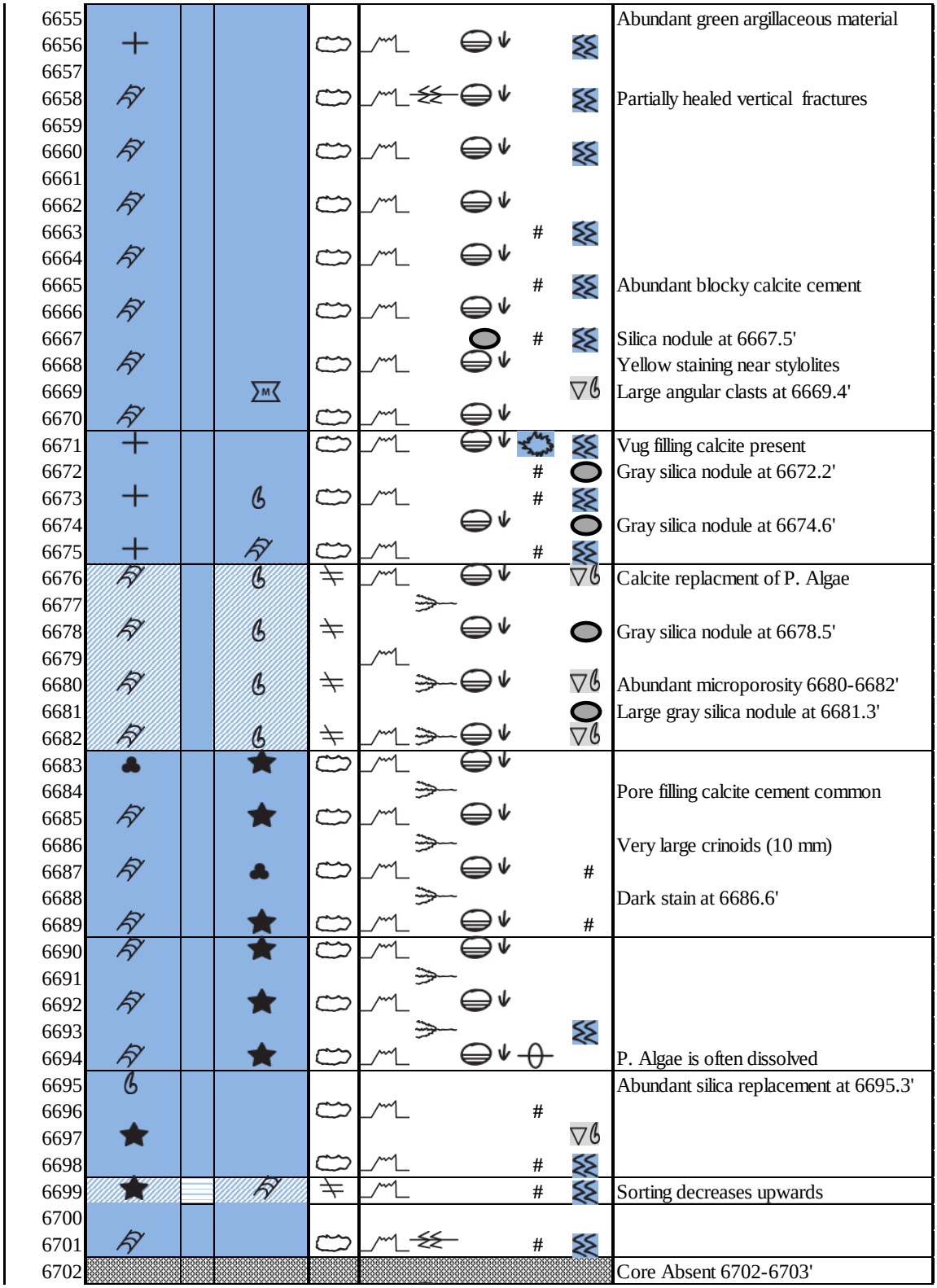
6655
6656
6657
6658
6659
6660
6661
6662
6663
6664
6665
6666
6667
6668
6669
6670
6671
6672
6673
6674
6675
6676
6677
6678
6679
6680
6681
6682
6683
6684
6685
6686
6687
6688
6689
6690
6691
6692
6693
6694
6695
6696
6697
6698
6699
6700
6701
6702
Abundant green argillaceous material
Partially healed vertical fractures
Abundant blocky calcite cement
Silica nodule at 6667.5'
Yellow staining near stylolites
Large angular clasts at 6669.4'
Vug filling calcite present
Gray silica nodule at 6672.2'
Gray silica nodule at 6674.6'
Calcite replacment of P. Algae
Gray silica nodule at 6678.5'
Abundant microporosity 6680-6682'
Large gray silica nodule at 6681.3'
Pore filling calcite cement common
Very large crinoids (10 mm)
Dark stain at 6686.6'
P. Algae is often dissolved
Abundant silica replacement at 6695.3'
Sorting decreases upwards
Core Absent 6702-6703'

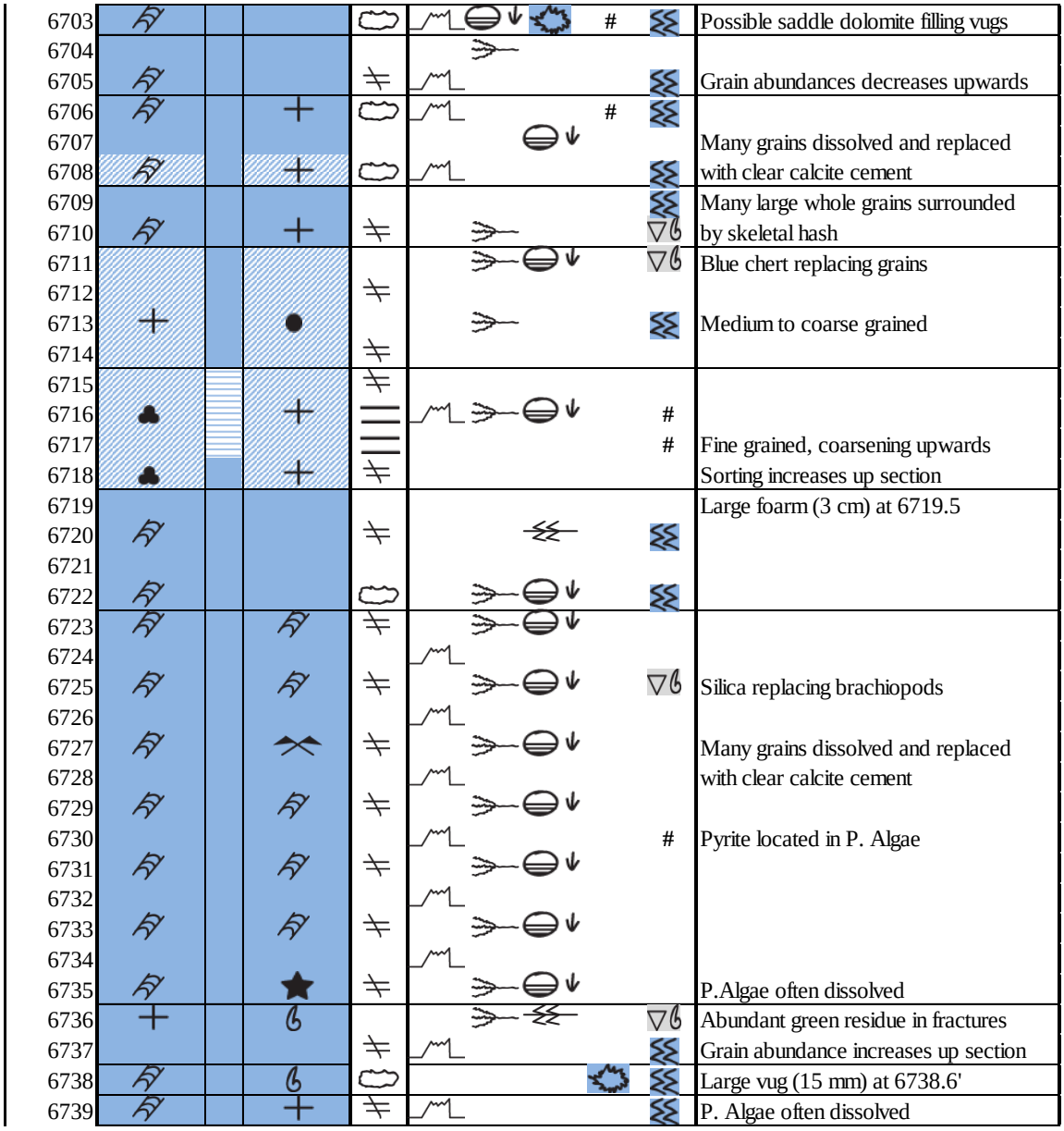
6703
6704
6705
6706
6707
6708
6709
6710
6711
6712
6713
6714
6715
6716
6717
6718
6719
6720
6721
6722
6723
6724
6725
6726
6727
6728
6729
6730
6731
6732
6733
6734
6735
6736
6737
6738
6739
Possible saddle dolomite filling vugs
Grain abundances decreases upwards
Many grains dissolved and replaced with clear calcite cement
Many large whole grains surrounded by skeletal hash
Blue chert replacing grains
Medium to coarse grained
Fine grained, coarsening upwards
Sorting increases up section
Large foarm (3 cm) at 6719.5
Silica replacing brachiopods
Many grains dissolved and replaced with clear calcite cement
Pyrite located in P. Algae
P.Algae often dissolved
Abundant green residue in fractures
Grain abundance increases up section
Large vug (15 mm) at 6738.6'
P. Algae often dissolved

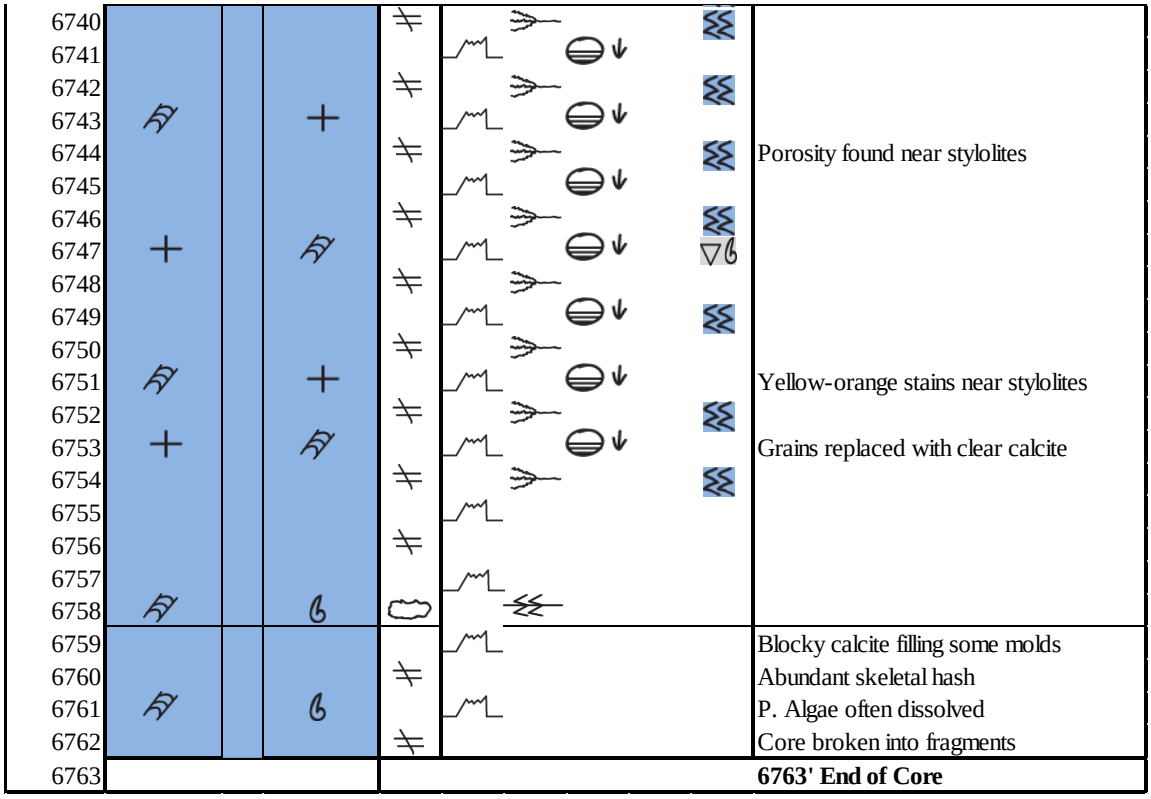
6740
6741
6742
6743
6744
6745
6746
6747
6748
6749
6750
6751
6752
6753
6754
6755
6756
6757
6758
6759
6760
6761
6762
6763
Porosity found near stylolites
Yellow-orange stains near stylolites
Grains replaced with clear calcite
Blocky calcite filling some molds
Abundant skeletal hash
P. Algae often dissolved
Core broken into fragments
6763' End of Core

Well : Jade #1

Depth (feet)	Lithology	Bddg	Structures	Accessories	Comments
6745				#	**6745' Top of Core**
6746					Unusual bright orange deposit present
6747					Abundant argillaceous material
6748					
6749					
6750					
6751					Fine grained, coarsens upwards
6752					
6753					
6754					
6755					Blue silica replacment common
6756					
6757					Abundant fractures
6758					
6759					Large crinoid fragments common
6760					
6761					Moderate to poor sorting
6762					P. algae often dissolved
6763					
6764					Very fine grained
6765	M				Large angular micritic clasts
6766					
6767					
6768					Moderately sorted
6769					Parellel layering of forams
6770					Abundant stylolites and dis. seams
6771					Poorly sorted
6772					
6773					
6774					
6775					
6776					Grains often replaced with clear calcite
6777					Packstone is poorly sorted
6778					
6779					
6780					
6781					Moderate sorting
6782					Micritic clasts present
6783					
6784					

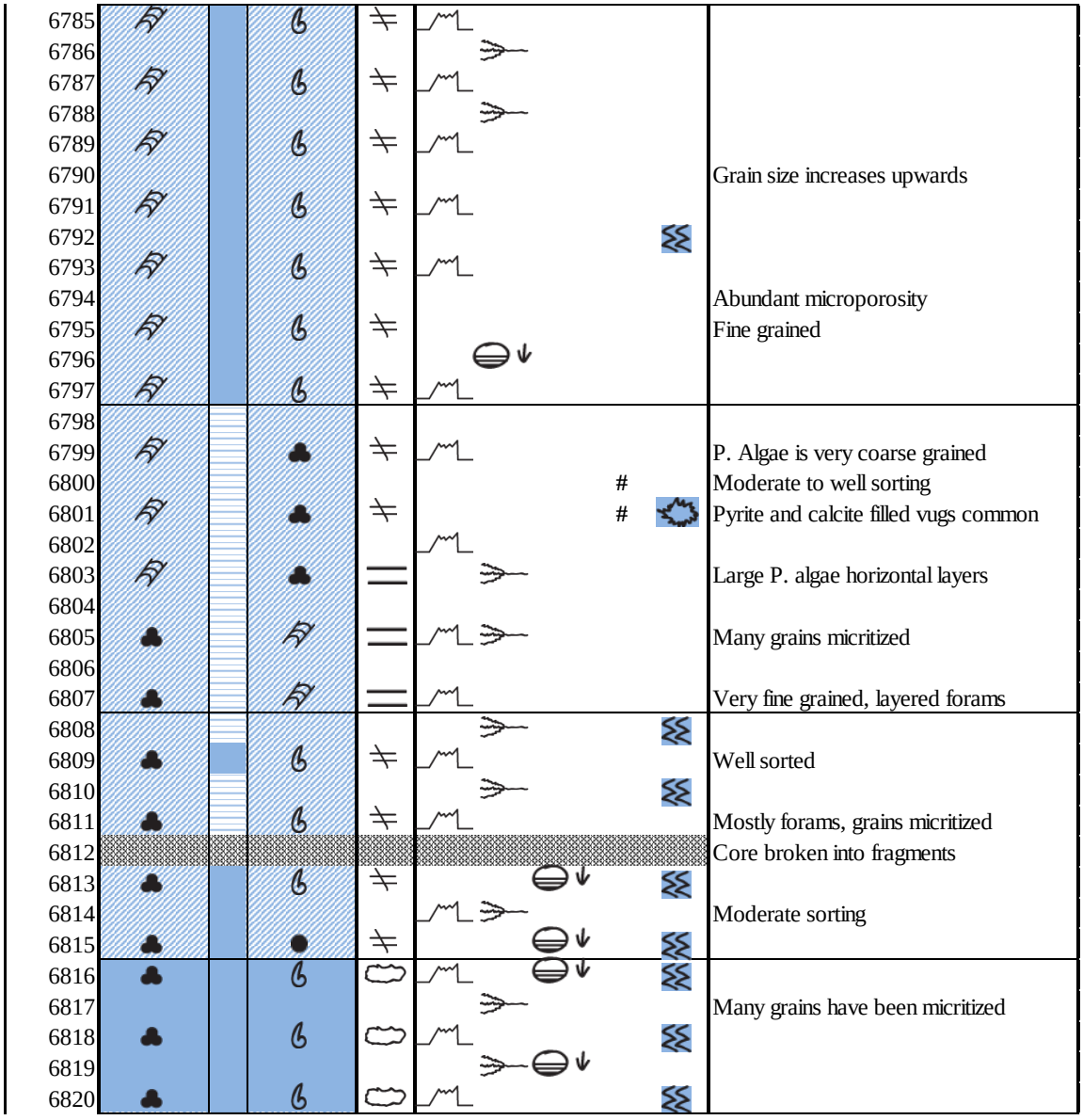
6785
6786
6787
6788
6789
6790
6791
6792
6793
6794
6795
6796
6797
6798
6799
6800
6801
6802
6803
6804
6805
6806
6807
6808
6809
6810
6811
6812
6813
6814
6815
6816
6817
6818
6819
6820
Grain size increases upwards
Abundant microporosity
Fine grained
P. Algae is very coarse grained
Moderate to well sorting
Pyrite and calcite filled vugs common
Large P. algae horizontal layers
Many grains micritized
Very fine grained, layered forams
Well sorted
Mostly forams, grains micritized
Core broken into fragments
Moderate sorting
Many grains have been micritized

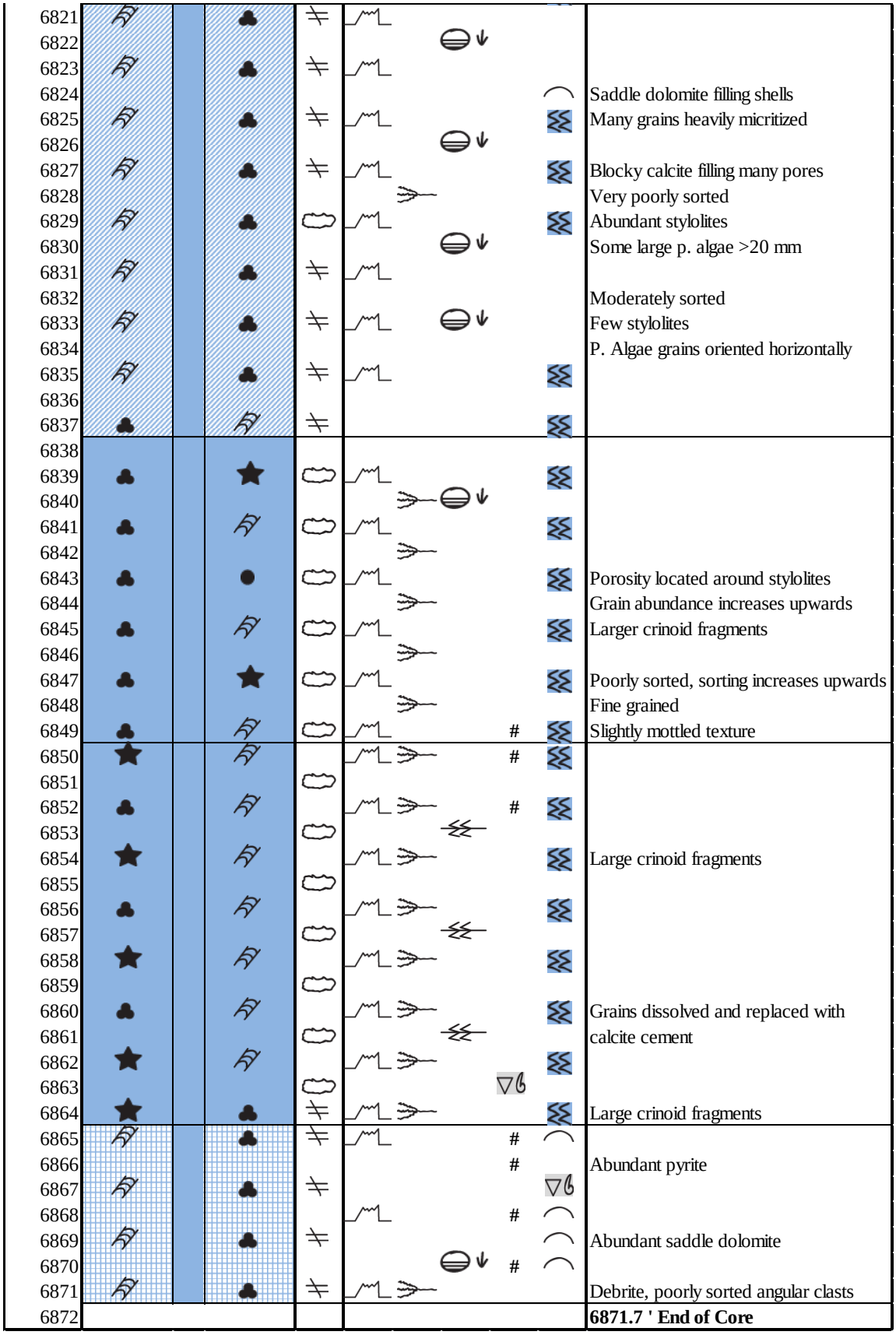
6821
6822
6823
6824
6825
6826
6827
6828
6829
6830
6831
6832
6833
6834
6835
6836
6837
6838
6839
6840
6841
6842
6843
6844
6845
6846
6847
6848
6849
6850
6851
6852
6853
6854
6855
6856
6857
6858
6859
6860
6861
6862
6863
6864
6865
6866
6867
6868
6869
6870
6871
6872
Saddle dolomite filling shells
Many grains heavily micritized
Blocky calcite filling many pores
Very poorly sorted
Abundant stylolites
Some large p. algae >20 mm
Moderately sorted
Few stylolites
P. Algae grains oriented horizontally
Porosity located around stylolites
Grain abundance increases upwards
Larger crinoid fragments
Poorly sorted, sorting increases upwards
Fine grained
Slightly mottled texture
Large crinoid fragments
Grains dissolved and replaced with calcite cement
Large crinoid fragments
Abundant pyrite
Abundant saddle dolomite
Debrite, poorly sorted angular clasts
6871.7 ' End of Core

Well : Topaz #1

Depth (feet)	Lithology	Bddg	Structures	Accessories	Comments
6706					**6706' Top of Core**
6707					Alternating layers of brown micrite and
6708					light calcite cement, fine grained
6709					
6710					Medium to coarse grained
6711					
6712					
6713					
6714					
6715					Grain abundance increases upwards
6716					
6717					Moderately sorted
6718					
6719					
6720					Porosity near stylolites
6721					Core absent 6721.2 - 6722.0'
6722					Moderately sorted
6723					
6724					P. algae often dissolved and replaced
6725					with calcite
6726					Core not recovered 6726.0 - 6750.0'
6727					
6728					
6729					
6730					
6731					
6732					
6733					
6734					
6735					
6736					
6737					
6738					
6739					
6740					
6741					
6742					
6743					
6744					
6745					
6746					
6747					
6748					
6749					Core not recovered 6726.0 - 6750.0'
6750					
6751					Moderately sorted
6752					Phylloid algae dissolved into molds

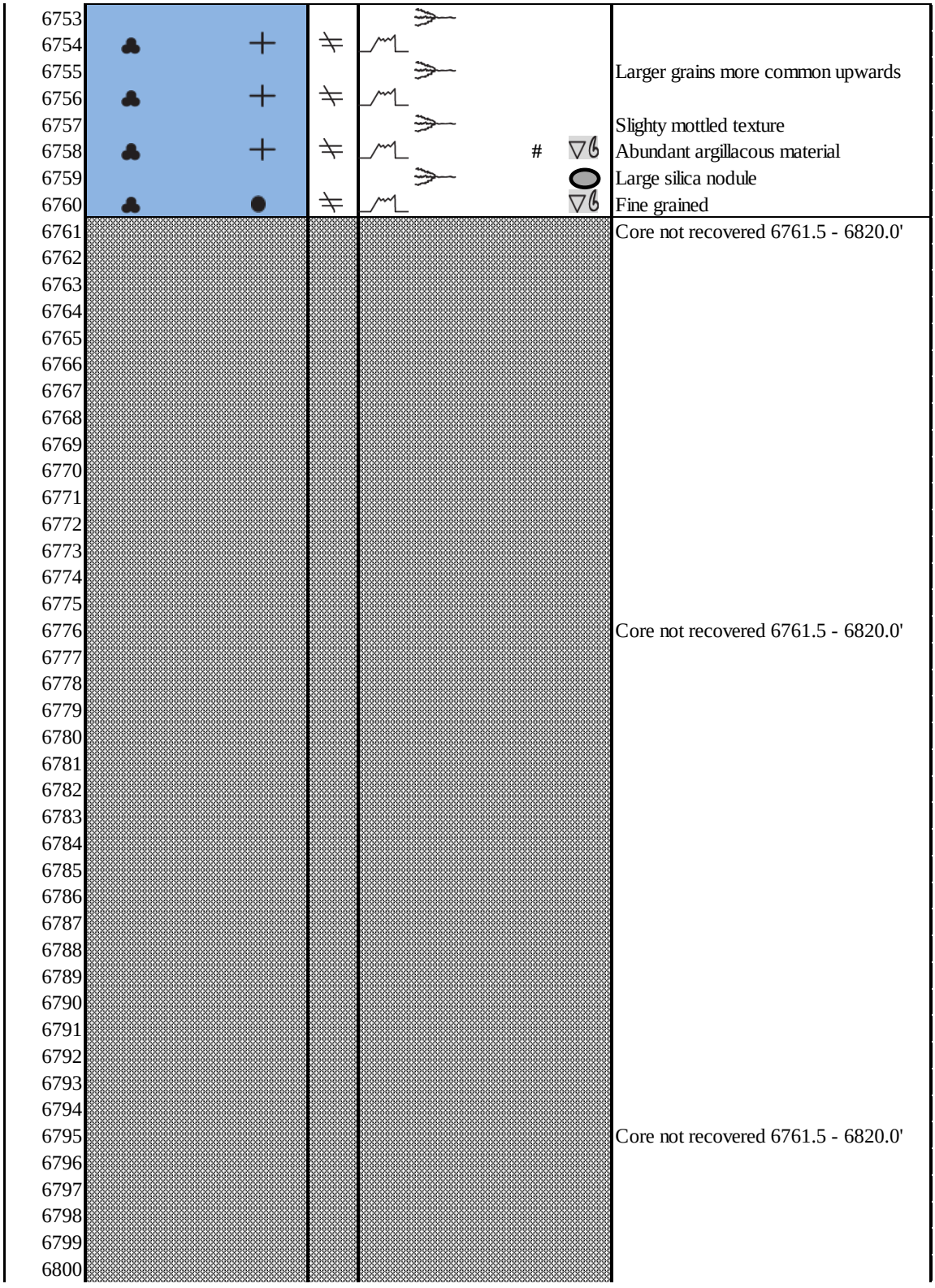
6753
6754
6755
6756
6757
6758
6759
6760
6761
6762
6763
6764
6765
6766
6767
6768
6769
6770
6771
6772
6773
6774
6775
6776
6777
6778
6779
6780
6781
6782
6783
6784
6785
6786
6787
6788
6789
6790
6791
6792
6793
6794
6795
6796
6797
6798
6799
6800
#
Larger grains more common upwards
Slighty mottled texture
Abundant argillacous material
Large silica nodule
Fine grained
Core not recovered 6761.5 - 6820.0'
Core not recovered 6761.5 - 6820.0'
Core not recovered 6761.5 - 6820.0'

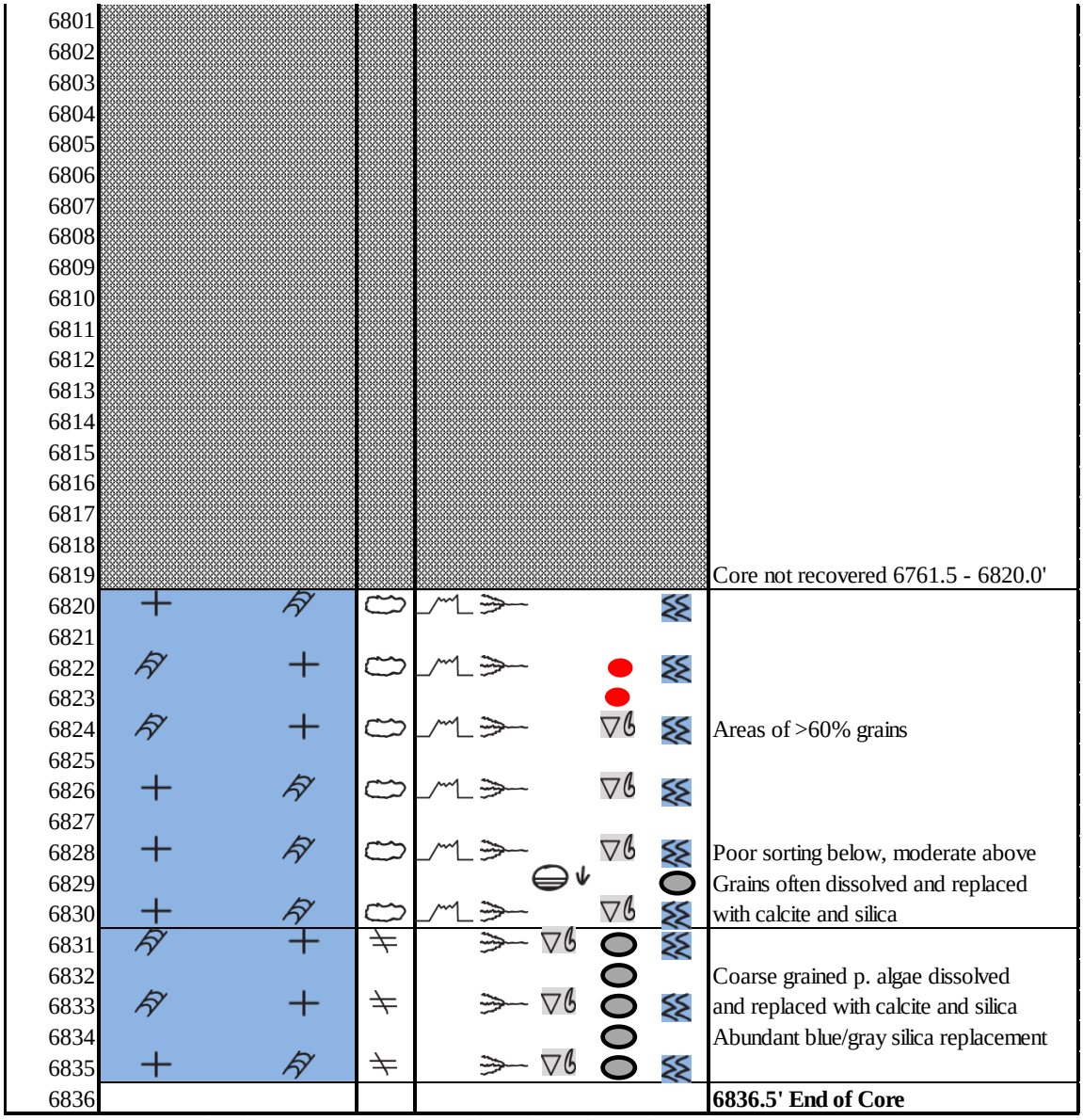
6801
6802
6803
6804
6805
6806
6807
6808
6809
6810
6811
6812
6813
6814
6815
6816
6817
6818
6819
Core not recovered 6761.5 - 6820.0'
6820
6821
6822
6823
6824
6825
6826
6827
6828
6829
6830
Areas of >60% grains
Poor sorting below, moderate above
Grains often dissolved and replaced
with calcite and silica
6831
6832
6833
6834
6835
Coarse grained p. algae dissolved
and replaced with calcite and silica
Abundant blue/gray silica replacement
6836
6836.5' End of Core

APPENDIX C

CORE PHOTOGRAPHS

Figure C.1: Grainstone/Packstone Facies in Emerald #1 well at 6717'. Note the parallel layering of grains. All core photographs are 3 inches across.

Figure C.2: Reef 1 Facies in Jade #1 well at 6764'. Note the heavily mottled texture.

Figure C.3: Reef 2 Facies in Jade #1 well at 6847'. Stylolites present as well as large crinoid fragments.

Figure C.4: Reef 3 Facies in Topaz #1 well at 6834'. Note the large amount of dark gray silica replacement.

Figure C.5: Debris Facies in Jade #1 well at 6868'.

Figure C.6: Large vugs in Reef 1 Facies, Topaz #1 at 6752'.

Figure C.7: White saddle dolomite in Debris facies, Jade #1 well, at 6870’.

APPENDIX D

THIN SECTION DESCRIPTION

Table D.1
Summary of Thin Section Analysis

Well	Thin Section Locations (ft)	Facies	Hybrid 1 Pore Type
Emerald	6614.3	GS/PS	Be
Emerald	6621.9	GS/PS	Ae
Emerald	6626.4	GS/PS	Br
Emerald	6631.8	GS/PS	Br
Emerald	6637.8	GS/PS	Be
Emerald	6645.9	GS/PS	Br
Emerald	6649.8	GS/PS	Ae
Emerald	6654.6	GS/PS	Br
Emerald	6656.6	R1	Be
Emerald	6668.6	R1	Be
Emerald	6675.5	R1	Ce
Emerald	6676.6	R1	Be
Emerald	6679.3	R1	Ae
Emerald	6684.4	R1	Be
Emerald	6694.7	R1	Be
Emerald	6699.4	R1	Br
Emerald	6700.5	R1	Be
Emerald	6703.6	R1	Be
Emerald	6712.2	GS/PS	Br
Emerald	6717.4	GS/PS	Ae
Emerald	6718.5	GS/PS	Br
Emerald	6726.8	R2	Br
Emerald	6736.8	R2	Ae
Emerald	6742.7	R2	Be
Emerald	6758.4	R2	Be
Jade	6747.6	R1	Ae
Jade	6767.5	R1	Ae
Jade	6769.3	R1	Ar
Jade	6771.9	R1	Be
Jade	6784.4	R1	Be

Table D.1 Continued,

Well	Thin Section Locations (ft)	Facies	Hybrid 1 Pore Type
Jade	6785.5	GS/PS	Be
Jade	6795.2	GS/PS	Be
Jade	6799.9	GS/PS	Br
Jade	6805.9	GS/PS	Be
Jade	6811.5	GS/PS	Br
Jade	6817.9	GS/PS	Ar
Jade	6822.8	GS/PS	Br
Jade	6823.8	GS/PS	Be
Jade	6829.9	GS/PS	Be
Jade	6843.6	R2	Br
Jade	6865.5	DEB	Be
Jade	6869.9	DEB	Be
Topaz	6707.1	GS/PS	Be
Topaz	6707.7	GS/PS	Be
Topaz	6712.9	GS/PS	Be
Topaz	6713.9	R1	Be
Topaz	6716.5	R1	Be
Topaz	6751.7	R1	Be
Topaz	6752.9	R1	Be
Topaz	6755.2	R1	Be
Topaz	6760.2	R1	Be
Topaz	6820.9	R3	Ar
Topaz	6828.8	R3	Ar
Topaz	6832.4	R3	Cr

THIN SECTION DESCRIPTION – EMERALD #1

Sample: Emerald 1 – 6614.3'

Depositional Characteristics

Rock Type: Limestone
Dunham/Riding Classification: Packstone
Grains Present:

- *Dominant:* Crinoids, Forams
- *Common:* Fusulinids, Brachiopods
- *Present:* Phylloid Algae (broken), Bivalves, Bryozoans, Echinoid Spines

Comments: Many grains fragmented

Sedimentary Structures: N/A
Bedding: N/A
Sorting: Moderate

Diagenetic Characteristics

Cementation: Present small blocky calcite and syntaxial overgrowth of crinoids
Recrystallization: Abundant micritization of grains, common neomorphism of micrite
Dissolution: Present dissolution of matrix and cement
Replacement: Present trace amounts of pyrite
Mechanical Compaction: N/A
Chemical Compaction: N/A
Other: N/A

Porosity

Visual Estimate: 5%

- *Dominant:* Partial molds – 85%
- *Common:* SE Interparticle – 10%
- *Present:* Intraparticle – 5%

Ahr Genetic Pore Type: **Hybrid 1B - Enhanced**

Sample: Emerald 1 – 6621.9’

Depositional Characteristics

Rock Type: Limestone
Dunham/Riding Classification: Automicrite
Grains Present:

- *Dominant:* Crinoids, Forams
- *Common:* Fusulinids
- *Present:* Brachiopods, Bivalves, Phylloid Algae (broken), Sponge Spicules

Comments: Phylloid algae and sponge spicules dissolved

Sedimentary Structures: N/A
Bedding: N/A
Sorting: Moderate

Diagenetic Characteristics

Cementation: Present pore filling small blocky calcite and grain replacing large blocky calcite
Recrystallization: Common micritization of grains and neomorphism of micrite
Dissolution: Present grain leaching
Replacement: Common saddle dolomite
Mechanical Compaction: N/A
Chemical Compaction: N/A
Other: N/A

Porosity

Visual Estimate: 10%

- *Dominant:* Moldic – 95%
- *Common:*
- *Present:* Intraparticle – 5%

Ahr Genetic Pore Type: **Hybrid 1A** (low end) **- Enhanced**

Sample: Emerald 1 – 6626.4’

Depositional Characteristics

Rock Type: Limestone
Dunham/Riding Classification: Automicrite
Grains Present:

- *Dominant:* Phylloid Algae, Crinoids, Forams
- *Common:* Brachiopods, Fusulinids, Sponge Spicules
- *Present:* Bryozoans, Gastropods, Trilobite Shell, Encrusting Algae

Comments: Many grains are completely dissolved and replaced with calcite, mainly phylloid algae, crinoids, and forams

Sedimentary Structures: N/A
Bedding: N/A
Sorting: Poor

Diagenetic Characteristics

Cementation: Abundant large blocky calcite replacing grains (mainly phylloid algae and crinoids), and small blocky calcite filling pores
Recrystallization: Common micritization of grains
Dissolution: Common grain leaching
Replacement: Present pore filling and grain replacing silica
Mechanical Compaction: Common brittle grain deformation and fractures
Chemical Compaction: Common stylolites
Other: Some dissolution near stylolites, grains near stylolites deformed. Nearly all grains micritized and replaced with blocky calcite.

Porosity

Visual Estimate: 1%

- *Dominant:*
- *Common:*
- *Present:* Fracture

Ahr Genetic Pore Type: **Hybrid 1B - Reduced**

Sample: Emerald 1 – 6631.8’

Depositional Characteristics

Rock Type: Limestone
Dunham/Riding Classification: Grainstone
Grains Present:

- *Dominant:* Crinoids, Phylloid Algae (broken)
- *Common:* Forams, Brachiopods, Gastropods
- *Present:* Skeletal Hash, Trilobite Spine

Comments:

Sedimentary Structures: N/A
Bedding: N/A
Sorting: Well

Diagenetic Characteristics

Cementation: Abundant pore filling and grain replacing small and large blocky calcite
Recrystallization: Common micritization of grains
Dissolution: Present grain leaching (later filled by calcite)
Replacement: Common silica replacing grains, usually crinoids. Present pyrite at bottom of slide
Mechanical Compaction: N/A
Chemical Compaction: N/A
Other: N/A

Porosity

Visual Estimate: 0%

- *Dominant:*
- *Common:*
- *Present:*

Ahr Genetic Pore Type: **Hybrid 1B - Reduced**

Sample: Emerald 1 – 6637.8’

Depositional Characteristics

Rock Type: Limestone
Dunham/Riding Classification: Packstone/Grainstone
Grains Present:

- *Dominant:* Forams, Crinoids
- *Common:* Fusulinids, Brachiopods
- *Present:* Peloids, Micritic Clasts, Phylloid Algae, Bryozoans

Comments: Top of slide grainstone, bottom of slide packstone. A stylolite separates the two areas.

Sedimentary Structures: N/A
Bedding: N/A
Sorting: Moderate

Diagenetic Characteristics

Cementation: Common small blocky calcite filling pores, present syntaxial overgrowth on crinoids
Recrystallization: Abundant micritization of grains
Dissolution: Present grain and matrix leaching
Replacement: Common pyrite near bottom of slide, present silica replacement of grains, mainly crinoids
Mechanical Compaction: N/A
Chemical Compaction: Present stylolites
Other: Large high amplitude stylolite present

Porosity

Visual Estimate: 5-10 %

- *Dominant:* SE Interparticle - 85%
- *Common:* Moldic – 10%
- *Present:* Intraparticle -5%

Ahr Genetic Pore Type: **Hybrid 1B** (high end) **- Enhanced**

Sample: Emerald 1 – 6645.9’

Depositional Characteristics

Rock Type: Limestone
Dunham/Riding Classification: Grainstone/Packstone
Grains Present:

- *Dominant:* Fusulinids, Forams
- *Common:* Phylloid Algae (broken)
- *Present:* Brachiopods, Sponge Spicules, Crinoids, Peloids

Comments: Forams heavily micritized, phylloid algae dissolved

Sedimentary Structures: N/A
Bedding: N/A
Sorting: Moderate

Diagenetic Characteristics

Cementation: Abundant pore filling and grain replacing small and large blocky calcite
Recrystallization: Abundant micritization of grains
Dissolution: Present grain and matrix leaching
Replacement: Present grain replacing silica
Mechanical Compaction: Present partially healed fractures
Chemical Compaction: N/A
Other: Cement partially filling molds and fractures

Porosity

Visual Estimate: 2-5%

- *Dominant:* Moldic – 85%
- *Common:* Vuggy – 10%
- *Present:* SE Interparticle – 3% , Fracture – 2%

Ahr Genetic Pore Type: **Hybrid 1B - Reduced**

Sample: Emerald 1 – 6649.8’

Depositional Characteristics

Rock Type: Limestone
Dunham/Riding Classification: Grainstone
Grains Present:

- *Dominant:*Forams, Fusulinids
- *Common:*Brachiopods
- *Present:* Sponge Spicules, Phylloid Algae (broken), Bivalves, Peloids

Comments: Forams heavily micritized

Sedimentary Structures: N/A
Bedding: N/A
Sorting: Moderate

Diagenetic Characteristics

Cementation: Small and large pore filling blocky calcite: Present top 80% of slide, abundant bottom 20% of slide
Recrystallization: Abundant micritization of grains, common neomorphism of micrite
Dissolution: N/A
Replacement: Present silica replacement of grains
Mechanical Compaction: N/A
Chemical Compaction: N/A
Other: N/A

Porosity

Visual Estimate: 1% near bottom of slide, 15-20% for the rest of the slide

- *Dominant:* SE Interparticle – 75%
- *Common:* SE Intraparticle – 25%
- *Present:*

Ahr Genetic Pore Type: **Hybrid 1A – Enhanced**
Comments: Irregular boundary near bottom of slide separates porous and non porous zones

Sample: Emerald 1 – 6654.6’

Depositional Characteristics

Rock Type: Limestone
Dunham/Riding Classification: Packstone
Grains Present:

- *Dominant:* Forams, Brachiopods
- *Common:* Crinoids, Phylloid Algae, Fusulinids
- *Present:* Bivalves, Sponge Spicules, Peloids

Comments: Similar to Emerald 1 – 6649.8’, Forams heavily micritized

Sedimentary Structures: N/A
Bedding: N/A
Sorting: Poor

Diagenetic Characteristics

Cementation: Abundant small and large blocky calcite filling all pores
Recrystallization: Abundant micritization
Dissolution: N/A
Replacement: N/A
Mechanical Compaction: N/A
Chemical Compaction: N/A
Other: N/A

Porosity

Visual Estimate: 0%

- *Dominant:*
- *Common:*
- *Present:*

Ahr Genetic Pore Type: **Hybrid 1B - Reduced**

Sample: Emerald 1 – 6656.6’

Depositional Characteristics

Rock Type: Limestone
*Dunham/Riding Classification:*Automicrite
Grains Present:

- *Dominant:*
- *Common:*
- *Present:* Brachiopods, Fusulinids, Forams, Phylloid Algae (broken), sponge spicules

Comments: Mostly micrite, around 10% grains, prismatic microstructure seen in brachiopods shells

*Sedimentary Structures:*N/A
*Bedding:*Mottled Texture
*Sorting:*Moderate

Diagenetic Characteristics

Cementation: Present small blocky calcite filling pores,
Recrystallization: Common micritization of grains and neomorphism of micrite
*Dissolution:*N/A
*Replacement:*N/A
*Mechanical Compaction:*N/A
*Chemical Compaction:*N/A
*Other:*N/A

Porosity

*Visual Estimate:*5%

- *Dominant:*Incomplete molds – 75%
- *Common:*SE Intraparticle – 10%
- *Present:*Vuggy – 5%

Ahr Genetic Pore Type: **Hybrid 1B** (high end) **- Enhanced**

Sample: Emerald 1 – 6668.6’

Depositional Characteristics

*Rock Type:*Limestone
*Dunham/Riding Classification:*Automicrite
Grains Present:

- *Dominant:*
- *Common:*
- *Present:*Brachiopods, Bivalves, Crinoids, Phylloid Algae (broken), Forams, Skeletal Hash

Comments: Fragmented grains, mostly micritic matrix

*Sedimentary Structures:*N/A
*Bedding:*N/A
*Sorting:*Poor

Diagenetic Characteristics

*Cementation:*Present small blocky calcite in pores
*Recrystallization:*Abundant neomorphism of micrite, present micritization of grains
*Dissolution:*N/A
*Replacement:*N/A
*Mechanical Compaction:*N/A
*Chemical Compaction:*N/A
*Other:*N/A

Porosity

*Visual Estimate:*10-15 %

- *Dominant:* Vuggy – 80%
- *Common:*Moldic – 20%
- *Present:*

Ahr Genetic Pore Type: **Hybrid 1B** (low end) **– Enhanced**
Comments: Solution enhanced molds often turning vuggy

Sample: Emerald 1 – 6675.5’

Depositional Characteristics

*Rock Type:*Limestone
*Dunham/Riding Classification:*Automicrite
Grains Present:

- *Dominant:* Forams, Bivalves
- *Common:*
- *Present:*Brachiopods, Sponge Spicules, Crinoids, Phylloid Algae, Bryozoans, Peloids

Comments: Mostly micritic matrix, phylloid algae and sponge spicules often dissolved or replaced, Forams heavily micritized

*Sedimentary Structures:*N/A
*Bedding:*N/A
*Sorting:*Moderate

Diagenetic Characteristics

*Cementation:*Present small amounts of pore filling small blocky calcite
Recrystallization: Abundant micritization of grains, common neomorphism of micrite
*Dissolution:*Common grain and matrix leaching
*Replacement:*Common pyrite replacement near stylolite at bottom of slide
*Mechanical Compaction:*N/A
*Chemical Compaction:*Present stylolites
*Other:*High amplitude stylolite present

Porosity

*Visual Estimate:*20%

- *Dominant:*SE Vuggy to Cavernous – 75%
- *Common:* Moldic – 23%
- *Present:*Interparticle – 2%

Ahr Genetic Pore Type: **Hybrid 1C** (high end) **- Enhanced**

Sample: Emerald 1 – 6676.6’

Depositional Characteristics

*Rock Type:*Limestone
*Dunham/Riding Classification:*Automicrite
Grains Present:

- *Dominant:*Crinoids, Brachiopods
- *Common:*Fusulinids, Forams
- *Present:* Coral, Bryozoans, Sponge Spicules

Comments: Mostly fined grained, except large fusulinids and coral. Sponge spicules dissolved

*Sedimentary Structures:*N/A
*Bedding:*N/A
*Sorting:*Moderate

Diagenetic Characteristics

*Cementation:*Common pore filling small and large blocky calcite
*Recrystallization:*Abundant neomorphism of micrite, common micritization of grains
*Dissolution:*Present grain, matrix, and cement leaching
*Replacement:*N/A
Mechanical Compaction: Brittle grain deformation (broken shells)
*Chemical Compaction:*Present stylolites
*Other:*N/A

Porosity

*Visual Estimate:*5%

- *Dominant:*Moldic – 85%
- *Common:* SE Intercrystalline – 10%
- *Present:*Intraparticle – 5%

Ahr Genetic Pore Type: **Hybrid 1B - Enhanced**

Sample: Emerald 1 – 6679. 3’

Depositional Characteristics

*Rock Type:*Limestone
*Dunham/Riding Classification:*Packstone
Grains Present:

- *Dominant:*Brachiopods
- *Common:*Corals, Crinoids
- *Present:*Forams, Sponge Spicules, Phylloid Algae

Comments: Roughly half micritic matrix and half grains. Shell structure in many grains perserved

*Sedimentary Structures:*N/A
*Bedding:*N/A
*Sorting:*Well

Diagenetic Characteristics

*Cementation:*Present small amounts of pore filling small blocky calcite
*Recrystallization:*Present micritization of grains
*Dissolution:*Present grain and cement leaching
*Replacement:*N/A
*Mechanical Compaction:*N/A
*Chemical Compaction:*N/A
*Other:*N/A

Porosity

*Visual Estimate:*5 %

- *Dominant:*SE Interparticle – 80%
- *Common:*Moldic – 10%, SE Intraparticle – 10%
- *Present:*

Ahr Genetic Pore Type: **Hybrid 1A - Enhanced**

Sample: Emerald 1 – 6684.4’

Depositional Characteristics

*Rock Type:*Limestone
*Dunham/Riding Classification:*Automicrite
Grains Present:

- *Dominant:*Forams, Crinoids
- *Common:*Brachiopods
- *Present:*Phylloid Algae, Sponge Spicules

Comments: Mostly neomorphosed micrite, phylloid algae and sponge spicules dissolved

*Sedimentary Structures:*N/A
*Bedding:*N/A
*Sorting:*Well

Diagenetic Characteristics

*Cementation:*Present very small amounts of pore filling small blocky calcite
*Recrystallization:*Abundant neomorphism of micrite
*Dissolution:*Abundant grain and matrix leaching
*Replacement:*N/A
*Mechanical Compaction:*N/A
*Chemical Compaction:*N/A
Other: Most grains are dissolved

Porosity

*Visual Estimate:*15-20 %

- *Dominant:* Vuggy –75%
- *Common:*Moldic – 25%
- *Present:*

Ahr Genetic Pore Type: **Hybrid 1B** (low end) **- Enhanced**

Sample: Emerald 1 – 6694.7’

Depositional Characteristics

*Rock Type:*Limestone
*Dunham/Riding Classification:*Automicrite
Grains Present:

- *Dominant:*
- *Common:*
- *Present:*Crinoids, Forams, Phylloid Algae (broken), Sponge Spicules

Comments: Very fine grained, mostly micritic matrix with very few grains, phylloid algae and sponge spicules often dissolved

*Sedimentary Structures:*N/A
*Bedding:*N/A
*Sorting:*Moderate

Diagenetic Characteristics

*Cementation:*Common small and large blocky calcite filling or partially filling dissolved grains and fractures
Recrystallization: Abundant neomorphism of micrite, common micritization of grains
*Dissolution:*Present cement leaching
*Replacement:*N/A
Mechanical Compaction: Common partially healed vertical fractures
*Chemical Compaction:*N/A
*Other:*N/A

Porosity

*Visual Estimate:*5 %

- *Dominant:*Moldic – 75%
- *Common:*Vuggy – 24%
- *Present:*Fracture – 1%

Ahr Genetic Pore Type: **Hybrid 1B – Enhanced**

Sample: Emerald 1 – 6699.4’

Depositional Characteristics

*Rock Type:*Limestone
*Dunham/Riding Classification:*Grainstone
Grains Present:

- *Dominant:* Phylloid Algae (broken), Forams
- *Common:*Fusulinids, Brachiopods, Crinoids
- *Present:* Peloids

Comments:Forams heavily micritized

*Sedimentary Structures:*N/A
*Bedding:*N/A
*Sorting:*Well

Diagenetic Characteristics

*Cementation:*Abundant small blocky calcite filling dissolved grains and large blocky calcite filling pores, present syntaxial overgrowth cement on crinoids
Recrystallization: Abundant micritization of grains, present neomorphism of micrite
*Dissolution:*Present grain and cement leaching
*Replacement:*N/A
*Mechanical Compaction:*Common brittle grain deformation
*Chemical Compaction:*N/A
*Other:*N/A

Porosity

*Visual Estimate:*5 %

- *Dominant:*SE Interparticle – 85%
- *Common:*Intercrystalline – 10%
- *Present:*SE Intramatrix, and Moldic – 5%

Ahr Genetic Pore Type: **Hybrid 1B – Reduced**
Comments: More porosity at top of slide than at bottom

Sample: Emerald 1 – 6700.5’

Depositional Characteristics

*Rock Type:*Limestone
*Dunham/Riding Classification:*Automicrite
Grains Present:

- *Dominant:*Forams , Brachiopods
- *Common:*Phylloid Algae, Sponge Spicules
- *Present:*Trilobite Fragments, Bryozoans, Crinoids, Peloids

Comments: Mostly fine grained material aside from large brachiopods, phylloid algae and sponge spicules often dissolved, Forams heavily micritized, prismatic microstructure seen in brachiopods.

*Sedimentary Structures:*N/A
*Bedding:*N/A
*Sorting:*Well, aside from large brachiopods

Diagenetic Characteristics

*Cementation:*Common small blocky calcite filling dissolved grains, present large blocky calcite filling pores
*Recrystallization:*Abundant micritization of grains, common neomorphism of micrite
*Dissolution:*Present grain leaching
*Replacement:*N/A
*Mechanical Compaction:*N/A
Chemical Compaction: Present stylolites
*Other:*Some porosity associated with stylolites

Porosity

*Visual Estimate:*3-5 %

- *Dominant:*Moldic – 95%
- *Common:*
- *Present:*Fracture – 5%

*Ahr Genetic Pore Type:***Hybrid 1B - Enhanced**

Sample: Emerald 1 – 6703.6’

Depositional Characteristics

Rock Type: Limestone
*Dunham/Riding Classification:*Automicrite
Grains Present:

- *Dominant:*Phylloid Algae, Forams, Brachiopods
- *Common:*Fusulinids, Crinoids, Bivalves, Sponge Spicules, Peloids
- *Present:*

Comments: Phylloid algae and sponge spicules often dissolved, Forams heavily micritized

*Sedimentary Structures:*N/A
*Bedding:*N/A
*Sorting:*Poor

Diagenetic Characteristics

*Cementation:*Common small and large blocky calcite filling pores and replacing grains
*Recrystallization:*Common neomorphism of micrite, present selective micritization of grians
*Dissolution:*Common grain, matrix, and cement leaching
*Replacement:*Common pyrite replacing matrix, common saddle dolomite in large pores
*Mechanical Compaction:*N/A
*Chemical Compaction:*N/A
*Other:*N/A

Porosity

*Visual Estimate:*10 %

- *Dominant:*Vuggy – 75%
- *Common:* Moldic – 25%
- *Present:*

Ahr Genetic Pore Type: **Hybrid 1B** (low end) **- Enhanced**

Sample: Emerald 1 – 6712.2’

Depositional Characteristics

*Rock Type:*Limestone
*Dunham/Riding Classification:*Grainstone
Grains Present:

- *Dominant:*Phylloid Algae, Forams
- *Common:*Fusulinids, Crinoids, Sponge Spicules, Bivalves
- *Present:* Peloids

Comments:Forams heavily micritized

*Sedimentary Structures:*N/A
*Bedding:*N/A
Sorting: Moderate

Diagenetic Characteristics

*Cementation:*Abundant small and large blocky calcite filling dissolved grains and pores, present drusy cement in some larger pores.
Recrystallization: Abundant micritization of grains
*Dissolution:*N/A
*Replacement:*N/A
*Mechanical Compaction:*N/A
*Chemical Compaction:*N/A
*Other:*N/A

Porosity

*Visual Estimate:*0 %

- *Dominant:*
- *Common:*
- *Present:*

Ahr Genetic Pore Type: **Hybrid 1B - Reduced**

Sample: Emerald 1 – 6717.4’

Depositional Characteristics

*Rock Type:*Limestone
*Dunham/Riding Classification:*Grainstone
Grains Present:

- *Dominant:*Forams
- *Common:*Bivalves, Fusulinids, Sponge Spicules, Brachiopods, Phylloid Algae (broken), Peloids
- *Present:*

Comments: Fine grained, Forams heavily micritized, phylloid algae and sponge spicules often dissolved

*Sedimentary Structures:*N/A
*Bedding:*Irregular bedding, a few layers of larger phylloid algae and fusulinids exist
*Sorting:*Well

Diagenetic Characteristics

*Cementation:*Common pore filling small blocky calcite, present large blocky calcite
*Recrystallization:*Abundant micritization of grains, present neomorphism of micrite
*Dissolution:*N/A
*Replacement:*Present saddle dolomite in larger pores
*Mechanical Compaction:*N/A
*Chemical Compaction:*N/A
*Other:*N/A

Porosity

*Visual Estimate:*5 %

- *Dominant:*SE Interparticle – 80%
- *Common:*Moldic – 15%
- *Present:*Intraparticle – 5%

Ahr Genetic Pore Type: **Hybrid 1A** (low end) **– Enhanced**
Comments: Porosity mainly located in top half of the slide

Sample: Emerald 1 – 6718.5’

Depositional Characteristics

*Rock Type:*Limestone
*Dunham/Riding Classification:*Grainstone/Packstone
Grains Present:

- *Dominant:*Forams
- *Common:*Crinoids, Fusulinids, Phylloid Algae (broken), Sponge Spicules
- *Present:* Peloids

Comments: Fine grained, over 75% of thin section is forams, forams heavily micritized

*Sedimentary Structures:*N/A
*Bedding:*N/A
*Sorting:*Well

Diagenetic Characteristics

*Cementation:*Abundant small blocky calcite filling pores, present large blocky calcite filling dissolved grains
Recrystallization: Abundant micritization of grains and neomorphism of micrite
*Dissolution:*N/A
*Replacement:*N/A
*Mechanical Compaction:*N/A
*Chemical Compaction:*N/A
*Other:*N/A

Porosity

*Visual Estimate:*1-2 %

- *Dominant:*Intraparticle – 75%
- *Common:*Interparticle – 25%
- *Present:*

Ahr Genetic Pore Type: **Hybrid 1B - Reduced**

Sample: Emerald 1 – 6726.8’

Depositional Characteristics

*Rock Type:*Limestone
*Dunham/Riding Classification:*Automicrite
Grains Present:

- *Dominant:*Phylloid Algae
- *Common:*Crinoids, Brachiopods, Bivalves, Forams
- *Present:*Sponge Spicules, Peloids

Comments: Nearly all grains dissolved and replaced with blocky calcite, Forams heavily micritized

*Sedimentary Structures:*N/A
*Bedding:*N/A
*Sorting:*Poor

Diagenetic Characteristics

*Cementation:*Abundant small and large blocky calcite filling all grains and pores
*Recrystallization:*Common neomorphism of micrite, present selective micritization of grains
*Dissolution:*N/A
*Replacement:*N/A
*Mechanical Compaction:*Present brittle grain deformation and fractures
*Chemical Compaction:*Present stylolites
*Other:*N/A

Porosity

Visual Estimate:< 1%

- *Dominant:*
- *Common:*
- *Present:*Fracture

Ahr Genetic Pore Type: **Hybrid 1B - Reduced**

Sample: Emerald 1 – 6736.8’

Depositional Characteristics

*Rock Type:*Limestone
*Dunham/Riding Classification:*Automicrite
Grains Present:

- *Dominant:*Phylloid Algae, Fusulinids, Crinoids
- *Common:*Forams, Bivalves, Brachiopods, Sponge Spicules
- *Present:* Peloids

Comments: Many grains have been altered, some forams have been heavily micritized

*Sedimentary Structures:*N/A
*Bedding:*N/A
*Sorting:*Poor

Diagenetic Characteristics

*Cementation:*Common small and large blocky calcite partially filling pores
*Recrystallization:*Abundant micritization of grains, common neomorphism of micrite
*Dissolution:*Present grain and matrix leaching
*Replacement:*Present pore filling saddle dolomite and grain replacing silica and pyrite
*Mechanical Compaction:*N/A
*Chemical Compaction:*Common stylolites, present sutured contacts
*Other:*Some porosity near stylolites

Porosity

*Visual Estimate:*15 %

- *Dominant:*Moldic – 70%
- *Common:*Vuggy – 20%
- *Present:*SE Interparticle – 10%

Ahr Genetic Pore Type: **Hybrid 1A** (low end) **- Enhanced**

Sample: Emerald 1 – 6742.7’

Depositional Characteristics

*Rock Type:*Limestone
*Dunham/Riding Classification:*Automicrite
Grains Present:

- *Dominant:*Phylloid Algae
- *Common:*Forams, Fusulinids, Brachiopods, Crinoids
- *Present:*Bivalves, Sponge Spicules, Peloids

Comments: Many forams have been heavily micritized

*Sedimentary Structures:*N/A
*Bedding:*N/A
*Sorting:*Moderate to Poor

Diagenetic Characteristics

*Cementation:*Present pore filling small blocky calcite that is mostly dissolved
*Recrystallization:*Abundant micritization of grains and neomorphism of micrite
*Dissolution:*Abundant grain, matrix, and cement leaching
*Replacement:*N/A
*Mechanical Compaction:*N/A
*Chemical Compaction:*N/A
*Other:*N/A

Porosity

*Visual Estimate:*25 %

- *Dominant:*Vuggy – 75%
- *Common:*Moldic – 20%
- *Present:* SE Interparticle and SE Intraparticle – 5%

Ahr Genetic Pore Type: **Hybrid 1B – Enhanced**
Comments: Patches of high porosity present throughout slide

Sample: Emerald 1 – 6758.4’

Depositional Characteristics

*Rock Type:*Limestone
*Dunham/Riding Classification:*Automicrite
Grains Present:

- *Dominant:*Forams, Phylloid Algae
- *Common:*Brachiopods, Crinoids, Fusulinids, Bivalves, Sponge Spicules
- *Present:* Peloids

Comments:Forams heavily micritized

*Sedimentary Structures:*N/A
*Bedding:*N/A
*Sorting:*Poor

Diagenetic Characteristics

*Cementation:*Present small and large blocky calcite partially filling pores and dissolved grains
*Recrystallization:*Common micritization of grains and neomorphism of micrite
*Dissolution:*Common grain and matrix leaching, present cement leaching
*Replacement:*Common saddle dolomite in pores
*Mechanical Compaction:*Present fractures
*Chemical Compaction:*N/A
*Other:*N/A

Porosity

*Visual Estimate:*15 %

- *Dominant:*Moldic – 49%, Vuggy 49%
- *Common:*
- *Present:*SE Interparticle – 2%

Ahr Genetic Pore Type: **Hybrid 1B - Enhanced**

THIN SECTION DESCRIPTION – JADE #1

Sample: Jade 1 – 6747.6’

Depositional Characteristics

*Rock Type:*Limestone
*Dunham/Riding Classification:*Automicrite
Grains Present:

- *Dominant:*Brachiopods, Peloids, Fusulinids
- *Common:*Phylloid Algae (broken), Crinoids, Sponge Spicules, Forams
- *Present:*Bryozoans

Comments: Many grains are fragmented

Sedimentary Structures: N/A
Bedding: N/A
*Sorting:*Poor

Diagenetic Characteristics

*Cementation:*Present small amounts of pore filling and grain replacing small and large blocky calcite
*Recrystallization:*Abundant micritization of grains, common neomorphism of micrite
*Dissolution:*N/A
*Replacement:*Present saddle dolomite and silica replacing grains and filling pores
Mechanical Compaction: Present small fractures
*Chemical Compaction:*Present small stylolites
Other: N/A

Porosity

*Visual Estimate:*5%

- *Dominant:*Moldic – 60%
- *Common:*SE Interparticle – 40%
- *Present:*

Ahr Genetic Pore Type: **Hybrid 1A** (low end) **- Enhanced**

Sample: Jade 1 – 6767.5’

Depositional Characteristics

*Rock Type:*Limestone
*Dunham/Riding Classification:*Grainstone at top and bottom of slide, Automicrite in middle
Grains Present:

- *Dominant:*Peloids
- *Common:*Brachiopods
- *Present:*Fusulinids, Forams, Sponge Spicules, Crinoids, Phylloid Algae

Comments: Well sorted peloidal layers at top and bottom of slide, moderate to poor sorted fossils and matrix in middle

*Sedimentary Structures:*N/A
*Bedding:*Parallel at top and bottom of slide
*Sorting:*Well sorted top and bottom of slide, moderate to poor sorted in middle

Diagenetic Characteristics

*Cementation:*Common pore filling small and large blocky calcite in well sorted peloidal layer
*Recrystallization:*Abundant micritization of grains, common neomorphism of micrite
*Dissolution:*Abundant grain and matrix leaching
*Replacement:*Present saddle dolomite replacing pore filling calcite
Mechanical Compaction: N/A
*Chemical Compaction:*Present low amplitude stylolites filled with insoluble carbonate residue
Other: N/A

Porosity

*Visual Estimate:*15-20 %

- *Dominant:*SE Interparticle – 80%
- *Common:*Moldic -10%
- *Present:*Vuggy and Intraparticle – 5%

Ahr Genetic Pore Type: **Hybrid 1A** (low end) **- Enhanced**

Sample: Jade 1 – 6769.3’

Depositional Characteristics

*Rock Type:*Limestone
*Dunham/Riding Classification:*Grainstone
Grains Present:

- *Dominant:*Peloids
- *Common:*Phylloid Algae, Brachiopods, Forams
- *Present:*Fusulinids, Sponge Spicules, Encrusting Algae

Comments:Fine grained peloids make up over 75% of the thin section, Forams heavily micritized, sponge spicules and phylloid algae are often dissolved

Sedimentary Structures: N/A
Bedding: N/A
*Sorting:*Moderate

Diagenetic Characteristics

*Cementation:*Abundant small blocky calcite filling pores and large blocky calcite replacing grains
*Recrystallization:*Abundant micritized grains, common neomorphism of micrite
Dissolution: N/A
*Replacement:*N/A
Mechanical Compaction: N/A
Chemical Compaction: N/A
Other: N/A

Porosity

*Visual Estimate:*1 %

- *Dominant:* SE Interparticle – 75%
- *Common:*SE Intraparticle – 25%
- *Present:*

Ahr Genetic Pore Type: **Hybrid 1A - Reduced**

Sample: Jade 1 – 6671.9’

Depositional Characteristics

*Rock Type:*Limestone
*Dunham/Riding Classification:*Automicrite
Grains Present:

- *Dominant:*Phylloid Algae (broken)
- *Common:*Crinoids, Sponge Spicules, Forams, Brachiopods
- *Present:*Fusulinids, Peloids

Comments: Many grains fragmented, Forams heavily micritized, phylloid algae and sponge spicules often dissolved

*Sedimentary Structures:*N/A
Bedding: N/A
*Sorting:*Poor

Diagenetic Characteristics

*Cementation:*Present small and large blocky calcite partially filled pores
*Recrystallization:*Abundant micritization of grains and neomorphism of micrite
*Dissolution:*Abundant grain and matrix leaching
*Replacement:*Present pore filling saddle dolomite and grain replacing silica
*Mechanical Compaction:*Common brittle deformation of grains
Chemical Compaction: N/A
Other: N/A

Porosity

*Visual Estimate:*10-15 %

- *Dominant:*Moldic – 75%
- *Common:*Vuggy – 25%
- *Present:*

*Ahr Genetic Pore Type:***Hybrid 1B** (high end) - **Enhanced**

Sample: Jade 1 – 6784.4’

Depositional Characteristics

*Rock Type:*Limestone
*Dunham/Riding Classification:*Automicrite
Grains Present:

- *Dominant:*
- *Common:*Brachiopods, Crinoids, Phylloid Algae (broken), Bivalves, Forams
- *Present:*Fusulinids, Sponge Spicules, Gastropods

Comments: Many grains deformed or broken, phylloid algae and sponge spicules often dissolved

Sedimentary Structures: N/A
Bedding: N/A
*Sorting:*Moderate

Diagenetic Characteristics

*Cementation:*Present small blocky calcite in a few pores
*Recrystallization:*Abundant micritization of grains and neomorphism of micrite
*Dissolution:*Common grain, matrix, and cement leaching
*Replacement:*Common pore filling saddle dolomite
*Mechanical Compaction:*Common brittle grain deformation
*Chemical Compaction:*Common stylolites
Other: N/A

Porosity

*Visual Estimate:*5-10 %

- *Dominant:*Moldic – 40% , Vuggy 40%
- *Common:*SE Interparticle – 20%
- *Present:*

Ahr Genetic Pore Type: **Hybrid 1B - Enhanced**

Sample: Jade 1 – 6785.5’

Depositional Characteristics

*Rock Type:*Limestone
*Dunham/Riding Classification:*Packstone
Grains Present:

- *Dominant:*Forams, Phylloid Algae (broken)
- *Common:*Brachiopods, Bivalves, Sponge Spicules, Crinoids
- *Present:* Peloids

Comments: Many grains dissolved leaving only a rim of neomorphosed micrite, Forams heavily micritized

Sedimentary Structures: N/A
Bedding: N/A
*Sorting:*Well

Diagenetic Characteristics

*Cementation:*Present small and large blocky calcite filling some pores and replacing some grains
*Recrystallization:*Abundant micritization of grains and neomorphism of micrite
*Dissolution:*Common grain and matrix leaching
*Replacement:*Present saddle dolomite filling some pores
Mechanical Compaction: N/A
Chemical Compaction: N/A
Other: N/A

Porosity

*Visual Estimate:*10-15%

- *Dominant:*Moldic – 85%
- *Common:*SE Interparticle – 10%
- *Present:*Intraparticle – 5%

Ahr Genetic Pore Type: **Hybrid 1B** (high end) **- Enhanced**

Sample: Jade 1 – 6795.2’

Depositional Characteristics

*Rock Type:*Limestone
*Dunham/Riding Classification:*Packstone/Grainstone
Grains Present:

- *Dominant:*Forams
- *Common:*Phylloid Algae (broken), Brachiopods, Crinoids, Fusulinids, Bivalves
- *Present:*Sponge Spicules, Peloids

Comments:Forams heavily micritized, phylloid algae and sponge spicules often dissolved

Sedimentary Structures: N/A
Bedding: N/A
*Sorting:*Well sorted at bottom of slide, moderately sorted at top

Diagenetic Characteristics

*Cementation:*Present pore filling small and large blocky calcite, mainly at the bottom of the slide
*Recrystallization:*Abundant micritization of grains and neomorphism of micrite
*Dissolution:*Present matrix and cement leaching
Replacement: Present pore filling saddle dolomite and grain replacing silica
Mechanical Compaction: N/A
Chemical Compaction: N/A
Other: N/A

Porosity

*Visual Estimate:*5-10 %

- *Dominant:*SE Interparticle – 80%
- *Common:*Moldic – 15%
- *Present:*Vuggy – 5%

Ahr Genetic Pore Type: **Hybrid 1B** (high end) **- Enhanced**

Sample: Jade 1- 6799.9’

Depositional Characteristics

*Rock Type:*Limestone
*Dunham/Riding Classification:*Grainstone
Grains Present:

- *Dominant:*Phylloid Algae
- *Common:*
- *Present:* Forams

Comments:Coarse grained phylloid algae dominated 90% of the slide, possible oil stains present

Sedimentary Structures: N/A
Bedding: N/A
*Sorting:*Well

Diagenetic Characteristics

*Cementation:*Abundant pore filling and grain replacing small and large blocky calcite, common drusy cement filing larger pores
*Recrystallization:*Common micritization of grains
Dissolution: Common cement leaching
*Replacement:*Present saddle dolomite replacing some large calcite crystals
Mechanical Compaction: N/A
Chemical Compaction: N/A
Other: N/A

Porosity

*Visual Estimate:*10 %

- *Dominant:*Intercrystalline – 80%
- *Common:*Moldic – 20%
- *Present:*

Ahr Genetic Pore Type: **Hybrid 1B** (low end) **- Reduced**

Sample: Jade 1 – 6805.9’

Depositional Characteristics

*Rock Type:*Limestone
*Dunham/Riding Classification:*Grainstone, with some areas of Packstone
Grains Present:

- *Dominant:*Forams, Phylloid Algae (broken)
- *Common:*Crinoids, Brachiopods, Bivalves, Sponge Spicules
- *Present:*Peloids

Comments:Forams heavily micritized, phylloid algae is often dissolved

Sedimentary Structures: N/A
Bedding: N/A
*Sorting:*Moderate

Diagenetic Characteristics

*Cementation:*Abundant pore filling and grain replacing large and small blocky calcite, common drusy cement filling larger pores
*Recrystallization:*Abundant micritization of grains, present neomorphism of micrite
Dissolution: Present grain and cement leaching
*Replacement:*N/A
Mechanical Compaction: N/A
*Chemical Compaction:*Present stylolites
Other: N/A

Porosity

*Visual Estimate:*5 %

- *Dominant:*SE Interparticle – 75%
- *Common:*Moldic – 20%
- *Present:*Vuggy – 5%

Ahr Genetic Pore Type: **Hybrid 1B** (high end) **– Enhanced**
Comments: Patches of high porosity and patches of no porosity in the thin section

Sample: Jade 1 – 6811.5’

Depositional Characteristics

*Rock Type:*Limestone
*Dunham/Riding Classification:*Grainstone
Grains Present:

- *Dominant:*Forams
- *Common:*Crinoids, Phylloid Algae (broken), Brachiopods, Bivalves, Sponge Spicules
- *Present:*Peloids

Comments: More than 80% of the slide is made up for forams, Forams heavily micritized

Sedimentary Structures: N/A
Bedding: N/A
*Sorting:*Well sorted with patches of moderate sorting

Diagenetic Characteristics

*Cementation:*Abundant pore filling small blocky calcite, present pore filling large blocky calcite
*Recrystallization:*Abundant micritization of grains
*Dissolution:*Present grain leaching
Replacement: N/A
Mechanical Compaction: N/A
Chemical Compaction: N/A
Other: N/A

Porosity

Visual Estimate:< 5 %

- *Dominant:*Moldic – 90%
- *Common:*SE Interparticle – 10%
- *Present:*

Ahr Genetic Pore Type: **Hybrid 1B** (high end) **- Reduced**

Sample: Jade 1 – 6817.9’

Depositional Characteristics

*Rock Type:*Limestone
*Dunham/Riding Classification:*Automicrite
Grains Present:

- *Dominant:*Skeletal Hash
- *Common:*
- *Present:* Brachiopods, Forams, Crinoids, Phylloid Algae (broken), Bivalves, Sponge Spicules

Comments: Mostly composed of very fine broken fragments, Forams heavily micritized, larger phylloid algae has been dissolved and replaced with calcite

Sedimentary Structures: N/A
Bedding: N/A
*Sorting:*Poor

Diagenetic Characteristics

*Cementation:*Abundant pore filling large blocky calcite, present pore filling small blocky calcite
*Recrystallization:*Abundant micritization of grains, present neomorphism of micrite
*Dissolution:*N/A
Replacement: N/A
Mechanical Compaction: N/A
Chemical Compaction: N/A
Other: N/A

Porosity

*Visual Estimate:*0 %

- *Dominant:*
- *Common:*
- *Present:*

Ahr Genetic Pore Type: **Hybrid 1A** (low end) **- Reduced**

Sample: Jade 1 – 6822.8’

Depositional Characteristics

*Rock Type:*Limestone
*Dunham/Riding Classification:*Packstone
Grains Present:

- *Dominant:*Forams, Phylloid Algae
- *Common:*Crinoids, Brachiopods, Bivalves, Sponge Spicules
- *Present:*Peloids

Comments:Forams heavily micritized, phylloid algae mostly dissolved and replaced with calcite

Sedimentary Structures: N/A
Bedding: N/A
*Sorting:*Poor

Diagenetic Characteristics

*Cementation:*Common small blocky calcite filling pores, and large blocky calcite replacing grains and filling large pores
*Recrystallization:*Abundant micritization of grains, present neomorphism of micrite
*Dissolution:*Present grain leaching
*Replacement:*Present pore filling saddle dolomite and grain replacing silica
Mechanical Compaction: N/A
Chemical Compaction: N/A
Other: N/A

Porosity

*Visual Estimate:*2-3 %

- *Dominant:*Moldic – 75%
- *Common:* SE Interparticle – 20%
- *Present:*Vuggy – 5%

Ahr Genetic Pore Type: **Hybrid 1B - Reduced**

Sample: Jade 1 – 6823.8’

Depositional Characteristics

*Rock Type:*Limestone
*Dunham/Riding Classification:*Automicrite with areas of Grainstone
Grains Present:

- *Dominant:*Forams, Phylloid Algae
- *Common:*Crinoids, Brachiopods, Bivalves, Sponge Spicules
- *Present:*Gastropods, Peloids

Comments: Patches of grainstone surrounded by automicrite, Forams heavily micritized

Sedimentary Structures: N/A
Bedding: N/A
*Sorting:*Poor

Diagenetic Characteristics

*Cementation:*Common pore filling small blocky calcite in grainstone areas, common pore filling large blocky calcite throughout
*Recrystallization:*Abundant micritization of grains, present neomorphism of micrite
*Dissolution:*Common grain and matrix leaching
*Replacement:*Common saddle dolomite filling pores
*Mechanical Compaction:*Present partially healed fractures
*Chemical Compaction:*Common stylolites
Other: N/A

Porosity

*Visual Estimate:*10 %

- *Dominant:*Moldic – 40% , Vuggy – 40%
- *Common:*SE Interparticle – 20%
- *Present:*

Ahr Genetic Pore Type: **Hybrid 1B - Enhanced**

Sample: Jade 1 – 6829.9’

Depositional Characteristics

*Rock Type:*Limestone
*Dunham/Riding Classification:*Packstone
Grains Present:

- *Dominant:*Forams
- *Common:*Crinoids, Bivalves, Brachiopods, Phylloid Algae
- *Present:*Sponge Spicules, Bryozoans, Peloids

Comments:Forams heavily micritized, phylloid algae is often dissolved

Sedimentary Structures: N/A
Bedding: N/A
*Sorting:*Poor

Diagenetic Characteristics

*Cementation:*Present small and large blocky calcite filling some pores, present syntaxial overgrowth on crinoids
*Recrystallization:*Abundant micritization of grains, common neomorphism of micrite
*Dissolution:*Abundant grain and matrix leaching
*Replacement:*Present pore filling saddle dolomite
Mechanical Compaction: N/A
Chemical Compaction: N/A
Other: N/A

Porosity

*Visual Estimate:*20 %

- *Dominant:* Vuggy – 75%
- *Common:* Moldic – 15% , SE Interparticle – 10%
- *Present:*

Ahr Genetic Pore Type: **Hybrid 1B** (low end) **- Enhanced**

Sample: Jade 1 – 6843.6’

Depositional Characteristics

*Rock Type:*Limestone
*Dunham/Riding Classification:*Automicrite
Grains Present:

- *Dominant:* Forams
- *Common:*Phylloid Algae, Brachiopods, Crinoids
- *Present:*Bivalves, Sponge Spicules, Peloids

Comments: Mostly fine grained, high grain abundance, Forams heavily micritized, phylloid algae is often dissolved and replaced, prismatic microstructure seen in brachiopods.

*Sedimentary Structures:*N/A
Bedding: N/A
*Sorting:*Well

Diagenetic Characteristics

*Cementation:*Common pore filling small blocky calcite and grain replacing large blocky calcite
*Recrystallization:*Abundant micritization of grains and neomorphism of micrite
*Dissolution:*Present grain and matrix leaching
Replacement: Present saddle dolomite is some pores
Mechanical Compaction: N/A
Chemical Compaction: N/A
Other: N/A

Porosity

*Visual Estimate:*2-3 %

- *Dominant:*Moldic – 40%, SE Interparticle – 40%
- *Common:* Vuggy – 20%
- *Present:*

Ahr Genetic Pore Type: **Hybrid 1B** (high end) **- Reduced**

Sample: Jade 1 – 6865.5’

Depositional Characteristics

*Rock Type:*Limestone
*Dunham/Riding Classification:*Packstone
Grains Present:

- *Dominant:*Forams
- *Common:*Phylloid Algae, Crinoids, Brachiopods, Sponge Spicules
- *Present:*Fusulinids, Bivalves, Peloids

Comments: Large phylloid algae, crinoids, and brachiopods. Forams heavily micritized

Sedimentary Structures: N/A
Bedding: N/A
*Sorting:*Poor

Diagenetic Characteristics

*Cementation:*Common pore filling large and small blocky calcite
Recrystallization: Abundant micritization of grains, common neomorphism of micrite
*Dissolution:*Present grain, matrix and cement leaching
*Replacement:*Common pore filling saddle dolomite, present silica replacement of some grains
Mechanical Compaction: N/A
*Chemical Compaction:*Common stylolites
Other: N/A

Porosity

*Visual Estimate:*5-10 %

- *Dominant:*Moldic – 40%, Vuggy – 40%
- *Common:*SE Interparticle – 20%
- *Present:*

Ahr Genetic Pore Type: **Hybrid 1B - Enhanced**

Sample: Jade 1 – 6869.9’

Depositional Characteristics

*Rock Type:*Limestone
*Dunham/Riding Classification:*Packstone
Grains Present:

- *Dominant:*Forams
- *Common:*Crinoids, Brachiopods, Phylloid Algae (broken)
- *Present:*Bivalves, Sponge Spicules, Peloids

Comments: Large angular clasts present, Forams heavily micritized

*Sedimentary Structures:*N/A
*Bedding:*Mottled texture
*Sorting:*Very poor

Diagenetic Characteristics

*Cementation:*Abundant small blocky calcite filling pores and large blocky calcite filling large pores and replacing grains (phylloid algae)
*Recrystallization:*Abundant micritization of grains and neomorphism of micrite
*Dissolution:*Common cement leaching
*Replacement:*Abundant saddle dolomite filling pores and replacing grains (nearly half of the slide)
Mechanical Compaction: N/A
Chemical Compaction: N/A
*Other:*Half of the slide replaced with saddle dolomite

Porosity

*Visual Estimate:*5 %

- *Dominant:*SE Interparticle and Intercrystalline – 75%
- *Common:*Vuggy – 25%
- *Present:*

Ahr Genetic Pore Type: **Hybrid 1B** (low end) - **Enhanced**

THIN SECTION DESCRIPTION – TOPAZ #1

Sample: Topaz 1 – 6701.1'

Depositional Characteristics

*Rock Type:*Limestone
*Dunham/Riding Classification:*Grainstone
Grains Present:

- *Dominant:*Peloids
- *Common:*Forams, Fusulinids
- *Present:* Bivalves, Crinoids, Sponge Spicules, Phylloid Algae (broken)

Comments: Crinoids often replaced with saddle dolomite, Forams heavily micritized, mostly fine grained

Sedimentary Structures: N/A
*Bedding:*N/A
*Sorting:*Well

Diagenetic Characteristics

*Cementation:*Abundant pore filling small and large blocky calcite
*Recrystallization:*Abundant micritization of grains, common neomorphism of micrite
*Dissolution:*Abundant grain and cement leaching
*Replacement:*Common saddle dolomite replacement of grains
Mechanical Compaction: N/A
Chemical Compaction: N/A
Other: N/A

Porosity

*Visual Estimate:*25%

- *Dominant:*Vuggy – 60% , Moldic – 40%
- *Common:*
- *Present:*

Ahr Genetic Pore Type: **Hybrid 1B - Enhanced**

Sample: Topaz 2 – 6707.7’

Depositional Characteristics

*Rock Type:*Limestone
*Dunham/Riding Classification:*Grainstone
Grains Present:

- *Dominant:*Peloids
- *Common:*Fusulinids, Brachiopods, Forams
- *Present:*Phylloid Algae (broken), Crinoids, Trilobite Fragments

Comments: Mostly fine grained peloidal grainstone with areas of peloidal/skeletal grainstone, Forams heavily micritized

*Sedimentary Structures:*N/A
*Bedding:*Some parallel layering in peloidal grainstone
*Sorting:*Well

Diagenetic Characteristics

*Cementation:*Common pore filling small blocky calcite, present pore filling large blocky calcite, present drusy cement in large pores, present poikilotopic cement
*Recrystallization:*Abundant micritization of grains, common neomorphism of micrite
*Dissolution:*Abundant grain and cement leaching
*Replacement:*Present saddle dolomite replacement of some grains
Mechanical Compaction: N/A
*Chemical Compaction:*Present stylolites
Other: N/A

Porosity

*Visual Estimate:*15-20 %

- *Dominant:*Moldic – 60%
- *Common:*SE Interparticle – 30%, Vuggy – 10%
- *Present:*

Ahr Genetic Pore Type: **Hybrid 1B** (high end) - **Enhanced**

Sample: Topaz 1 – 6712.9’

Depositional Characteristics

*Rock Type:*Limestone
*Dunham/Riding Classification:*Packstone
Grains Present:

- *Dominant:*Crinoids, Fusulinids, Brachiopods
- *Common:*Forams, Bivalves
- *Present:*Phylloid Algae (broken), Sponge Spicules

Comments: Crinoid fragments most common, fine to coarse grained

Sedimentary Structures: N/A
Bedding: N/A
*Sorting:*Moderate to Poor

Diagenetic Characteristics

*Cementation:*Present syntaxial overgrowth cement on crinoids, present drusy cement filling some large pores
Recrystallization: Abundant micritization of grains, common neomorphism of micrite
*Dissolution:*Abundant grain, matrix and cement leaching
Replacement: N/A
*Mechanical Compaction:*Common brittle grain deformation (shells crushed)
Chemical Compaction: N/A
Other: N/A

Porosity

*Visual Estimate:*20-25 %

- *Dominant:*Vuggy – 75%
- *Common:*Moldic – 25%
- *Present:*

Ahr Genetic Pore Type: **Hybrid 1B - Enhanced**

Sample: Topaz 1 – 6713.9’

Depositional Characteristics

*Rock Type:*Limestone
*Dunham/Riding Classification:*Packstone
Grains Present:

- *Dominant:*Crinoids
- *Common:*Fusulinids, Brachiopods, Phylloid Algae (broken), Forams
- *Present:*Bivalves, Sponge Spicules

Comments: Dominated by crinoids fragments, abundant micrite, phylloid algae and sponge spicules often dissolved, fine to coarse grained

Sedimentary Structures: N/A
Bedding: N/A
*Sorting:*Poor

Diagenetic Characteristics

*Cementation:*Common pore filling large blocky calcite, present pore filling small blocky calcite, present syntaxial overgrowth on crinoids
*Recrystallization:*Abundant micritization of grains and neomorphism of micrite
*Dissolution:*Abundant cement, matrix, and grain leaching
Replacement: N/A
*Mechanical Compaction:*Present brittle grain deformation
Chemical Compaction: N/A
Other: N/A

Porosity

*Visual Estimate:*10-15%

- *Dominant:*Vuggy – 85%
- *Common:*Moldic – 15%
- *Present:*

Ahr Genetic Pore Type: **Hybrid 1B - Enhanced**

Sample: Topaz 1 – 6716.5’

Depositional Characteristics

*Rock Type:*Limestone
*Dunham/Riding Classification:*Automicrite
Grains Present:

- *Dominant:*
- *Common:*
- *Present:*Fusulinids, Brachiopods, Crinoids, Bivalves, Trilobites, Sponge Spicules, Phylloid Algae (broken)

Comments: Mostly micrite, less than 20% grains

*Sedimentary Structures:*N/A
Bedding: N/A
*Sorting:*Moderate

Diagenetic Characteristics

*Cementation:*Present small blocky calcite in a few pores
*Recrystallization:*Abundant micritization of grains and neomorphism of micrite
*Dissolution:*Abundant matrix leaching, present grain leaching
Replacement: N/A
Mechanical Compaction: N/A
Chemical Compaction: N/A
Other: N/A

Porosity

*Visual Estimate:*10-15 %

- *Dominant:*Vuggy – 85%
- *Common:*Moldic – 15%
- *Present:*

Ahr Genetic Pore Type: **Hybrid 1B** (low end) **- Enhanced**

Sample: Topaz 1 – 6751.7’

Depositional Characteristics

*Rock Type:*Limestone
*Dunham/Riding Classification:*Automicrite
Grains Present:

- *Dominant:*Phylloid Algae (broken) , Peloids
- *Common:*Forams, Brachiopods, Bivalves, Crinoids, Sponge Spicules
- *Present:*

Comments: Phylloid algae mostly dissolved, Forams heavily micritized

Sedimentary Structures: N/A
Bedding: N/A
*Sorting:*Moderate

Diagenetic Characteristics

*Cementation:*Present small and large blocky calcite partially filling some proes
*Recrystallization:*Abundant micritization of grains and neomorphism of micrite
*Dissolution:*Abundant grain and matrix leaching
*Replacement:*Present silica replacement of some grains
Mechanical Compaction: N/A
*Chemical Compaction:*Present stylolites near top of slide
Other: N/A

Porosity

*Visual Estimate:*25 %

- *Dominant:*Vuggy to Cavernous – 80%
- *Common:*Moldic – 20%
- *Present:*

Ahr Genetic Pore Type: **Hybrid 1B** (low end) **- Enhanced**

Sample: Topaz 1 – 6752.9’

Depositional Characteristics

*Rock Type:*Limestone
*Dunham/Riding Classification:*Automicrite
Grains Present:

- *Dominant:* Forams
- *Common:*Crinoids, Brachiopods, Phylloid Algae (broken)
- *Present:*Fusulinids, Bivalves, Sponge Spicules

Comments: Many grains broken up, mostly micrite, prismatic microstructure seen in brachiopod

Sedimentary Structures: N/A
Bedding: N/A
*Sorting:*Moderate

Diagenetic Characteristics

*Cementation:*Present small and large blocky calcite partially filling some pores
*Recrystallization:*Abundant micritization of grains and neomorphism of micrite
*Dissolution:*Abundant grain and matrix leaching
Replacement: N/A
*Mechanical Compaction:*Common brittle grain deformation
*Chemical Compaction:*Present stylolites
Other: N/A

Porosity

*Visual Estimate:*20 %

- *Dominant:*Vuggy to Cavernous – 75%
- *Common:* Moldic – 25%
- *Present:*

Ahr Genetic Pore Type: **Hybrid 1B** (low end) **- Enhanced**

Sample: Topaz 1 – 6755.2’

Depositional Characteristics

*Rock Type:*Limestone
*Dunham/Riding Classification:*Automicrite with a few areas of Packstone
Grains Present:

- *Dominant:*Forams
- *Common:*Phylloid Algae (broken), Fusulinids, Brachiopods, Crinoids
- *Present:*Bivalves, Sponge Spicules, Peloids

Comments:Forams heavily micritized, phylloid algae and sponge spicules mostly dissolved

*Sedimentary Structures:*N/A
Bedding: N/A
*Sorting:*Well

Diagenetic Characteristics

*Cementation:*Common small blocky calcite in pores, present large blocky calcite in larger pores
*Recrystallization:*Abundant micritization of grains and neomorphism of micrite
*Dissolution:*Abundant grain and matrix leaching, common cement leaching
Replacement: N/A
Mechanical Compaction: N/A
Chemical Compaction: N/A
Other: N/A

Porosity

*Visual Estimate:*10 %

- *Dominant:*Moldic – 75%
- *Common:*SE Interparticle – 25%
- *Present:*

Ahr Genetic Pore Type: **Hybrid 1B** (high end) – **Enhanced**
Comments: Most of the SE interparticle porosity is in the packstone areas

Sample: Topaz 1 – 6760.2’

Depositional Characteristics

*Rock Type:*Limestone
*Dunham/Riding Classification:*Automicrite
Grains Present:

- *Dominant:*Forams, Sponge Spicules
- *Common:*Crinoids, Brachiopods, Bivalves
- *Present:*

Comments: Mostly fine grained sponge spicules and forams, about 80% of slide, many spicules are dissolved

Sedimentary Structures: N/A
Bedding: N/A
*Sorting:*Well

Diagenetic Characteristics

*Cementation:*Present small blocky calcite in some pores
*Recrystallization:*Abundant micritization of grains and neomorphism of micrite
*Dissolution:*Abundant grain leaching
Replacement: N/A
Mechanical Compaction: N/A
*Chemical Compaction:*Present stylolites near top of slide
Other: N/A

Porosity

*Visual Estimate:*5 %

- *Dominant:*Moldic – 90 %
- *Common:*SE Interparticle – 10%
- *Present:*

Ahr Genetic Pore Type: **Hybrid 1B** (high end) **- Enhanced**

Sample: Topaz 1 – 6820.9’

Depositional Characteristics

*Rock Type:*Limestone
*Dunham/Riding Classification:*Automicrite
Grains Present:

- *Dominant:*Forams
- *Common:*Brachiopods, Fusulinids, Phylloid Algae (broken)
- *Present:*Sponge Spicules, Peloids

Comments: Very fine grained foram areas and coarser grained fusilind, brachiopods, and phylloid algae areas. Forams heavily micritized

Sedimentary Structures: N/A
Bedding: N/A
*Sorting:*Poor

Diagenetic Characteristics

*Cementation:*Common pore filling small blocky calcite, present pore filling large blocky calcite
*Recrystallization:*Abundant micritization of grains, common neomorphism of micrite
Dissolution: N/A
Replacement: N/A
Mechanical Compaction: N/A
*Chemical Compaction:*Present stylolites
Other: N/A

Porosity

Visual Estimate:<1 %

- *Dominant:*
- *Common:*
- *Present:*Fracture

Ahr Genetic Pore Type: **Hybrid 1A** (low end) **- Reduced**

Sample: Topaz 11 – 6828.8’

Depositional Characteristics

*Rock Type:*Limestone
*Dunham/Riding Classification:*Automicrite
Grains Present:

- *Dominant:* Forams
- *Common:*Phylloid Algae (whole and broken)
- *Present:*Sponge Spicules, Brachiopods, Peloids

Comments: Less than 15 % grains, fine grained forams and larger phylloid algae, Forams heavily micritized

Sedimentary Structures: N/A
Bedding: N/A
Sorting: Well, aside from large phylloid algae

Diagenetic Characteristics

*Cementation:*Abundant large blocky calcite filling pores and replacing grains, present small blocky calcite filling pores
*Recrystallization:*Abundant micritization of grains and neomorphism of micrite
Dissolution: N/A
Replacement: N/A
Mechanical Compaction: N/A
Chemical Compaction: N/A
Other: N/A

Porosity

*Visual Estimate:*0 %

- *Dominant:*
- *Common:*
- *Present:*

Ahr Genetic Pore Type: **Hybrid 1A - Reduced**

Sample: Topaz 1 – 6832.4’

Depositional Characteristics

*Rock Type:*Limestone
*Dunham/Riding Classification:*Automicrite
Grains Present:

- *Dominant:*Skeletal Hash
- *Common:* Fusulinids, Brachiopods, Crinoids, Phylloid Algae (broken)
- *Present:*Bivalves

Comments: Around 50% grains, mostly fine skeletal hash, some large fusilinds

Sedimentary Structures: N/A
Bedding: N/A
*Sorting:*Poor

Diagenetic Characteristics

*Cementation:*Present small blocky calcite filling pores
*Recrystallization:*Abundant micritization of grains, common neomorphism of micrite
Dissolution: N/A
*Replacement:*Present silica replacement of some grains
*Mechanical Compaction:*Common brittle grain deformation
*Chemical Compaction:*Common stylolites
*Other:*Heavily altered

Porosity

Visual Estimate:< 1 %

- *Dominant:*
- *Common:*
- *Present:* Fracture

Ahr Genetic Pore Type: **Hybrid 1C** (high end) **- Reduced**

APPENDIX E

THIN SECTION PHOTOMICROGRAPHS

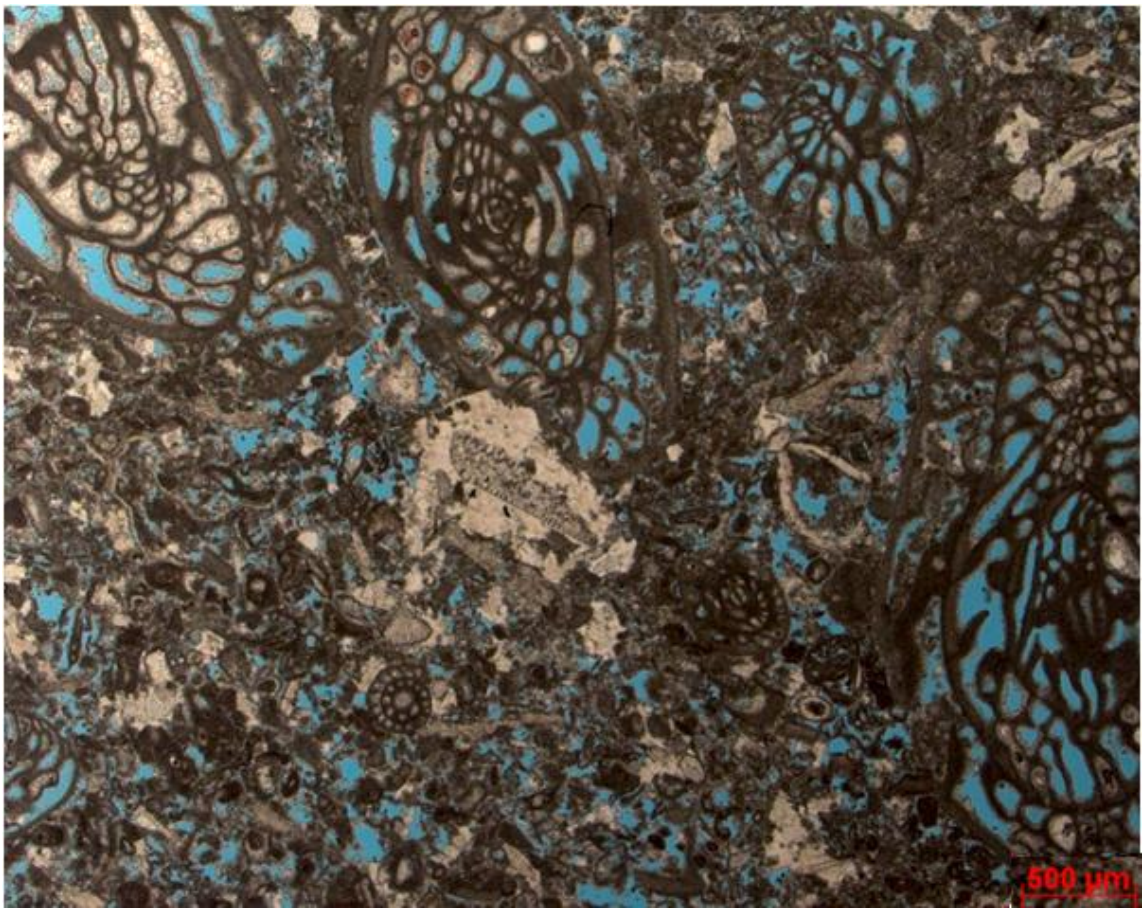

Figure E.1: Example of H1-Ae porosity. SE Interparticle and SE Intraparticle in Grainstone/Packstone facies. Sample Emerald 1, 6649.8'

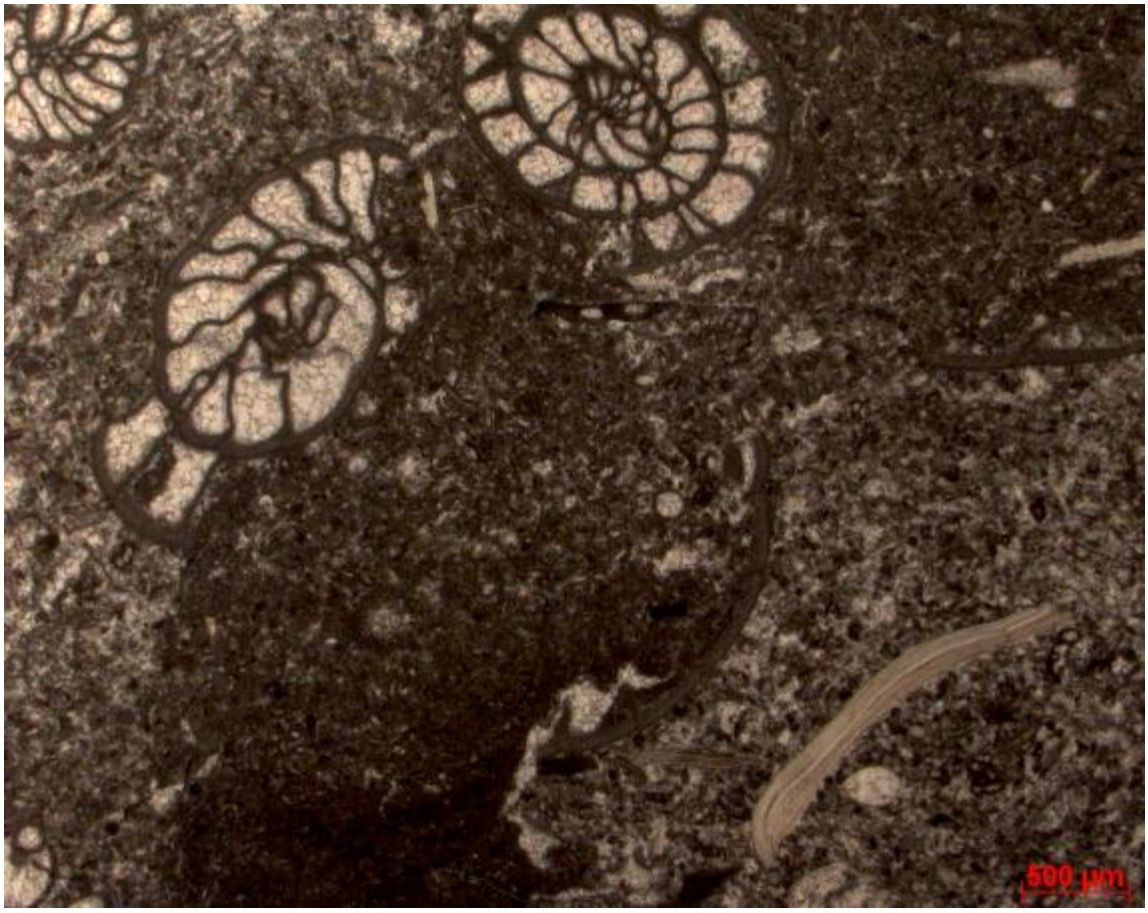

Figure E.2: Example of H1-Ar porosity. Small blocky calcite filling all the pores in the Reef 3 facies. Shell structure is well preserved and diagenetic alteration is not very extensive. Sample Topaz 1, 6820.9'

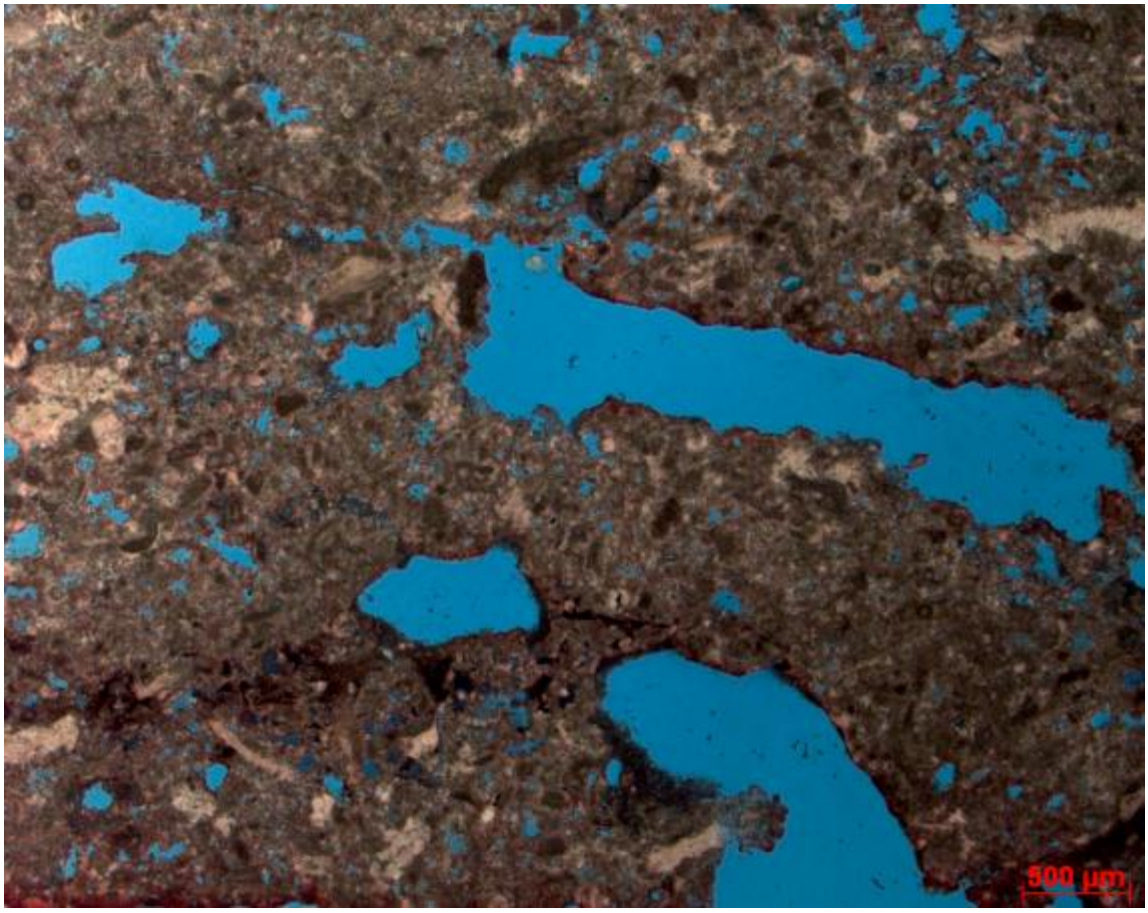

Figure E.3: Example of H1-Be porosity. Reef 2 facies, thin section dominated by large vugs and some molds. Sample Emerald 1, 6742.7'

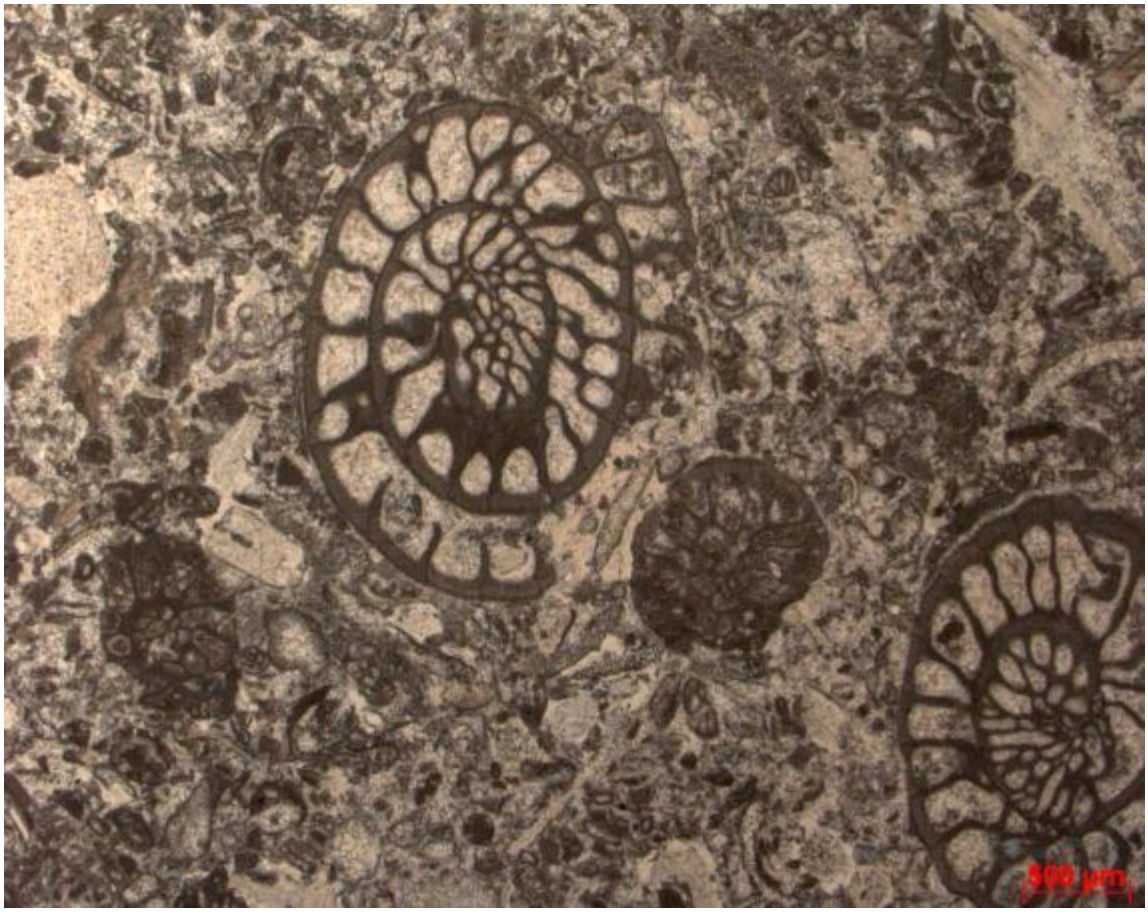

Figure E.4: Example of H1-Br porosity. Grainstone/Packstone facies completely cemented with large and small blocky calcite. Sample Emerald 1, 6654.6'

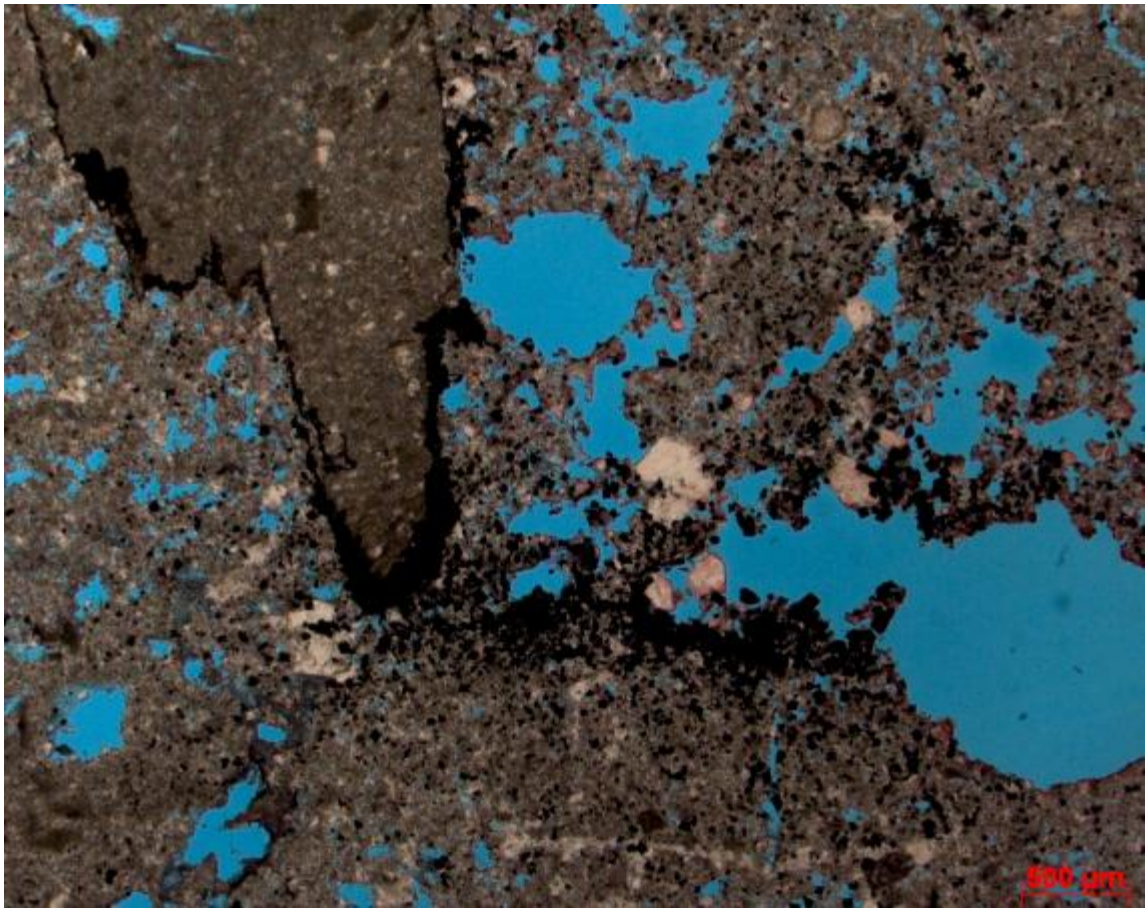

Figure E.5: Example of H1-Ce porosity. Reef 1 facies showing significant alteration. Stylolites present and pyrite abundant in this slide. Vugs and solution enhanced molds provide significant porosity. Sample Emerald 1, 6675.5'

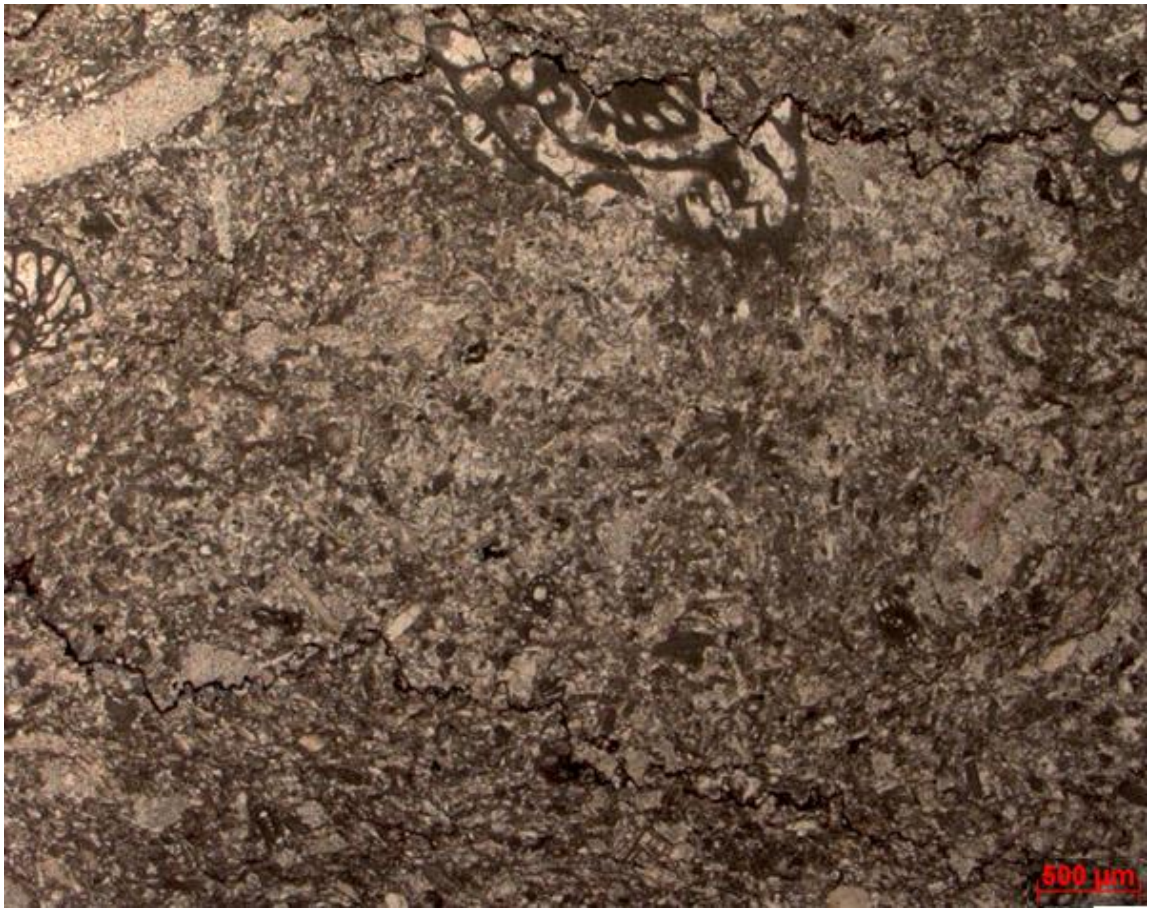

Figure E.6: Example of H1-Cr porosity. Reef 3 facies has been heavily altered. Mechanical and chemical compaction present, many grains fragmented. Abundant micritization of grains and neomorphism of micrite. Sample Topaz 1, 6832.4'

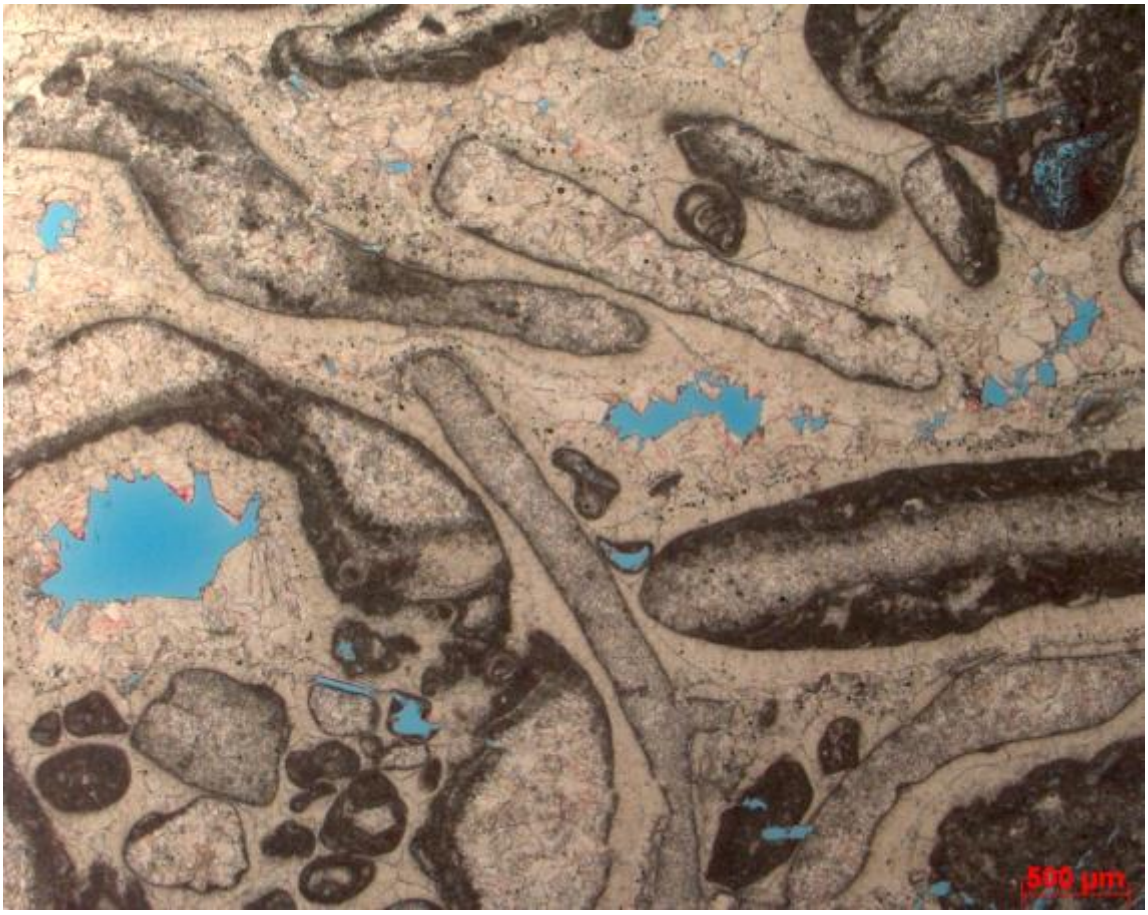

Figure E.7: H1-Br porosity in Grainstone/Packstone facies. Intercrystalline porosity in a phylloid algal grainstone. Small and large blocky calcite have filled almost all of the pores. Sample Jade 1, 6799.9'

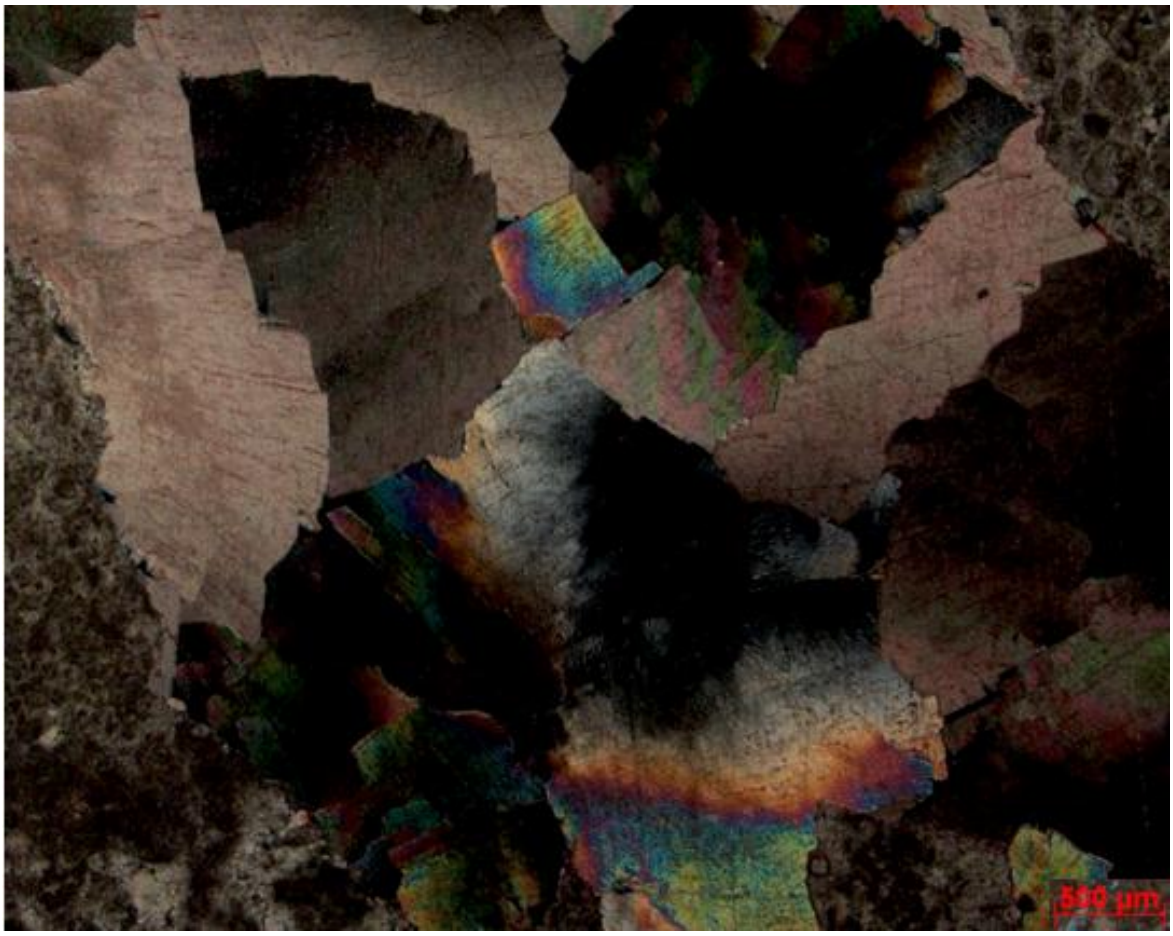

Figure E.8: Saddle dolomite replacement of a peloidal packstone in polarized light. Debris facies. Sample Jade 1, 6869.9’

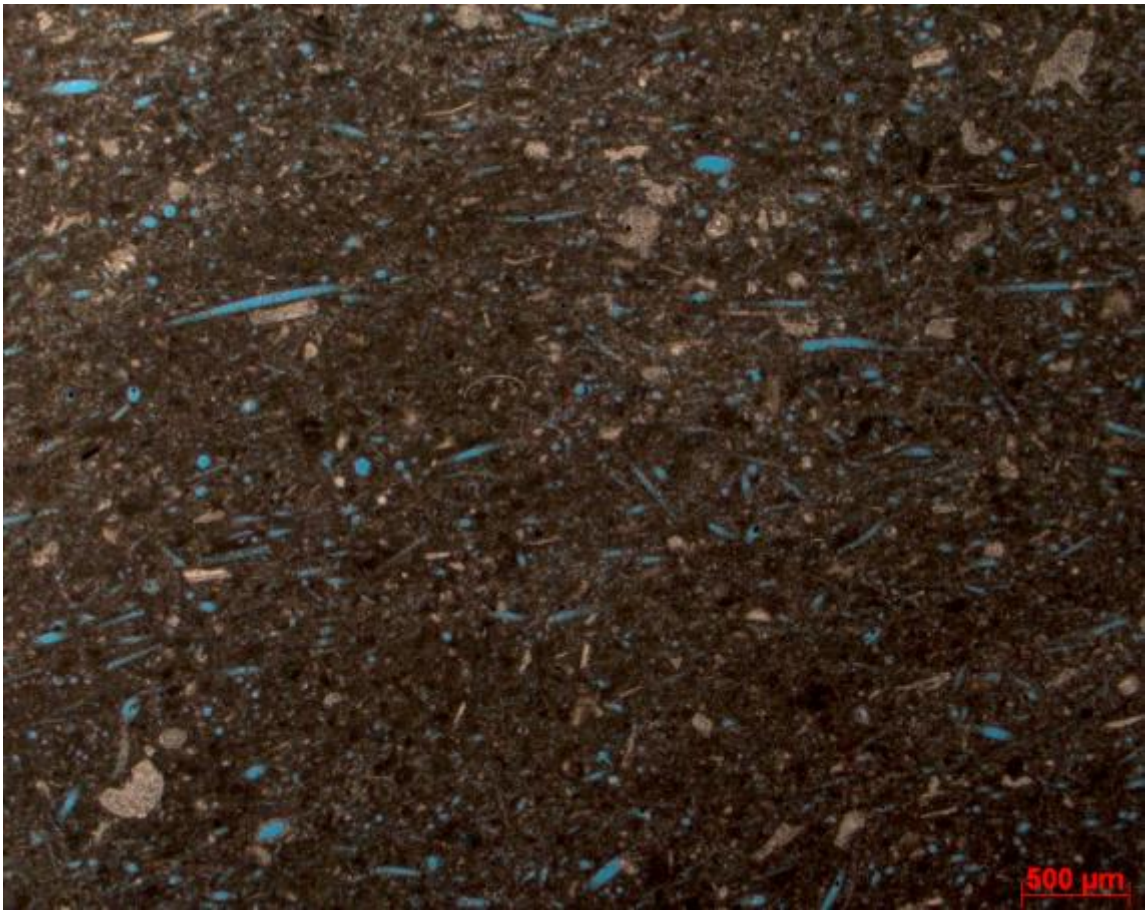

Figure E.9: Moldic porosity of sponge spicules in Reef 1 facies. H1-Be porosity. Sample Topaz 1, 6760.2’

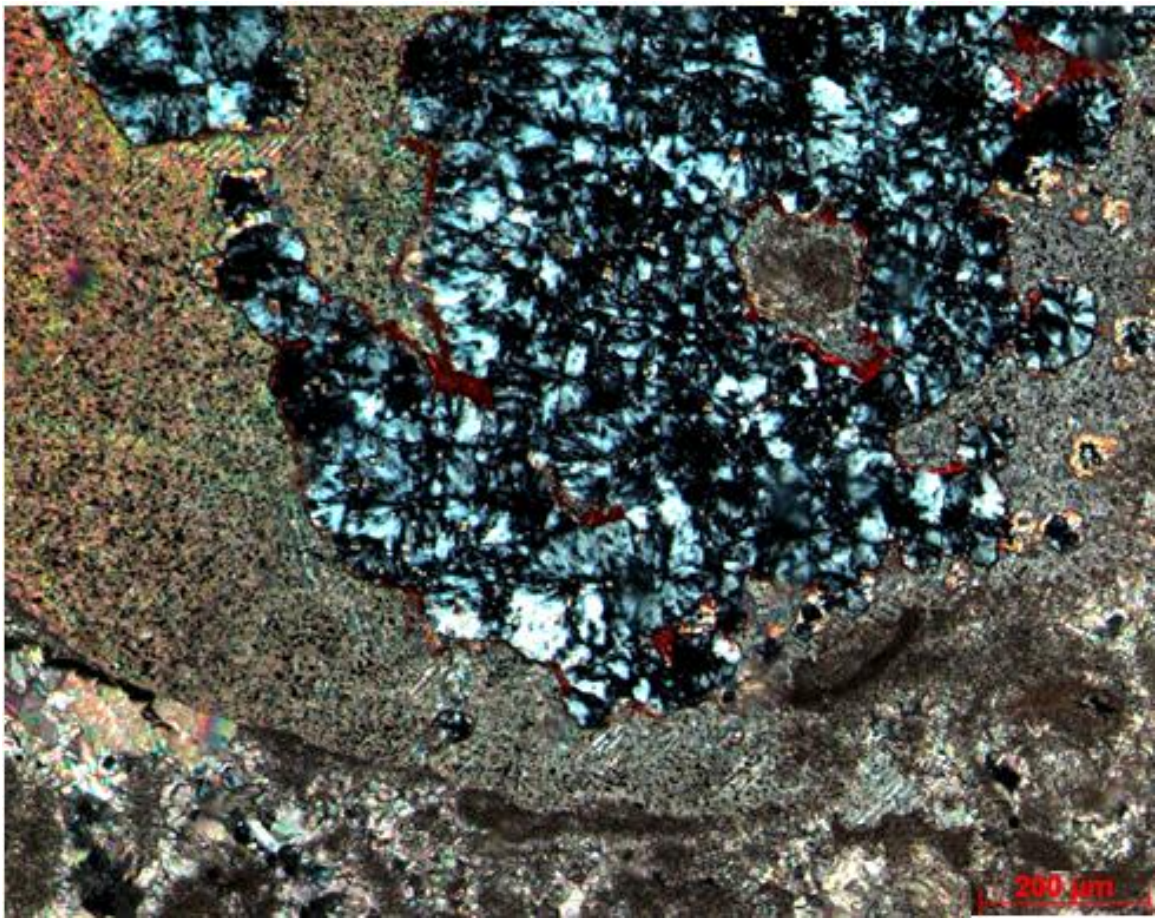

Figure E.10: Silica replacement of crinoid in polarized light in the grainstone/packstone facies. Sample Emerald 1, 6631.8’

APPENDIX F

FACIES DESCRIPTIONS

***Facies*: Grainstone/Packstone**

- *Color:* Tan to dark gray
- *Texture/Bedding:*Mostly indistinct bedding, but parallel layers are present throughout, mainly at the bottom erosional surface
- *Sedimentary Structures:*Present - Stylolites, Dissolution Seams, Calcite Filled Veins, and Geopetal Structures
- *Grain Size and Sorting:*Fine to coarse grained, moderate to well sorted
- *Dunham/Riding Classification:*Grainstone/Packstone, with patches of automicritic reef rock
- *Grains Present:*
    - *Dominant:*Forams, Phylloid Algae
    - *Common:* Bivalves, Brachiopods, Crinoids, Fusulinids
    - *Present:* Bryozoans, Gastropods, Peloids, Sponge Spicules
- *Accessory Minerals:*Present - Pyrite, Silica, and Saddle Dolomite
- *Porosity:*
    - *Dominant:* SE Interparticle
    - *Common:* Moldic
    - *Present:* SEIntercrystalline, SE Intraparticle, Vuggy
- *Comments:*

Pockets of automicritic reef rock usually around 4 feet thick are present in the Emerald and Jade wells. There are also separate zones of very large fusulinids and phylloid alage. Typically the phylloid algae range from 0.5 mm to 15 mm, and the fusulinids range from 0.5 to 5 mm. The color of the core roughly correlates to grain size. Tan areas are usually fined grained, brown areas are medium to coarse, and grey areas contain large phylloid algae.

***Facies*: Reef 1**

- *Color:* Light brown to dark gray
- *Texture/Bedding:*Mainly heavily mottled texture, but some parallel layers in grainstone/packstone areas
- *Sedimentary Structures:*Common- Calcite Filled Veins and Geopetal Structures , Present -Stylolites, Dissolution Seams
- *Grain Size and Sorting:* Fine to coarse grained, moderate to poor sorting, but some grainstone/packstone areas are well sorted
- *Dunham/Riding Classification:* Mainly automicrite. Areas of grainstone/packstone present
- *Grains Present:*
    - *Dominant:* Phylloid Algae, Brachipods, Forams
    - *Common:* Crinoids, Fusulinids
    - *Present:* Bryozoans, Gastropods, Micritic Clasts, Peloids, Trilobite fragments
- *Accessory Minerals:*Common - Silica nodules and grain replacing silica , Present – Pyrite, Saddle Dolomite
- *Porosity:*
    - *Dominant:* Vuggy
    - *Common:* Moldic
    - *Present:* SE Interparticle (in Grainstone/Packestone intervals), SE Intraparticle
- *Comments:*

Approximately half of this rock type is micritic, while sketeltal grains such as phylloid algae, brachiopods, and forams dominate the remaining half. A few detrital grainstone/packstone areas usually less than 3 feet thick are present in Emerald and Jade wells. These detrital grainstones/packstones often show parallel bedding and erosional truncation. Large silica nodules up to 5 cm are also present.

***Facies*: Reef 2**

- *Color:* Light to dark gray
- *Texture/Bedding:* Mostly indistinct bedding, but some areas are slightly mottled
- *Sedimentary Structures:* Common - Stylolites and Calcite Filled Veins, Present - Dissolution Seams and Geopetal Structures
- *Grain Size and Sorting:* Fine to coarse grained, moderate to poor sorting
- *Dunham/Riding Classification:* Automicrite
- *Grains Present:*
    - *Dominant:* Forams, Phylloid Algae,
    - *Common:* Brachiopods, Bivalves, Crinoids, Fusulinids, Sponge Spicules
    - *Present:* Bryozoans, Gastropods, Peloids
- *Accessory Minerals:*Present - Pyrite
- *Porosity:*
    - *Dominant:* Moldic
    - *Common:* Vuggy
    - *Present:* SE Interparticle, SE Intraparticle
- *Comments:*

Higher mud/grain ratio than Reef 1 facies. Approximately 2/3 of this rock is micritic, with the remaining 1/3 dominated by forams and phylloid algae. Crinoids are more common and larger (5-35 mm) than in Reef 1 facies. Reef 2 also has less visual porosity than Reef 1.

***Facies*: Reef 3**

- *Color:* Light to dark brown
- *Texture/Bedding:*Mottled texture for the top 2/3 of the section, but changes to indistinct bedding for the bottom 1/3 of the section.
- *Sedimentary Structures:* Common -Stylolites, dissolution seams, and calcite filled veins
- *Grain Size and Sorting:* Fine to coarse grained, mainly poor sorting with areas of moderate sorting.
- *Dunham/Riding Classification:* Automicrite
- *Grains Present:*
    - *Dominant:* Forams, Phylloid Algae
    - *Common:* Brachiopods, Crinoids, Fusulinids
    - *Present:* Bivalves, Peloids, Sponge Spicules
- *Accessory Minerals:*Abundant silica replacement
- *Porosity:*No porosity
- *Comments:*

Blue/gray silica is abundant, replacing about 30% of the section and often spanning across the entire width of the core. The section is mostly fine grained, but the phylloid algae, crinoids, and fusulinids are larger than the other grains (up to 20mm, 5mm, and 2mm respectively). This facies is only present at the very bottom of the Topaz #1 well and contains almost no porosity.

***Facies*: Debris**

- *Color:* Gray to dark gray
- *Texture/Bedding:*Indistinct bedding
- *Sedimentary Structures:*Present - Stylolites, Dissolution Seams, and Geopetal structures
- *Grain Size and Sorting:* Mostly large angular intraclasts, poorly sorted
- *Dunham/Riding Classification:* Packstone
- *Grains Present:*
    - *Dominant:*Forams, Phylloid Algae
    - *Common:* Bivalves, Brachiopods, Crinoids, Sponge spicules
    - *Present:* Bryozoans, Gastropods, Fusulinids, Peloids
- *Accessory Minerals:*Abundant Pyrite and Saddle dolomite, Present - Silica
- *Porosity:*
    - *Dominant:* Moldic
    - *Common:* SE Interparticle
    - *Present:*
- *Comments:*

A majority of the section is made of large angular intraclasts (10-40 mm), but micrite is also common. This facies is only present in the Jade #1 core, and is volumetrically insignificant at only 6 feet thick.

APPENDIX G

CROSS SECTIONS

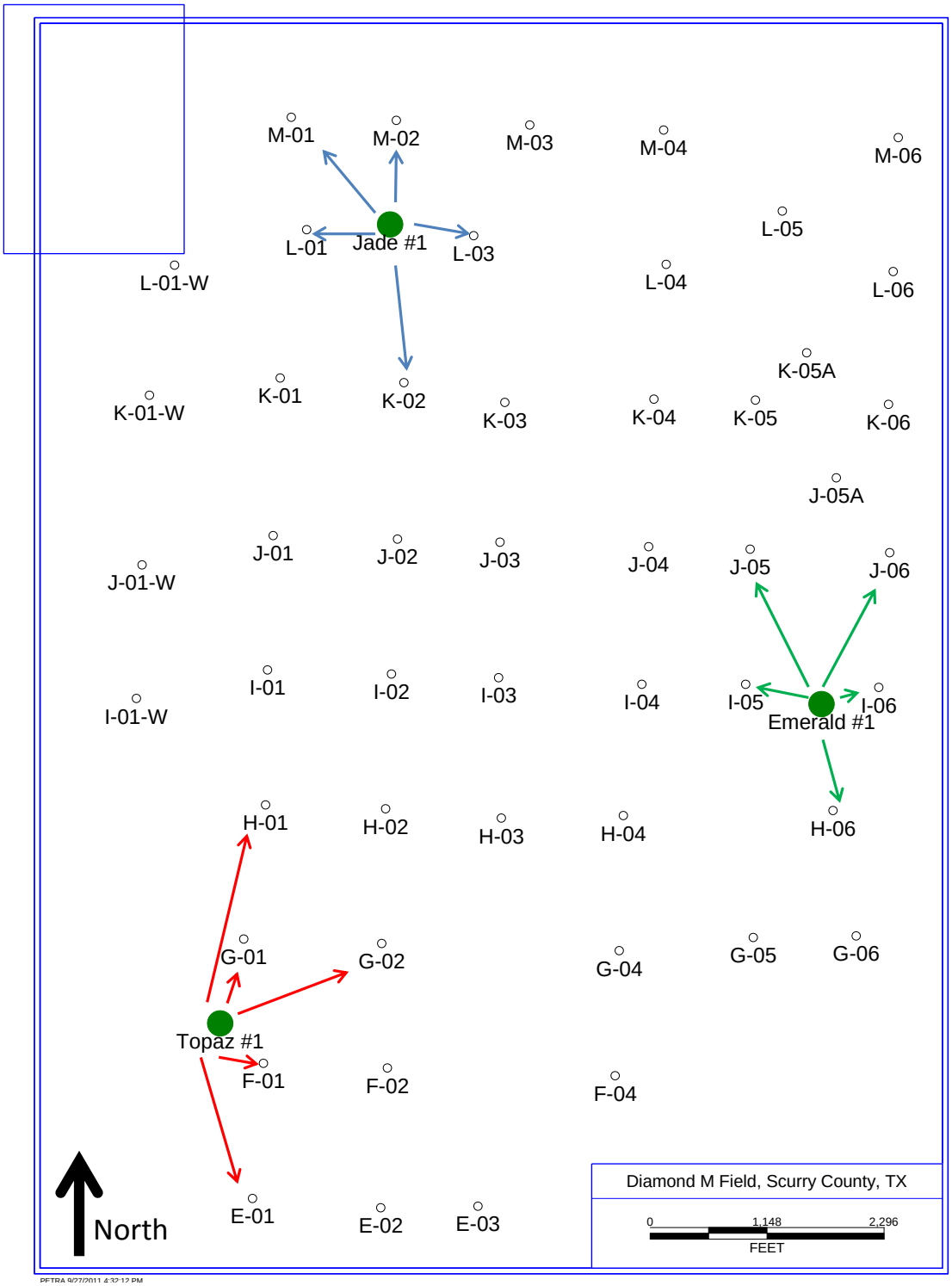

Figure G.1: Base map for Diamond M field. Arrows show which wells were correlated out from the cored wells.

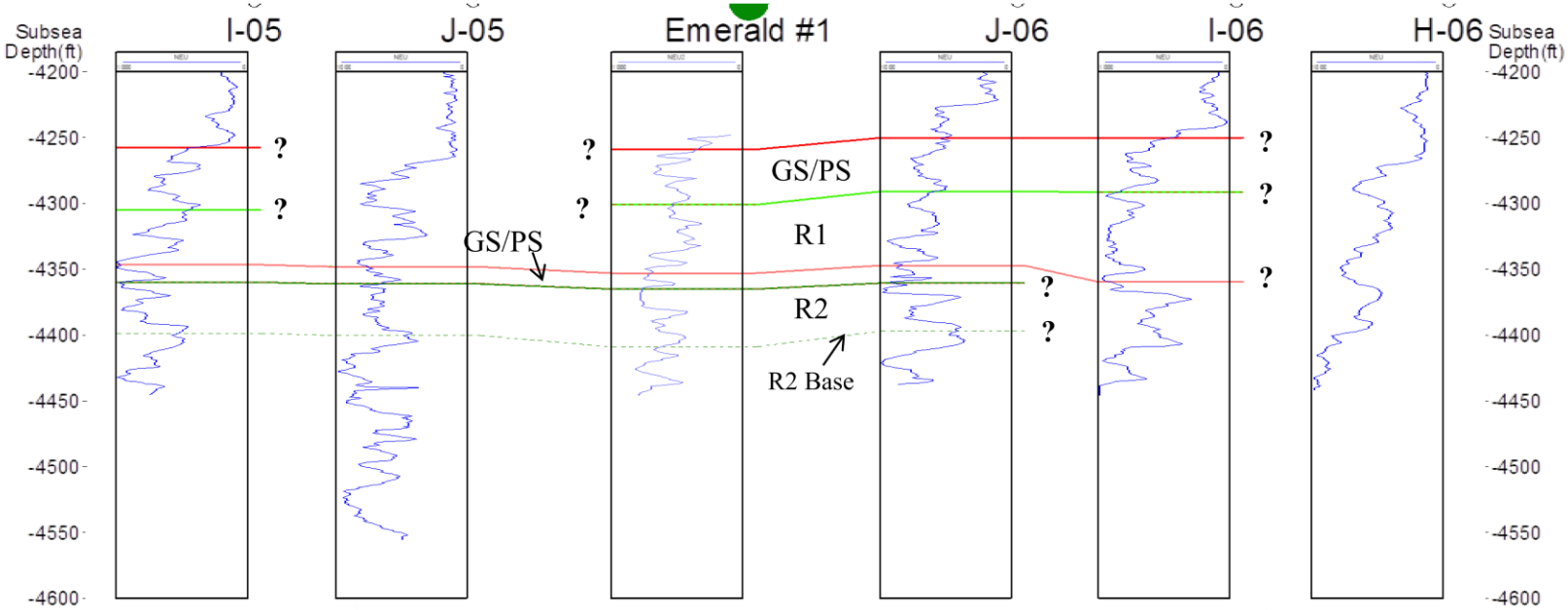

Figure G.2: Structural cross section for Emerald #1 Well

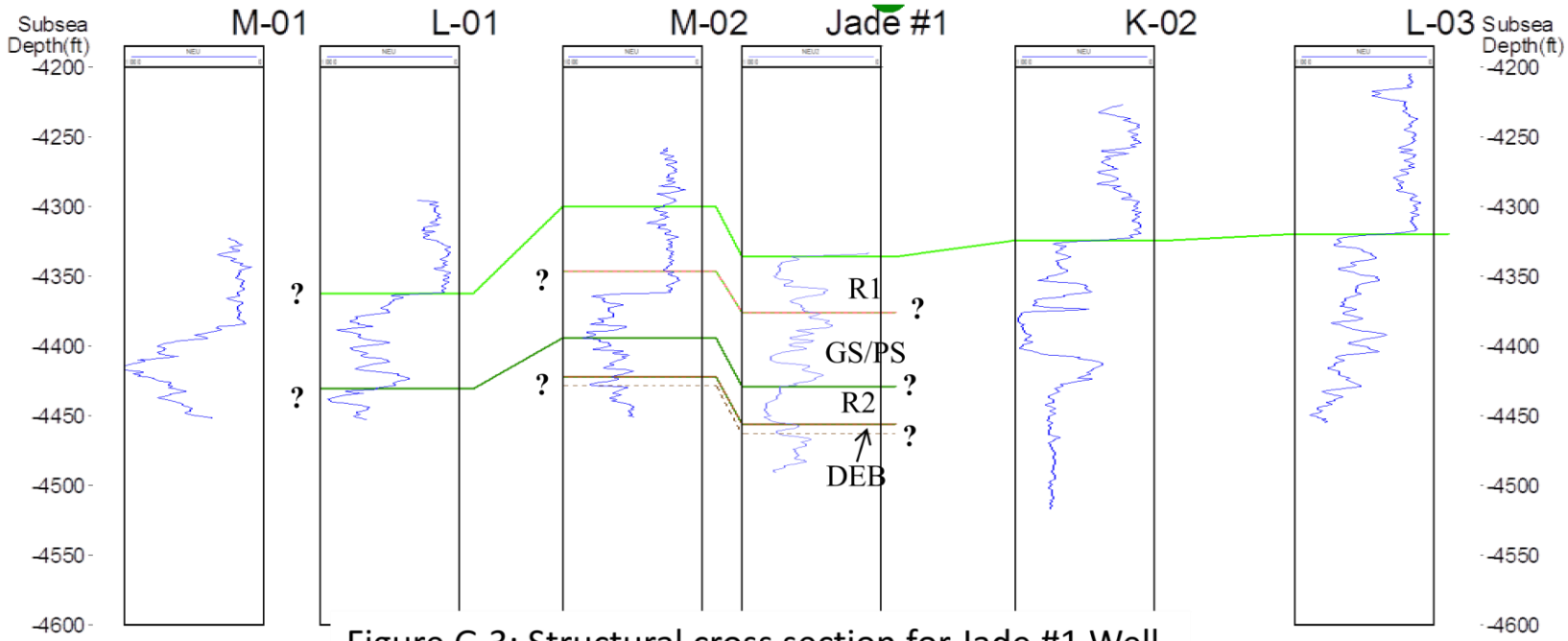

Figure G.3: Structural cross section for Jade #1 Well

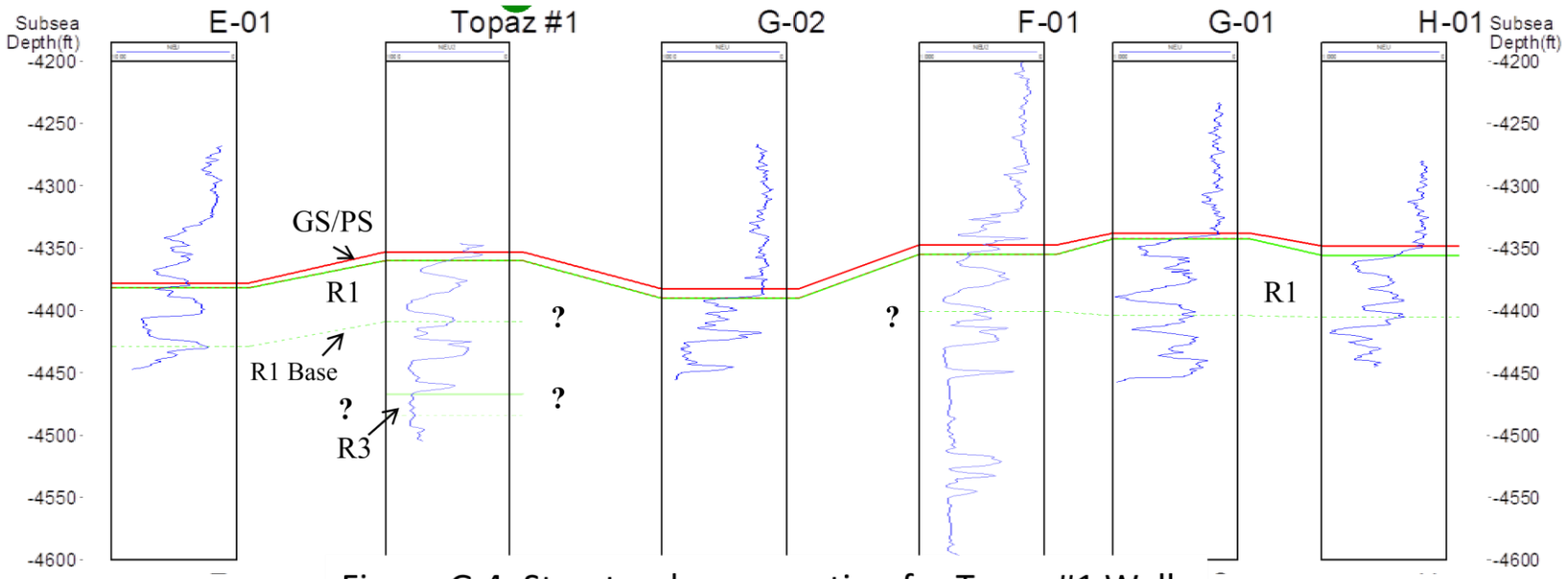

Figure G.4: Structural cross section for Topaz #1 Well

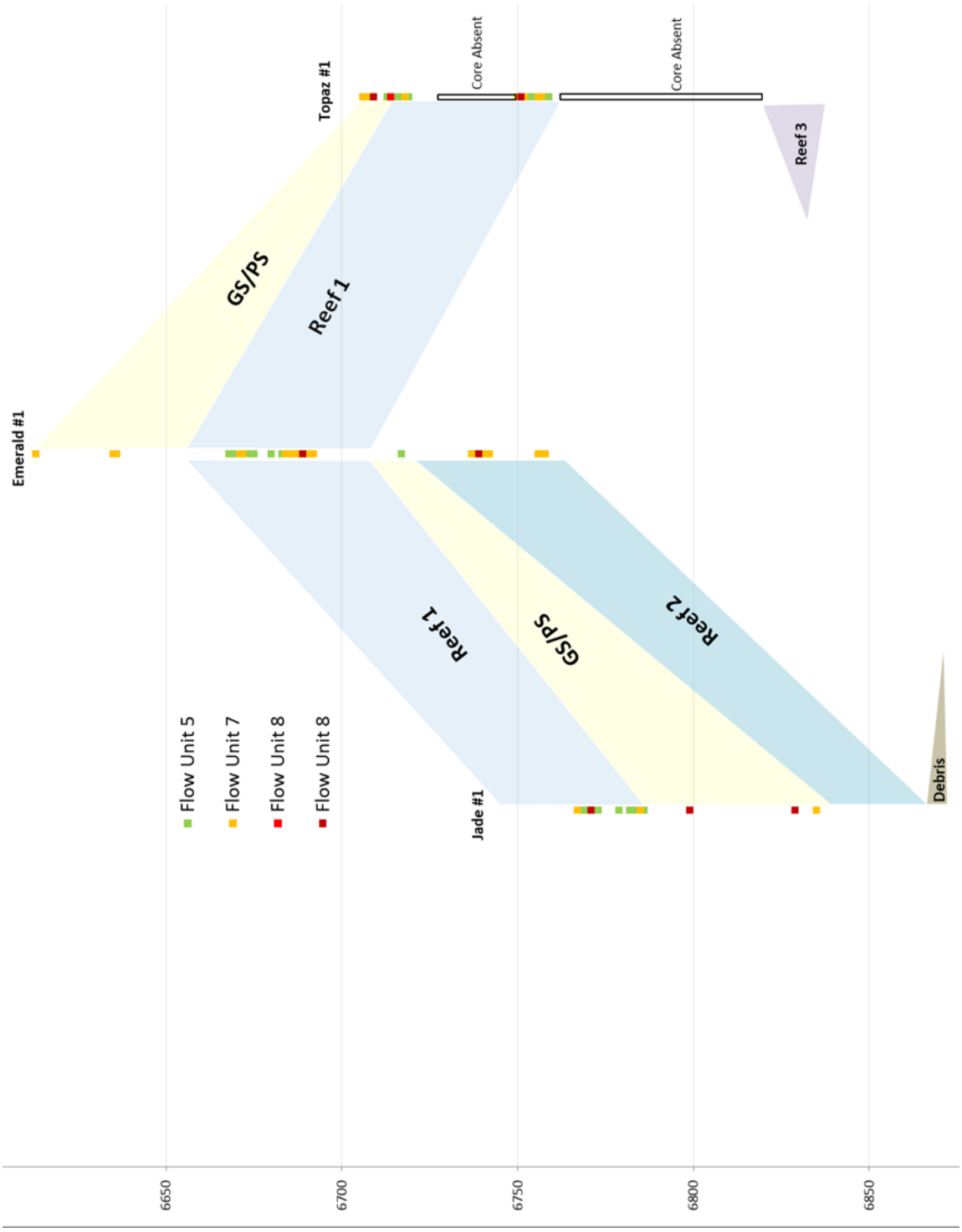

Figure G.5: Cross section showing depositional facies and good flow unit distribution between cored wells.

APPENDIX H

FIGURES

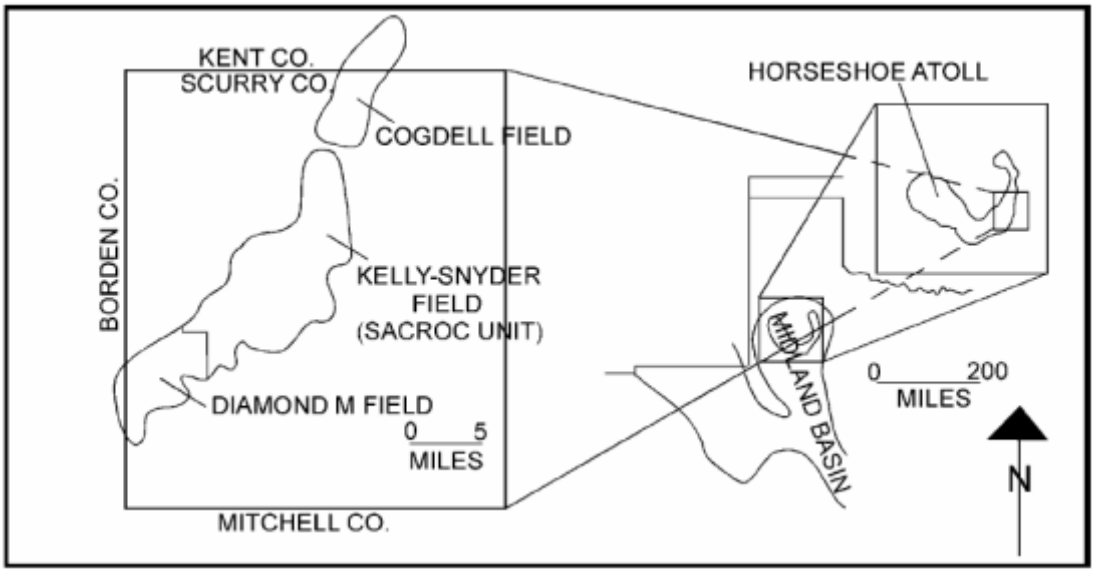

Figure H.1: Map of West Texas showing the Horseshoe atoll and Diamond M field
Source: Fisher (2005)

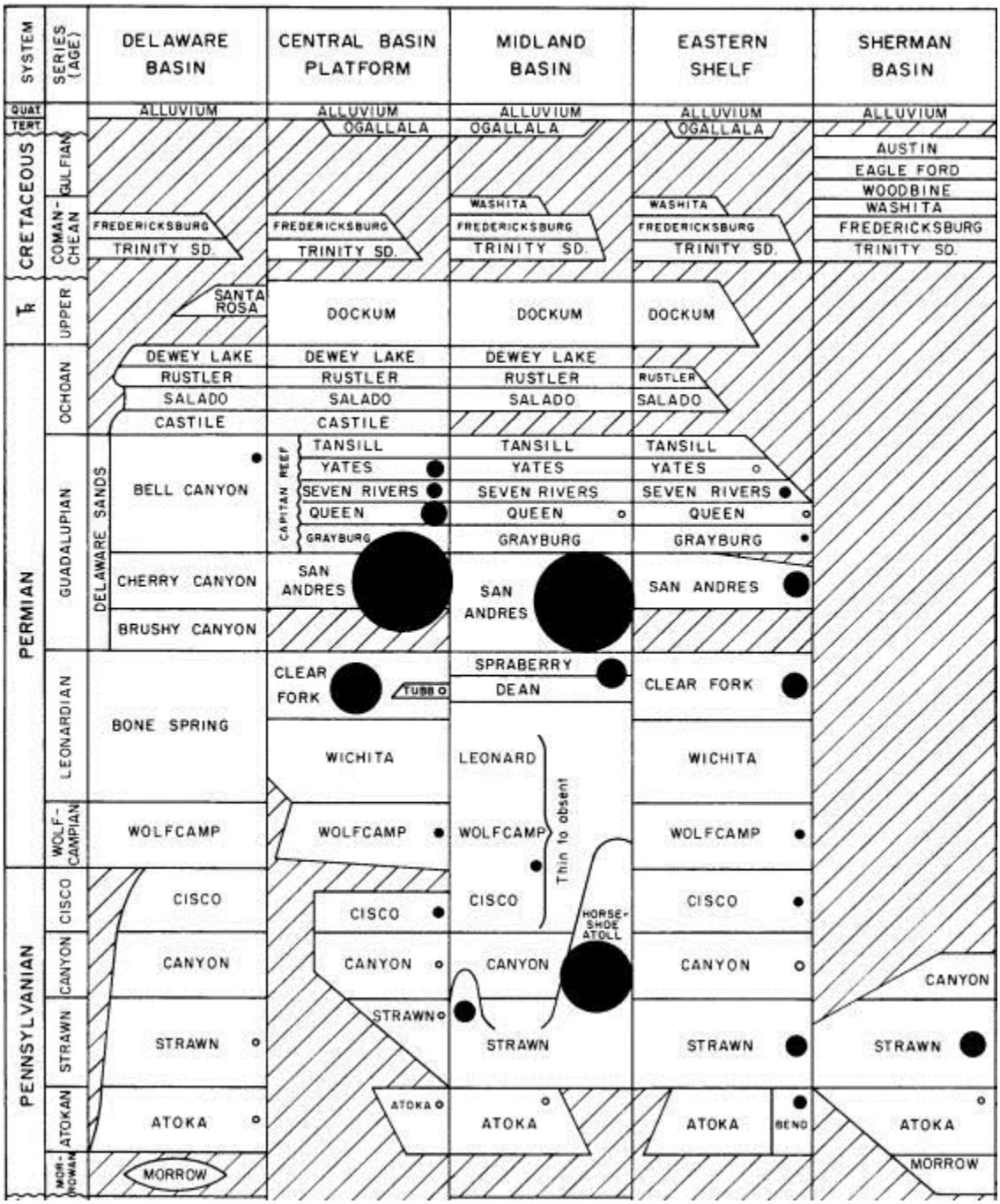

Figure H.2: Stratigraphic cross-section of Permian Basin region with black circles indicating the sizes of the oil reservoir. Source: Galloway et al. (1983) in Alnaji (2002)

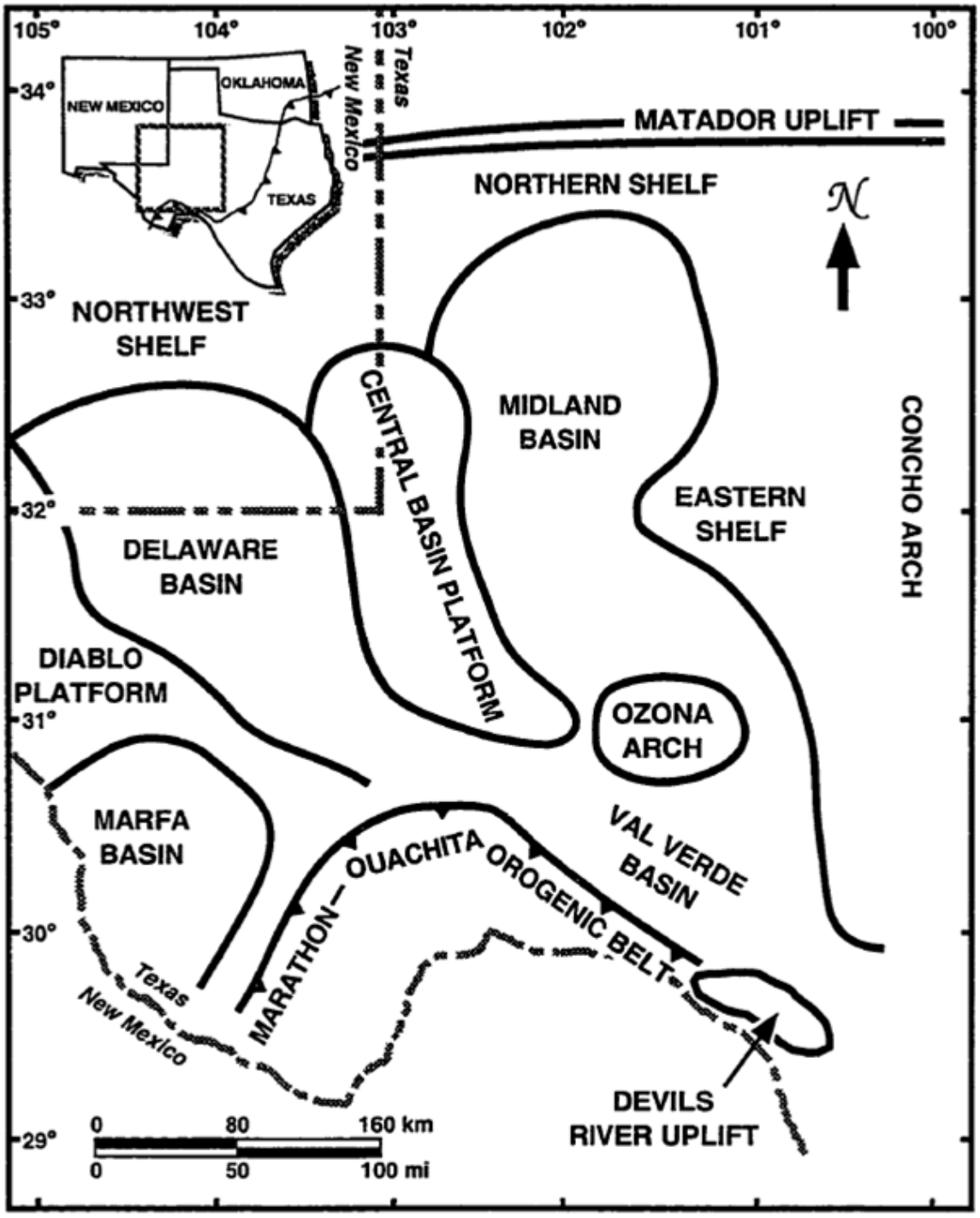

Figure H.3: Map of the Permian Basin region showing major paleotopographic and tectonic features of late Paleozoic age. Modified from Hanson et al. (1991). Source: Yang and Dorobek (1995a)

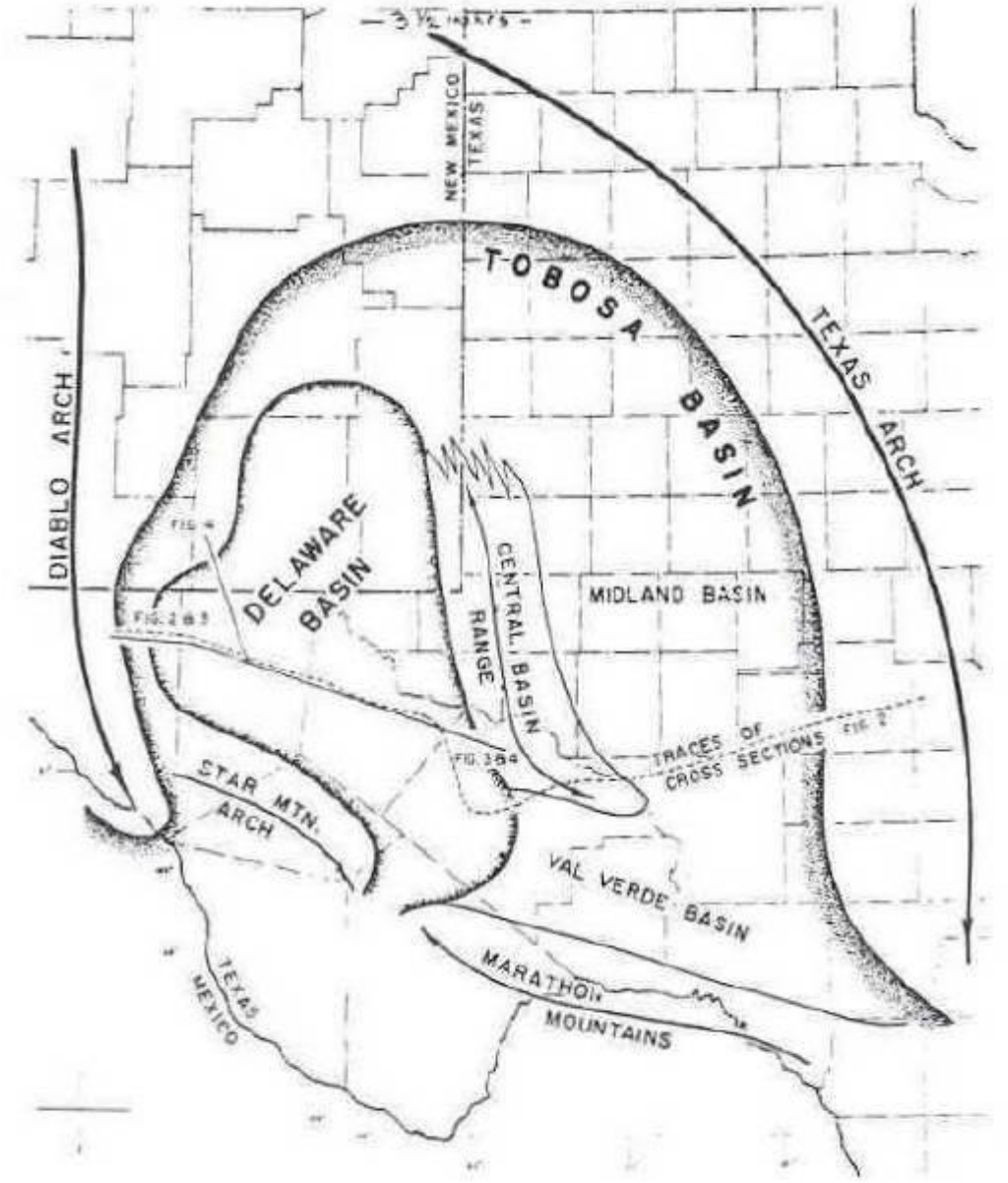

Figure H.4: The tectonic development of Tobosa Basin by the end of Mississippian, which originated the Delaware Basin, Central Basin Platform, and Midland Basin. Source: Adams (1965) in Alnaji (2002)

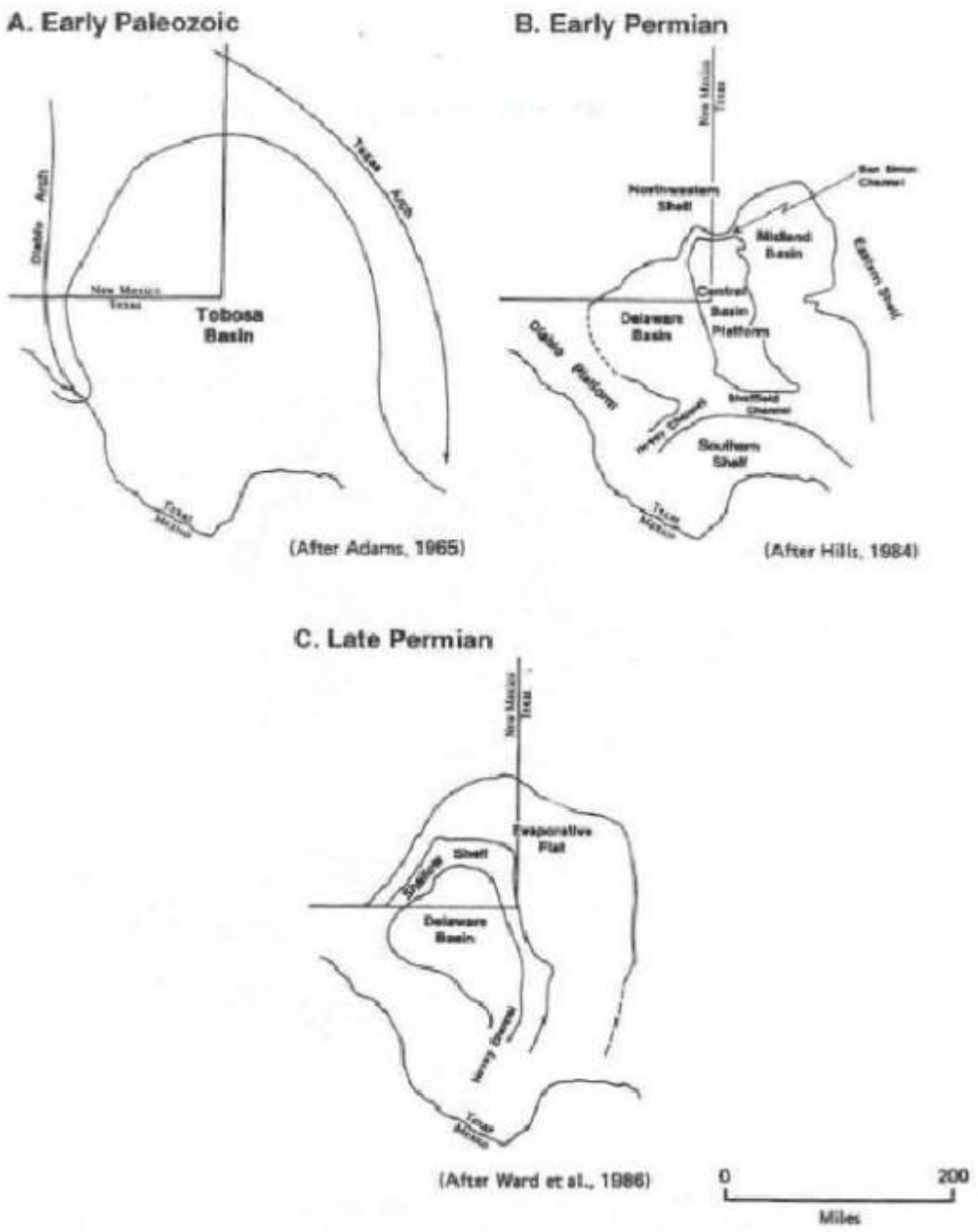

Figure H.5: Evolution of the Permian Basin, from Early Paleozoic to the Late Permian
Source: Garber et al. (1989) in Alnaji (2002)

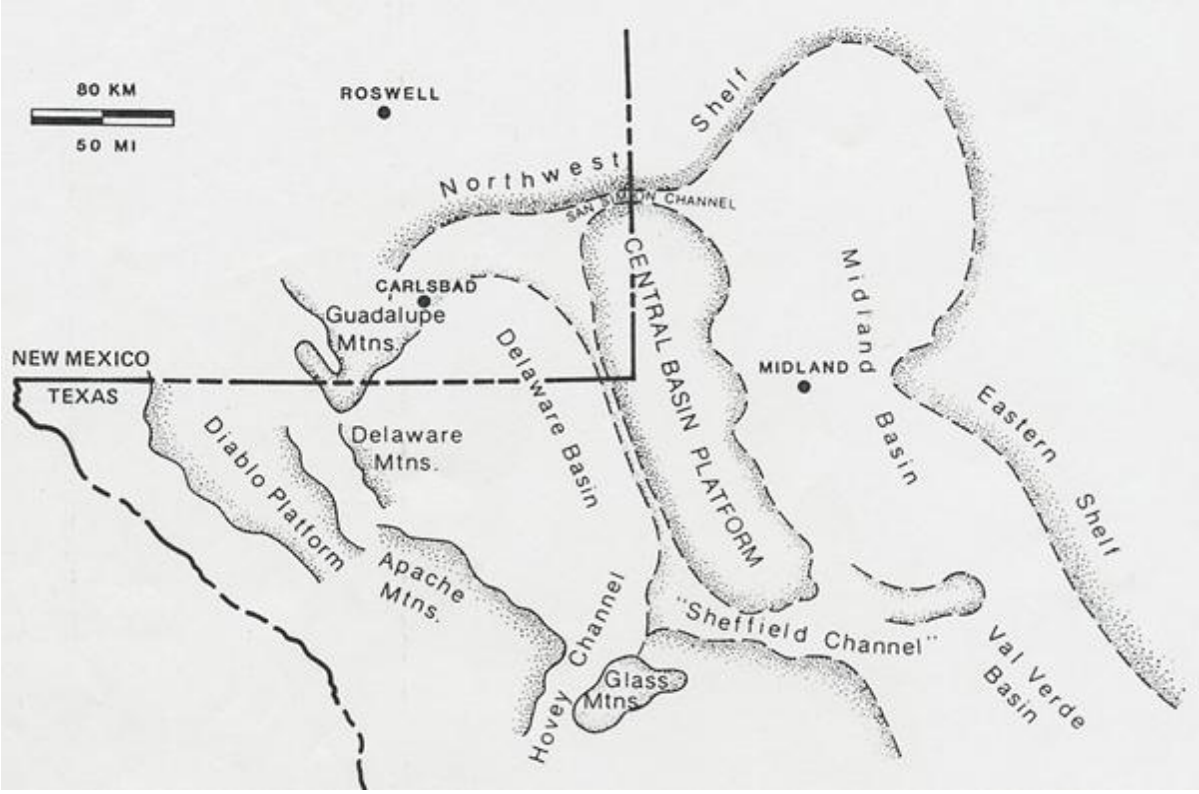

Figure H.6: Map of Permian Basin during Late Permian time. Source: Ward et al. (1986) in Alnaji (2002)

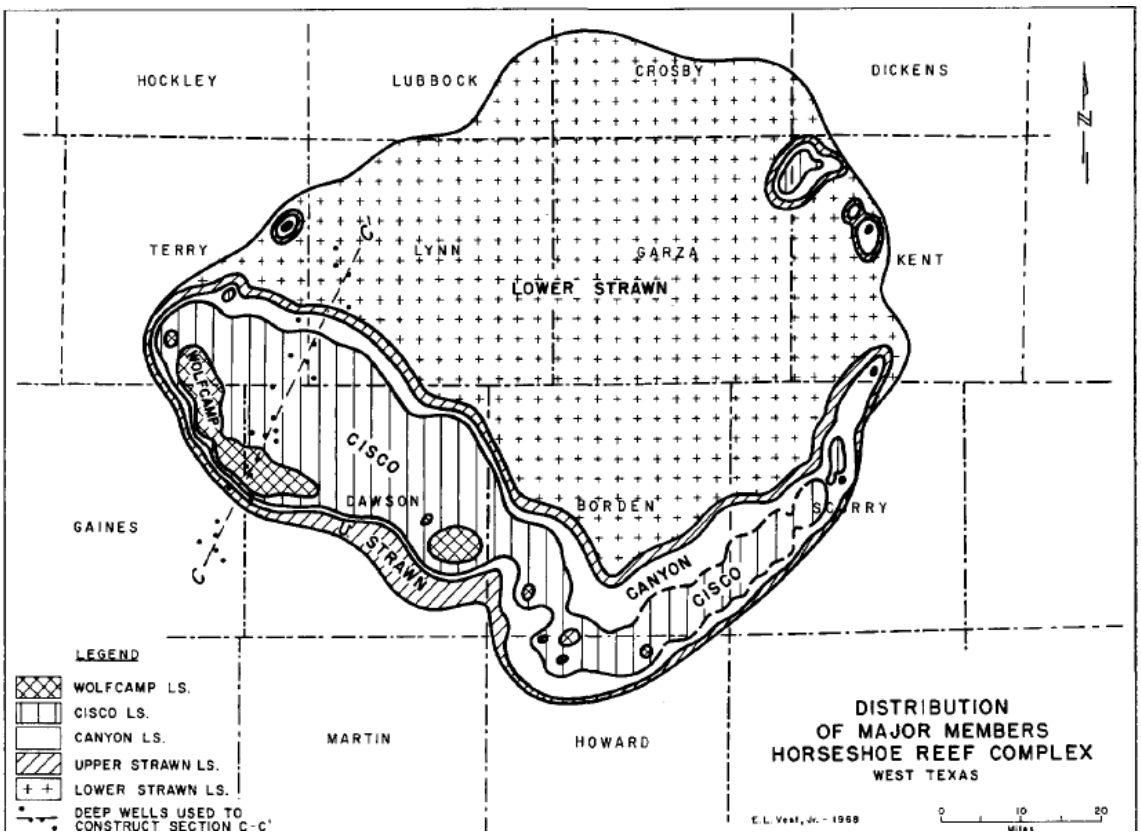

Figure H.7: Distribution of major units in the Horseshoe atoll. Source: Vest (1970)

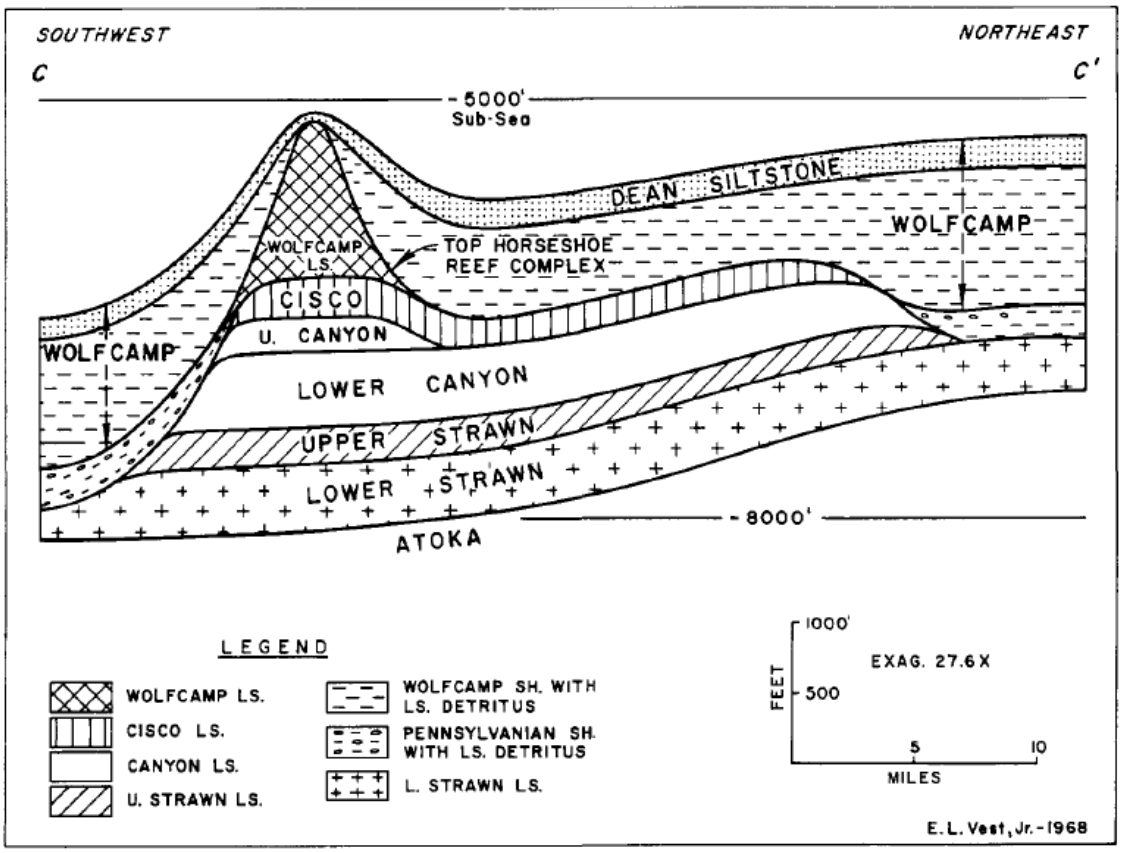

Figure H.8: Cross section from C-C' shown in Figure 7 through the thickest part of the Horseshoe atoll. Source: Vest (1970)

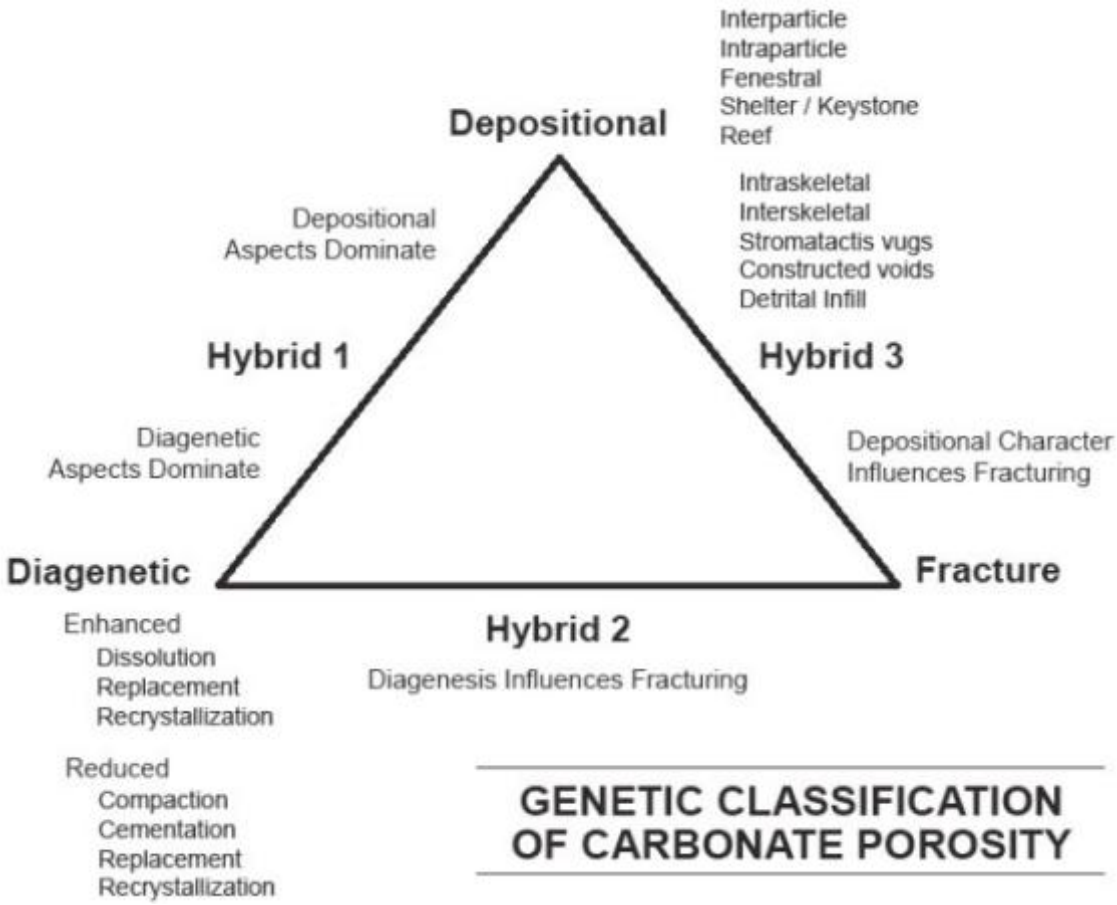

Figure H.9: Ahr genetic classification of carbonate porosity. Source: Ahr et al., (2005)

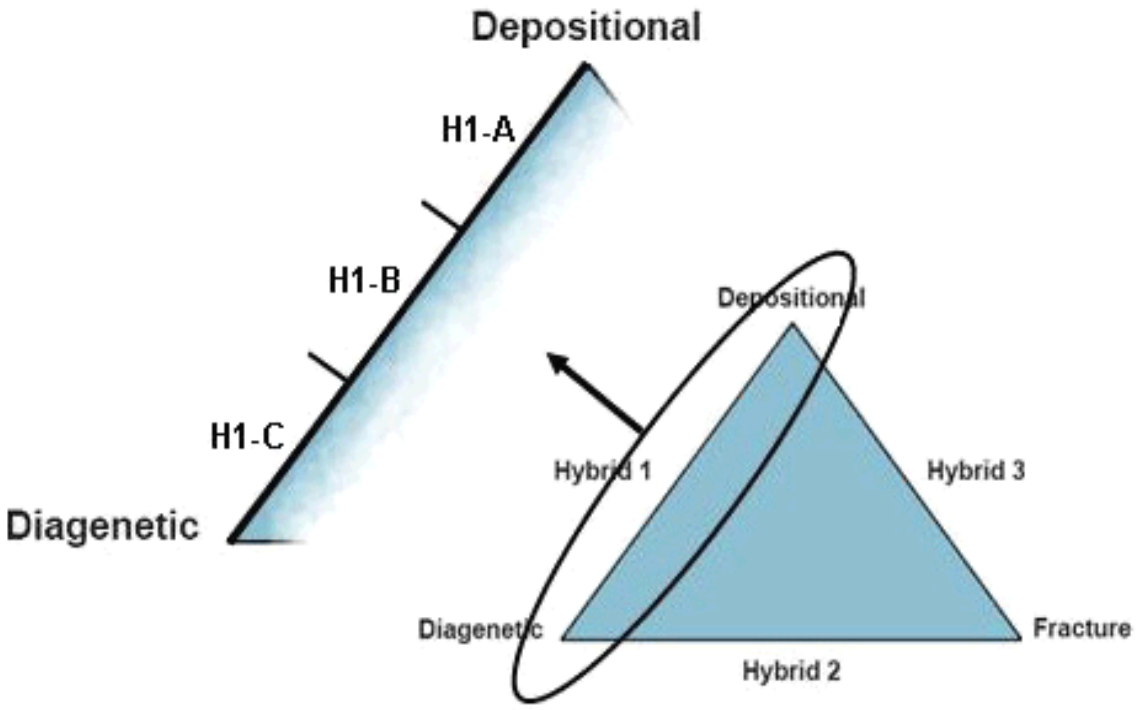

Figure H.10: Humbolt modification of the Ahr porosity classification. Source: Ahr et al. (2011)

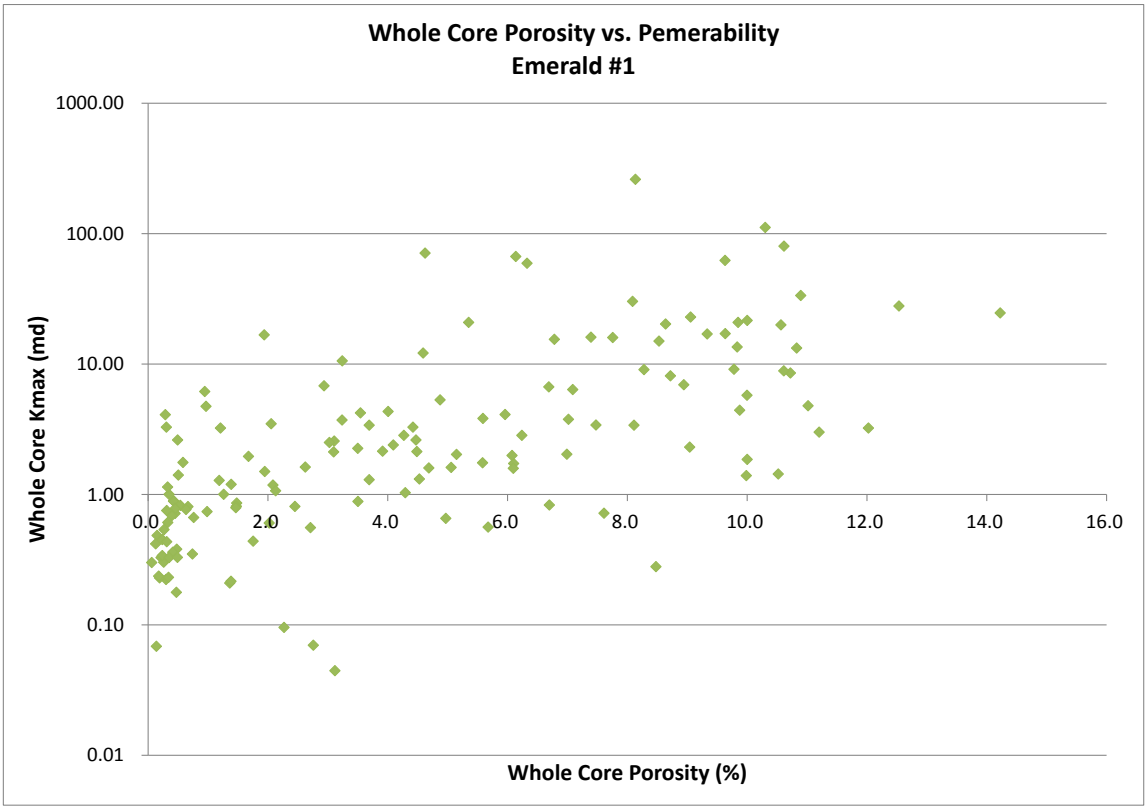

Figure H.11: Whole core porosity vs permeability for the Emerald #1 well. R^2 value on a linear trend line is 0.1104

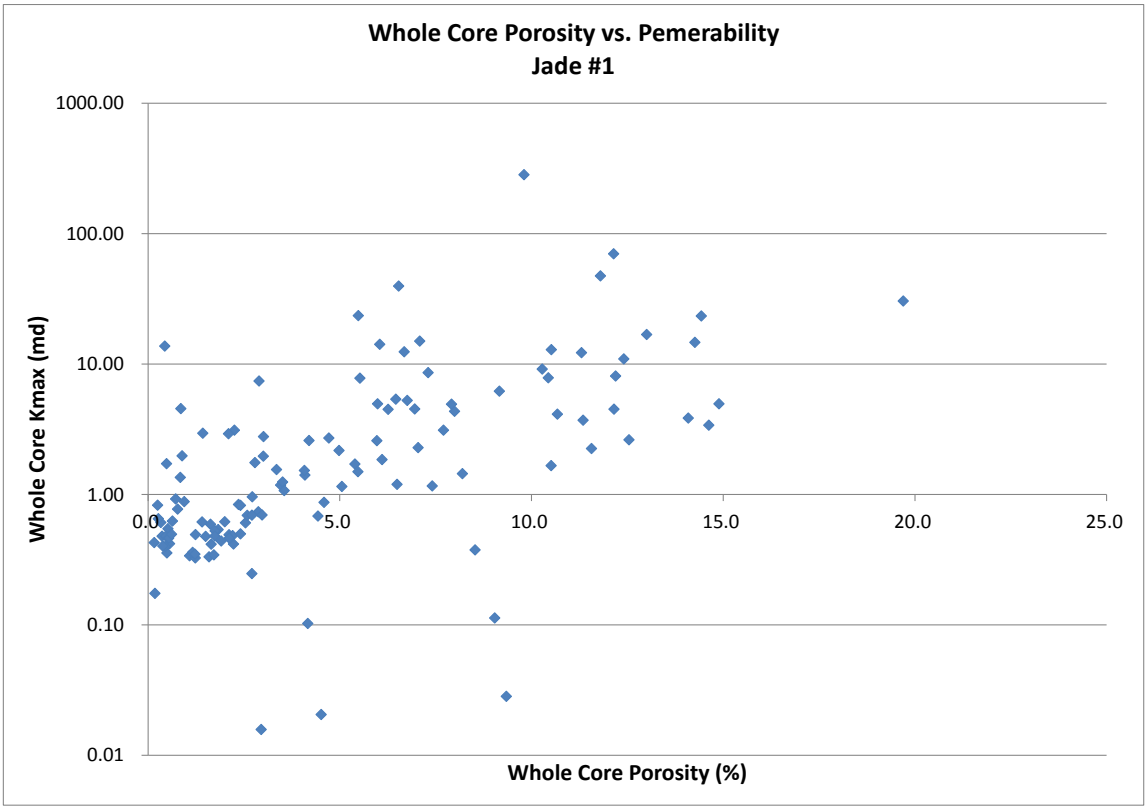

Figure H.12: Whole core porosity vs permeability for the Jade #1 well. R^2 value on a linear trend line is 0.073

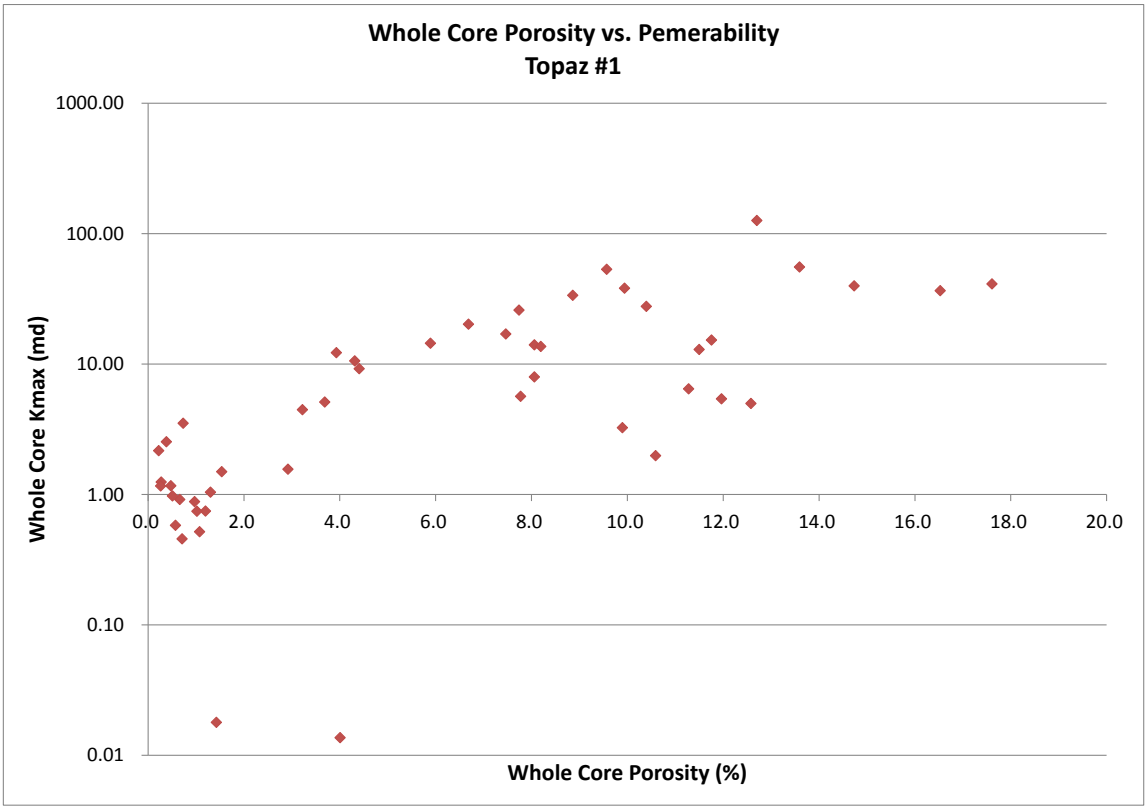

Figure H.13: Whole core porosity vs permeability for the Jade #1 well. R^2 value on a linear trend line is 0.3763

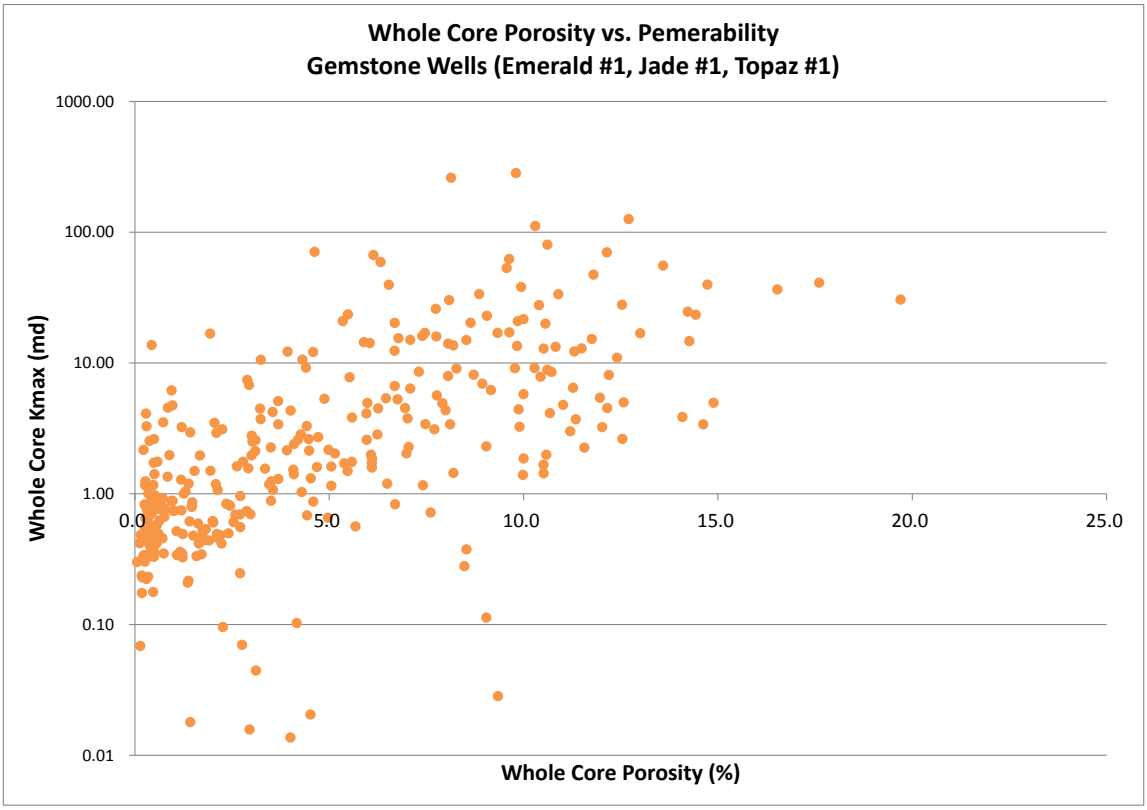

Figure H.14: Whole core porosity vs permeability for the all of the cored wells. R^2 value on a linear trend line is 0.1217

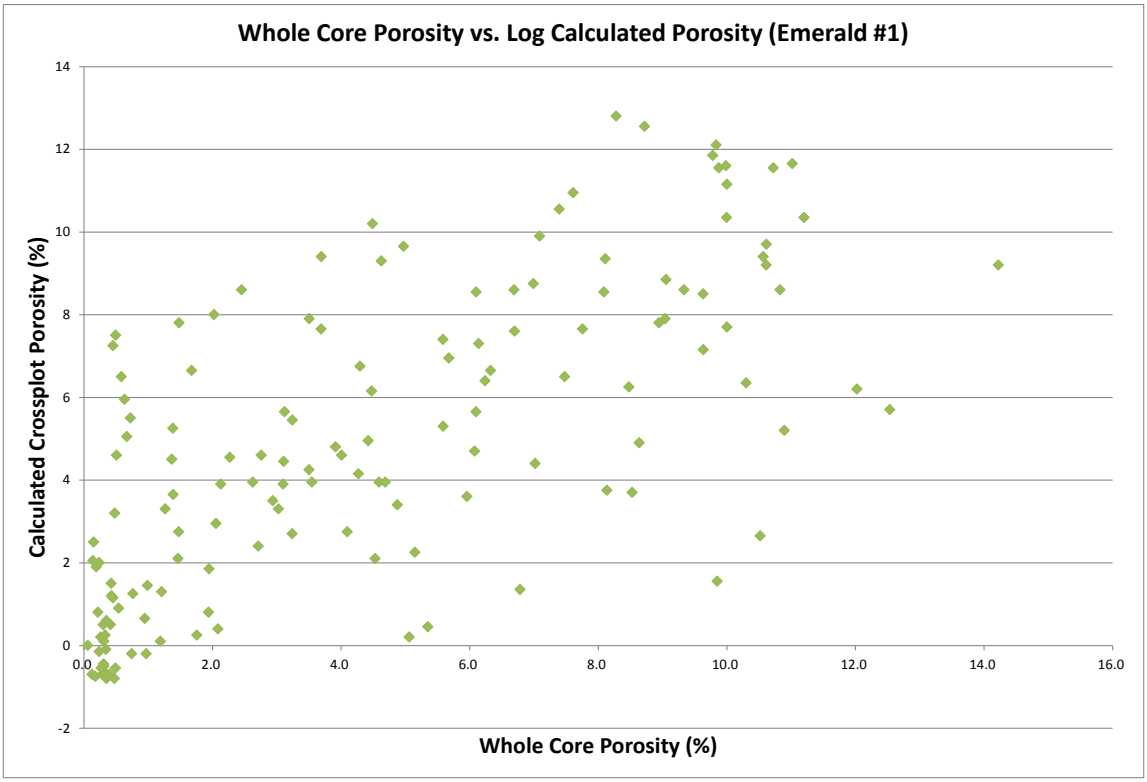

Figure H.15: Whole core porosity vs calculated log porosity for the Emerald #1 well. R^2 value on a linear trend line is 0.5041

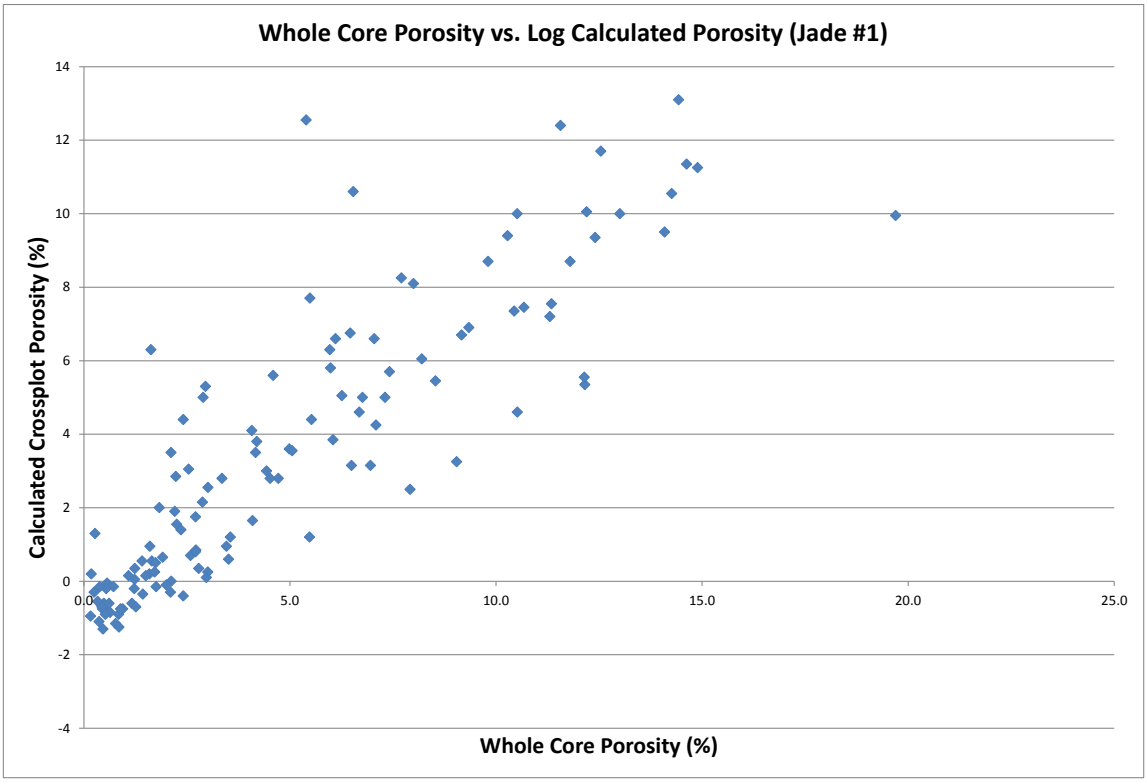

Figure H.16: Whole core porosity vs calculated log porosity for the Jade #1 well. R^2 value on a linear trend line is 0.7674

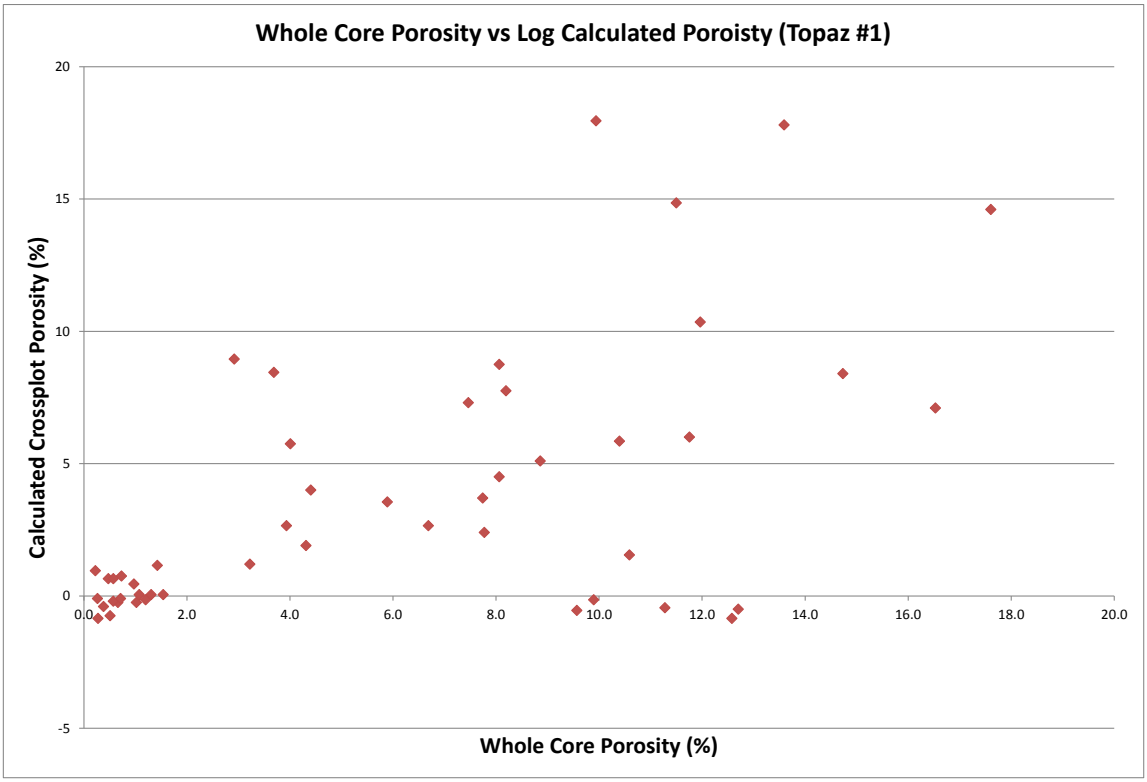

Figure H.17: Whole core porosity vs calculated log porosity for the Topaz #1 well. R^2 value on a linear trend line is 0.3493

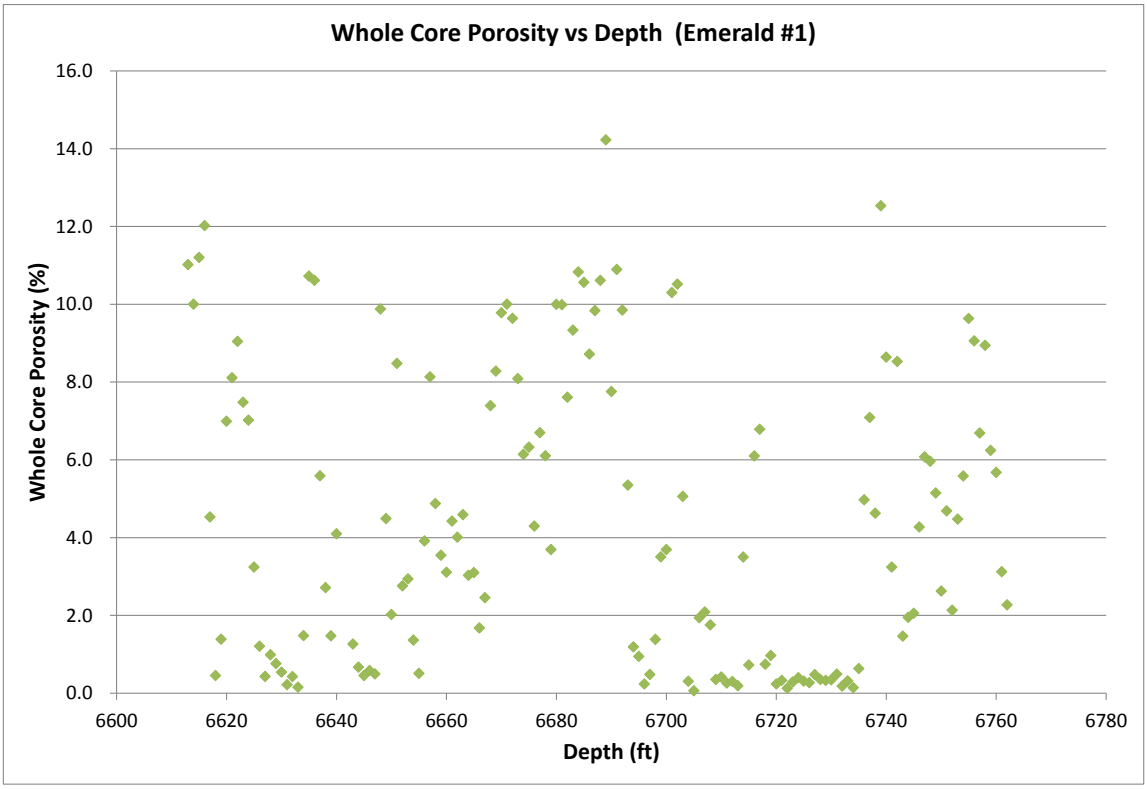

Figure H.18: Whole core porosity vs. depth for the Emerald #1 well. R^2 value on a linear trend line is 0.0114

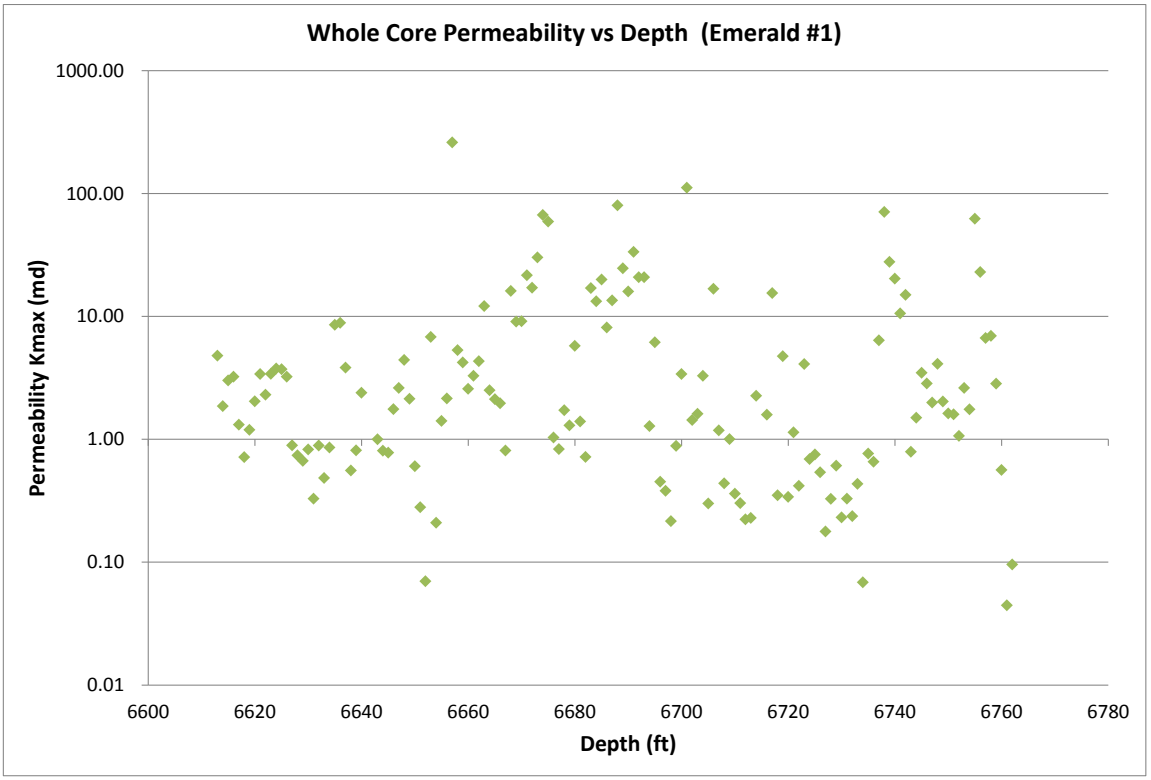

Figure H.19: Whole core permeability vs depth for the Emerald #1 well. R^2 value on a linear trend line is 0.000078

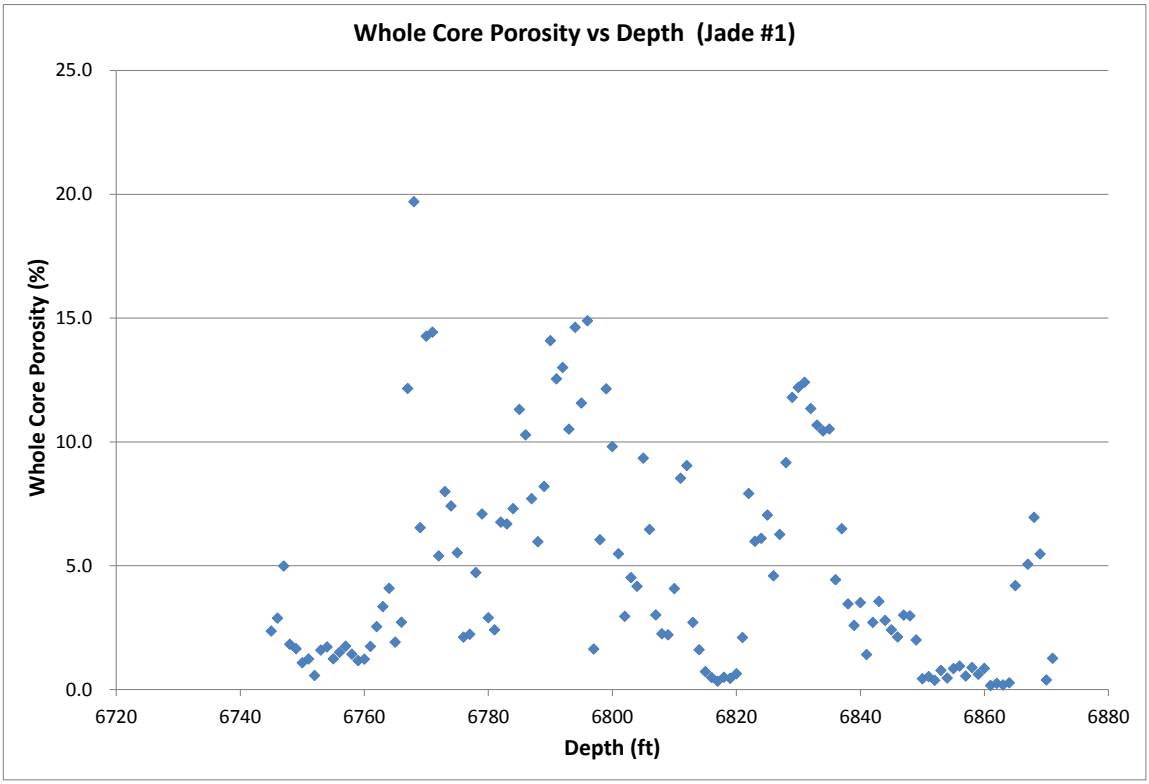

Figure H.20: Whole core porosity vs depth for the Jade #1 well. R^2 value on a linear trend line is 0.0285

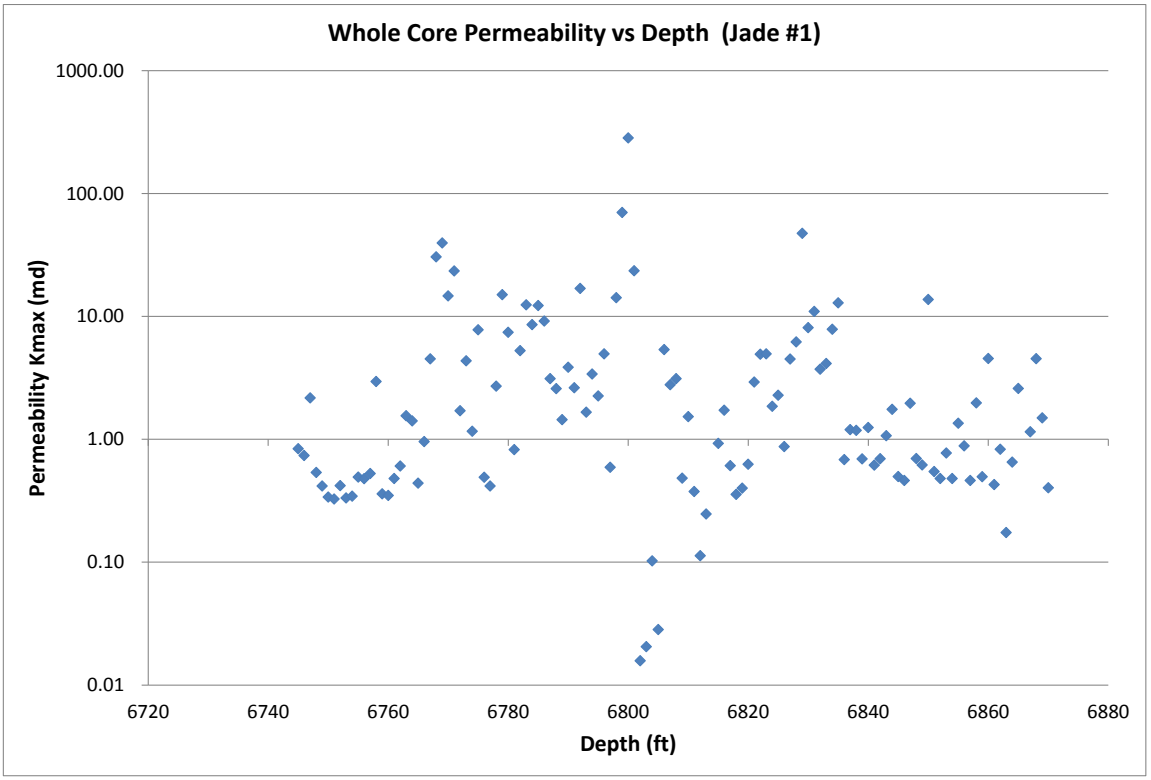

Figure H.21: Whole core permeability vs depth for the Jade #1 well. R^2 value on a linear trend line is 0.0026

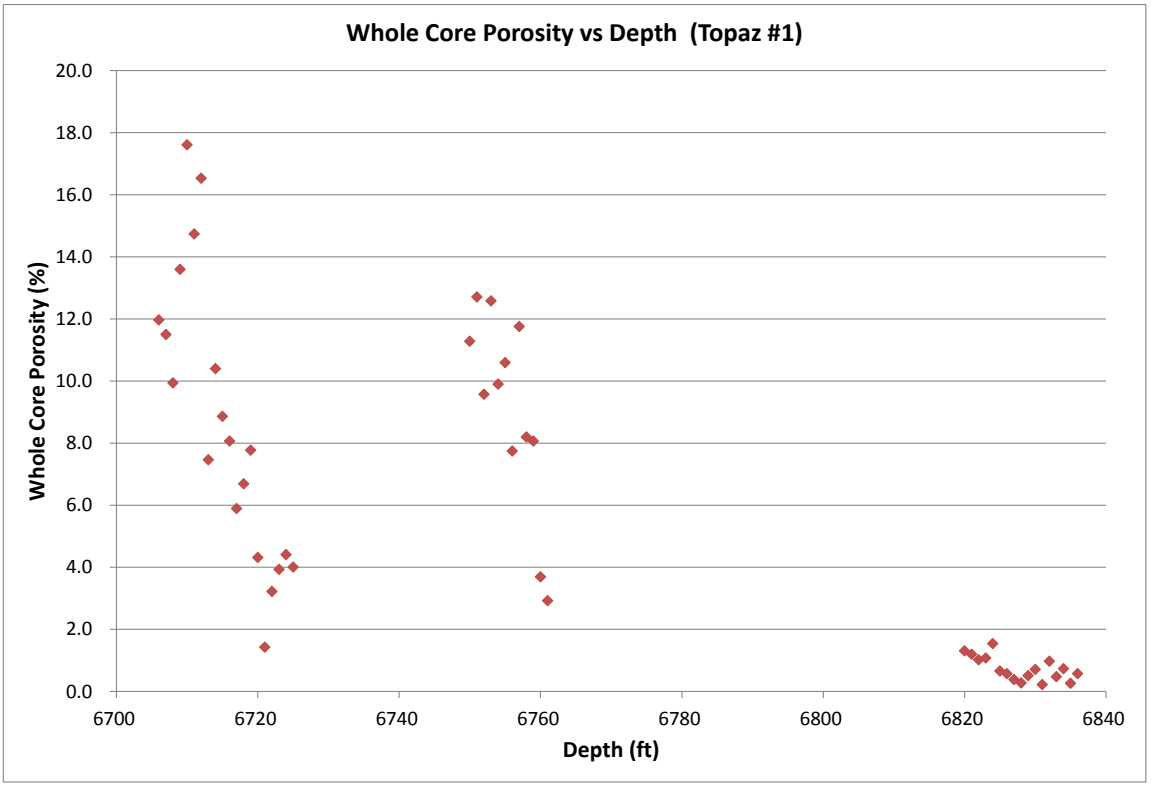

Figure H.22: Whole core porosity vs depth for the Topaz #1 well. R^2 value on a linear trend line is 0.5657

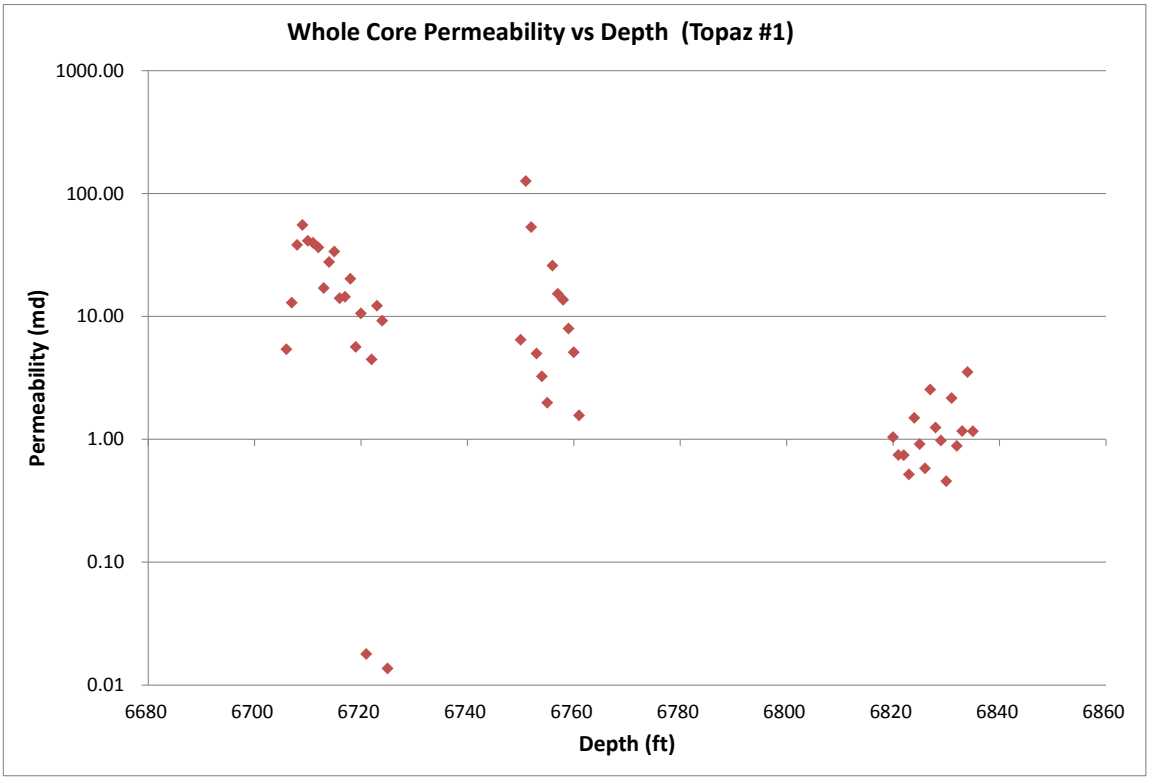

Figure H.23: Whole core permeability vs depth for the Topaz #1 well. R^2 value on a linear trend line is 0.1801

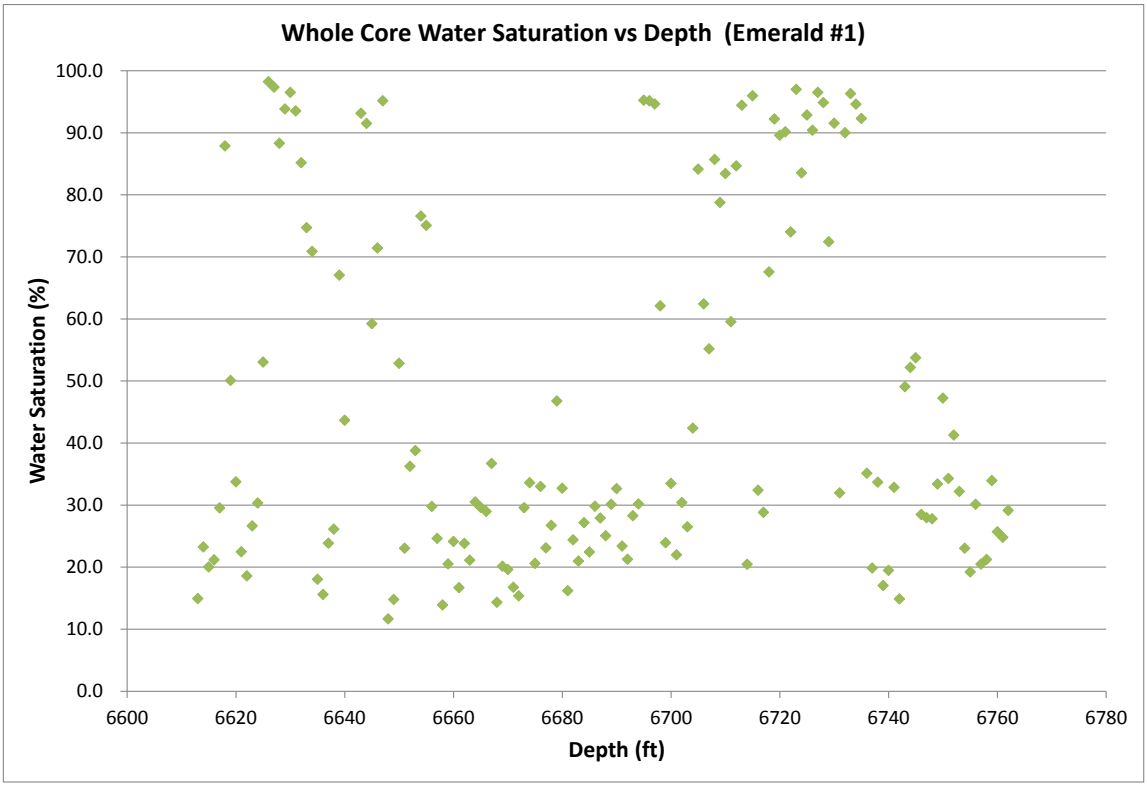

Figure H.24: Whole core water saturation vs depth for Emerald #1 well. R^2 value on a linear trend line is 0.0011

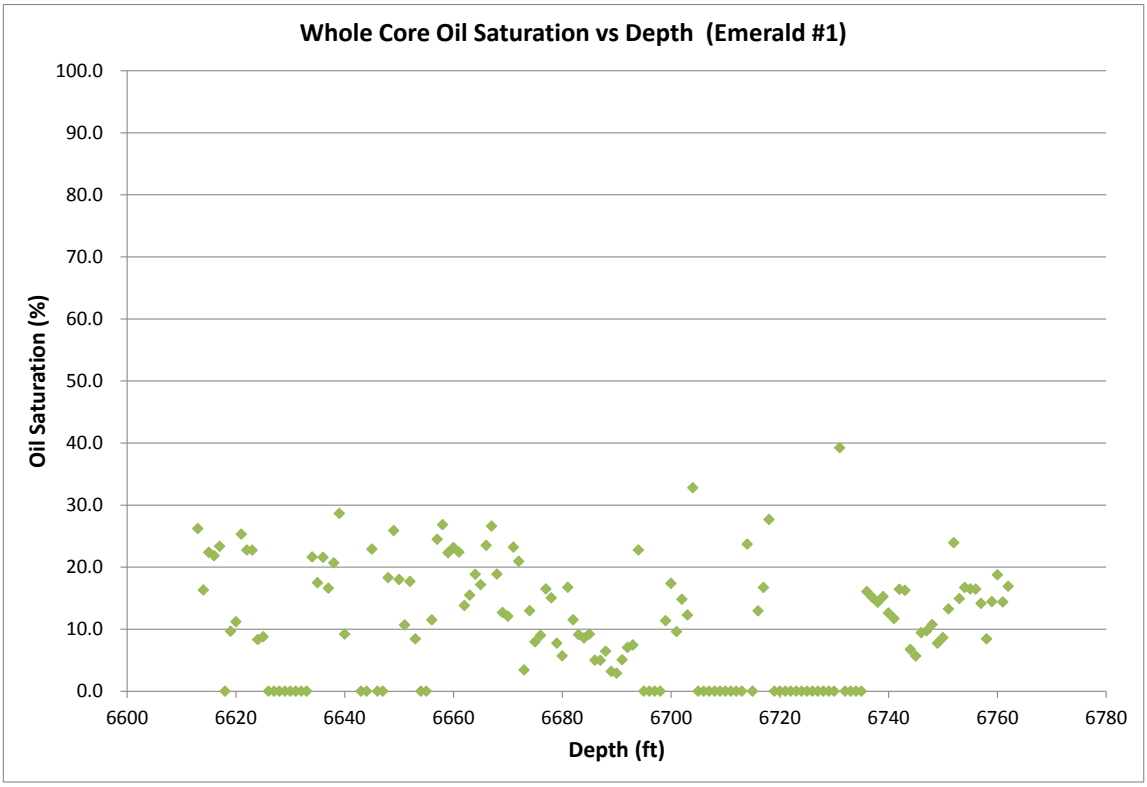

Figure H.25: Whole core oil saturation vs depth for Emerald #1 well. R^2 value on a linear trend line is 0.02

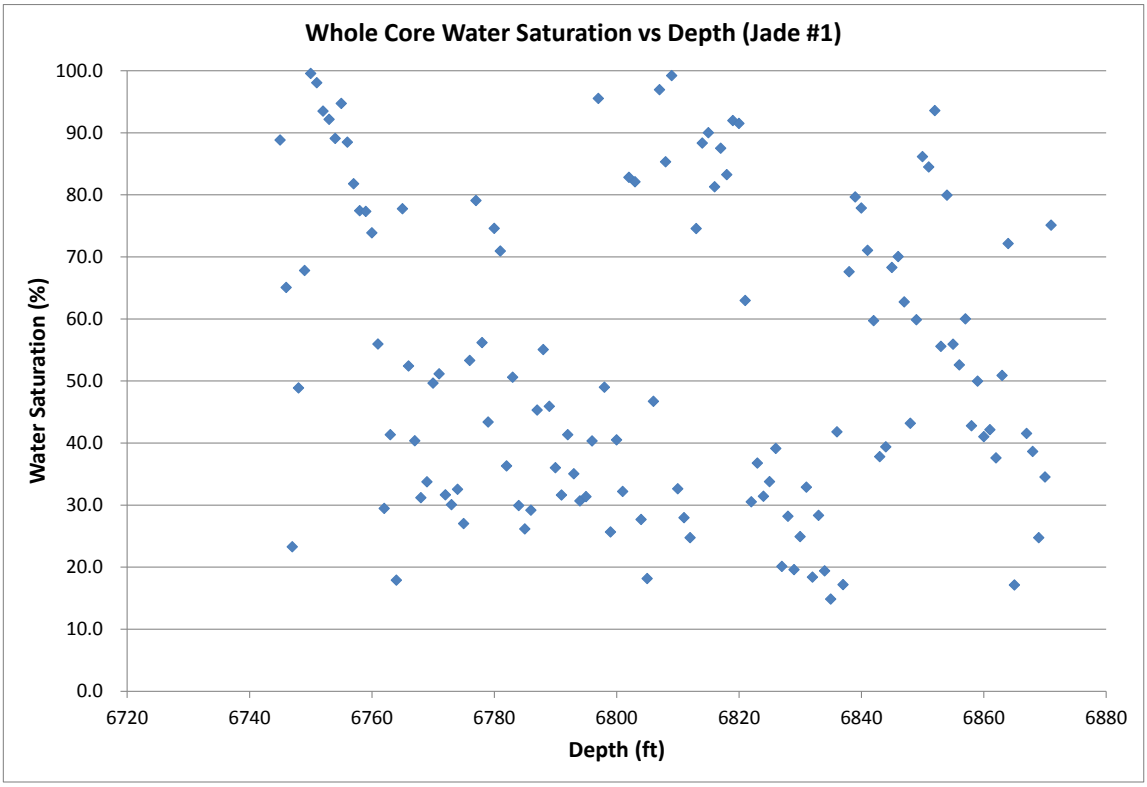

Figure H.26: Whole core water saturation vs depth for Jade #1 well. R^2 value on a linear trend line is 0.0214

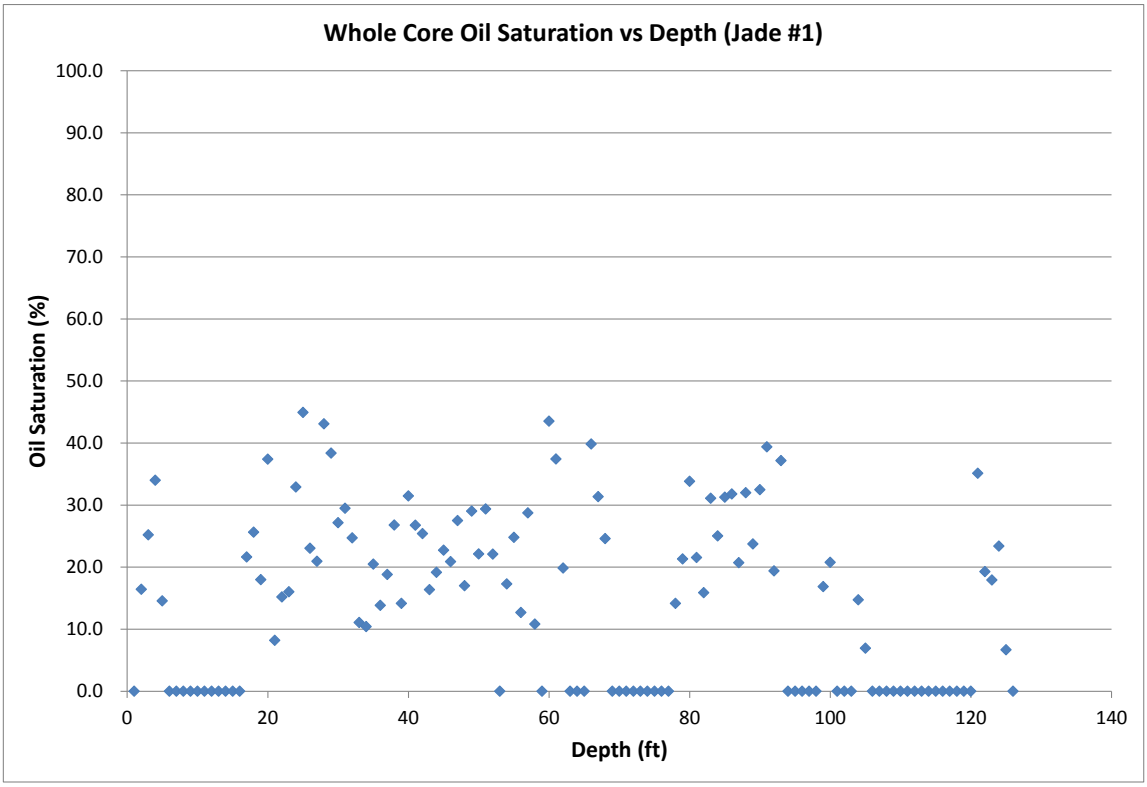

Figure H.27: Whole core oil saturation vs depth for Jade #1 well. R^2 value on a linear trend line is 0.0434

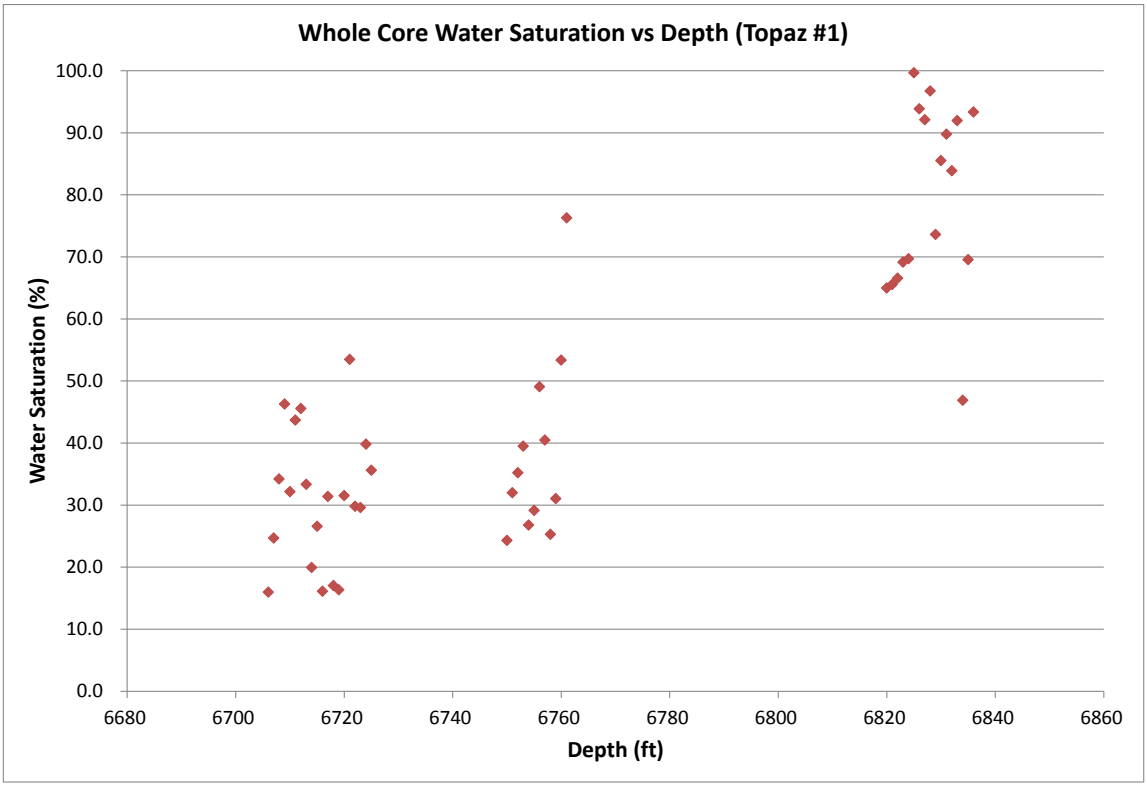

Figure H.28: Whole core water saturation vs depth for Topaz #1 well. R^2 value on a linear trend line is 0.7245

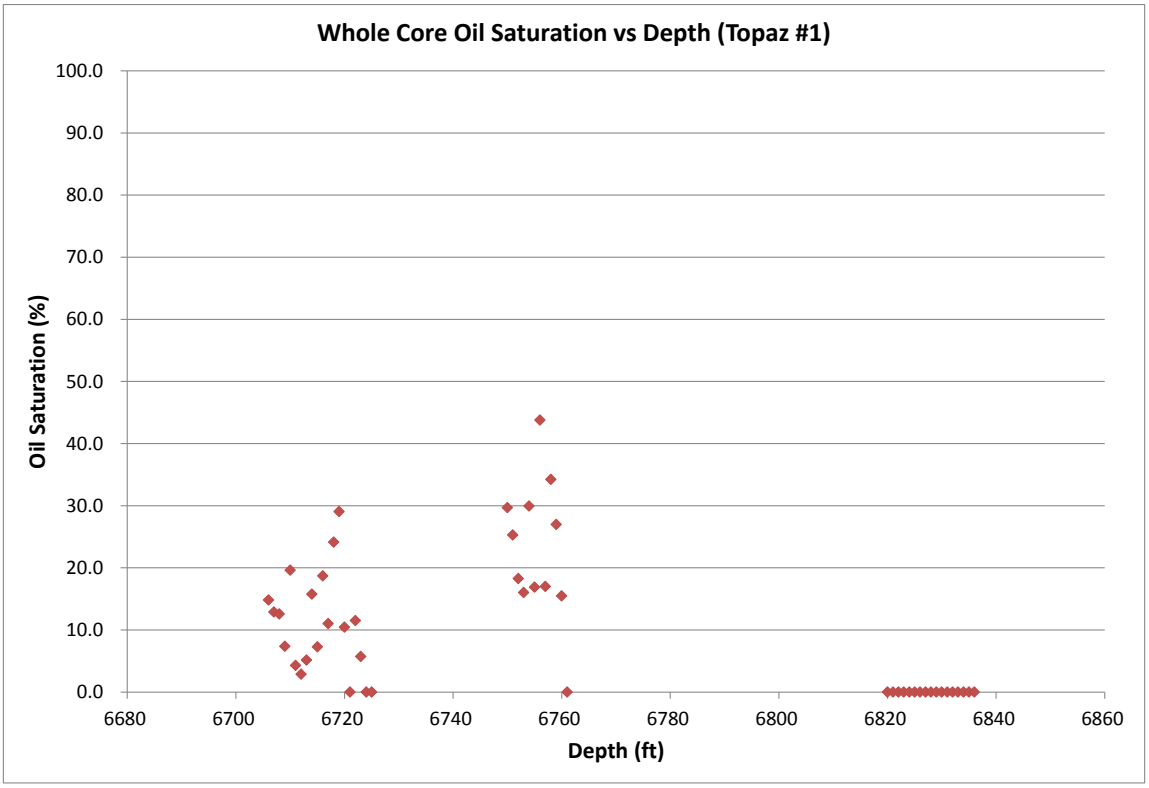

Figure H.29: Whole core oil saturation vs depth for Topaz #1 well. R^2 value on a linear trend line is 0.2319

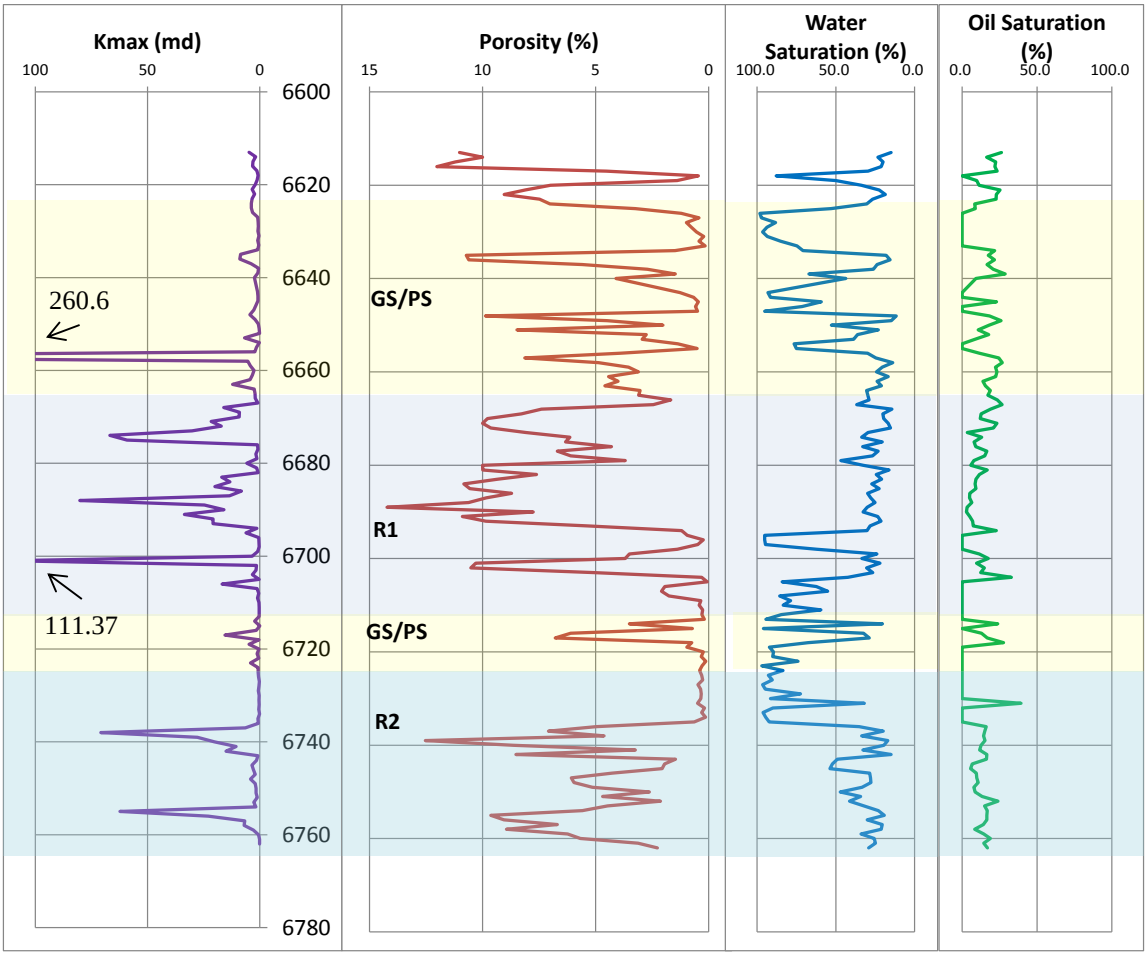

Figure H.30: Permeability, Porosity, and Fluid Saturation for Emerald #1 well. Observed lithofacies also noted.

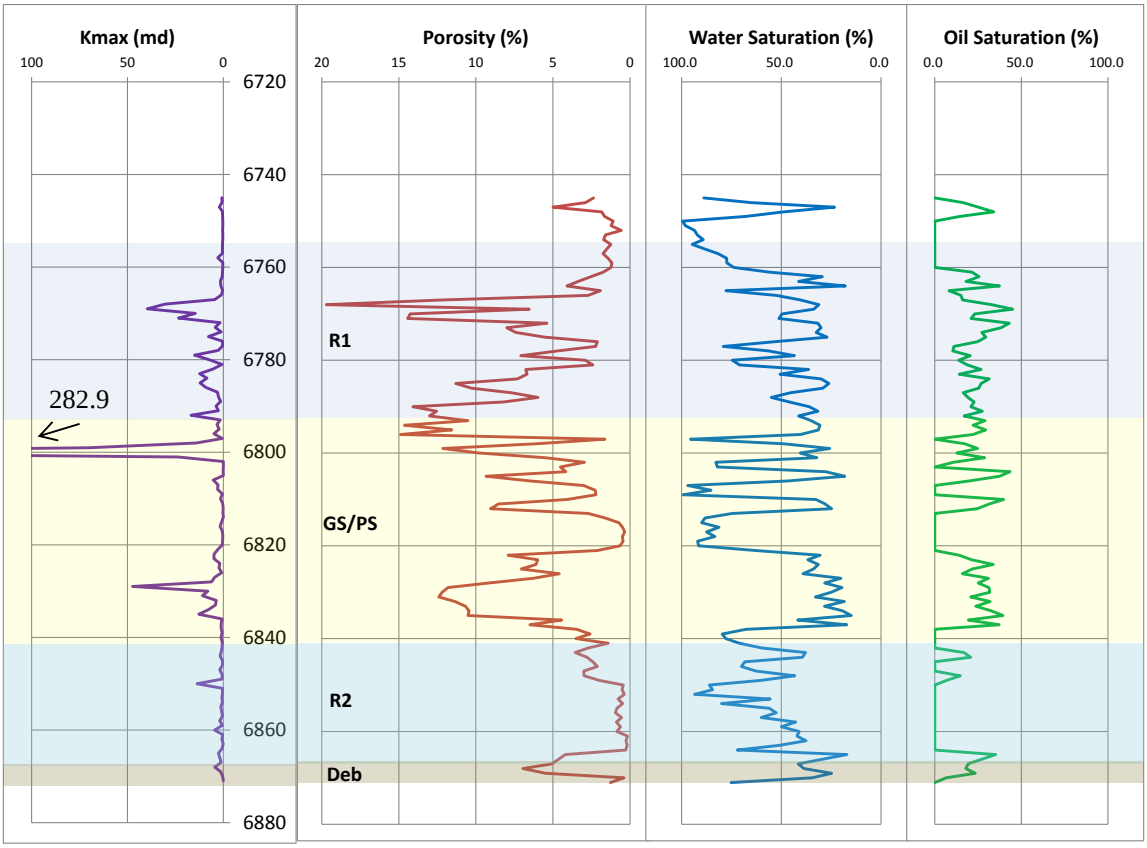

Figure H.31: Permeability, Porosity, and Fluid Saturation for Jade #1 well. Observed lithofacies also noted.

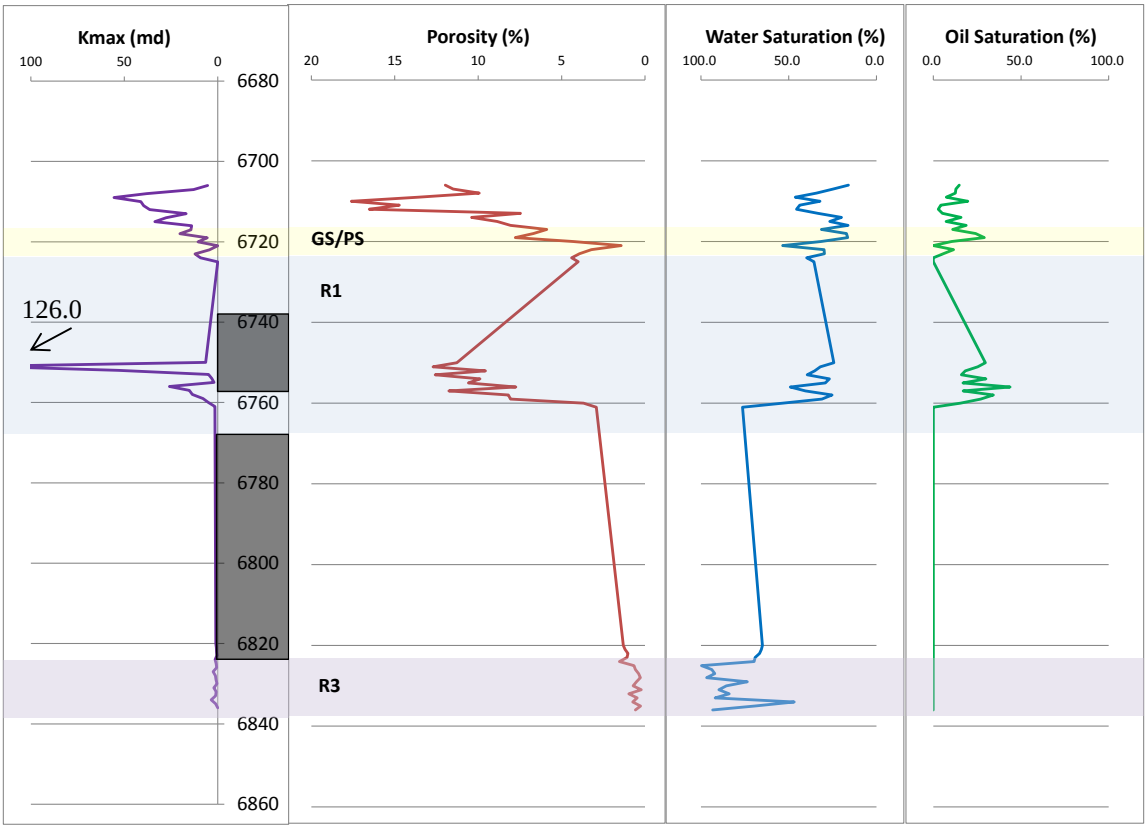

Figure H.32: Permeability, Porosity, and Fluid Saturation for Topaz #1 well. Observed lithofacies also noted. Dark gray areas are where core was absent.

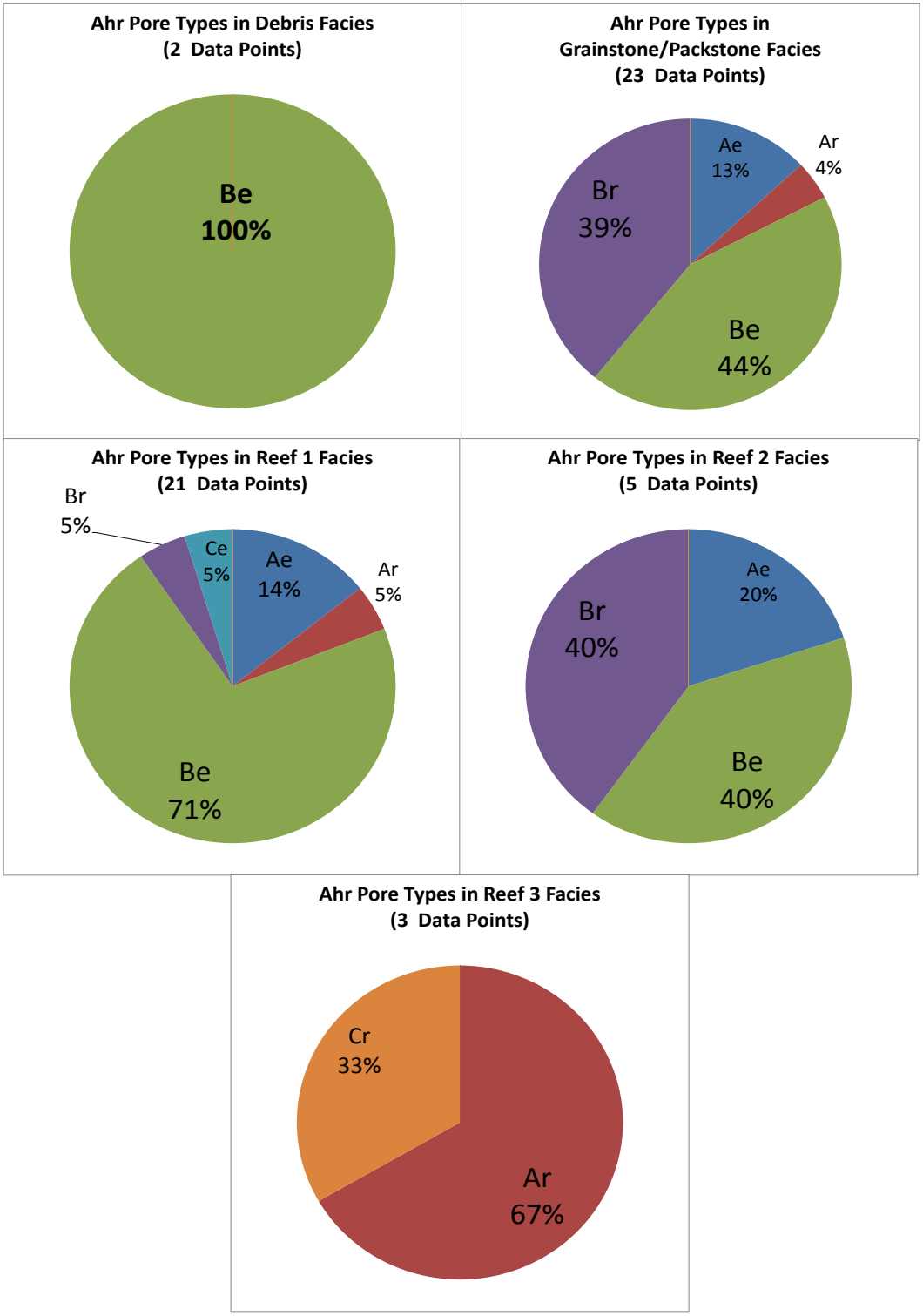

Figure H.33: Genetic pore type abundance by depositional facies. Data points indicate number of thin sections with observed pore types.

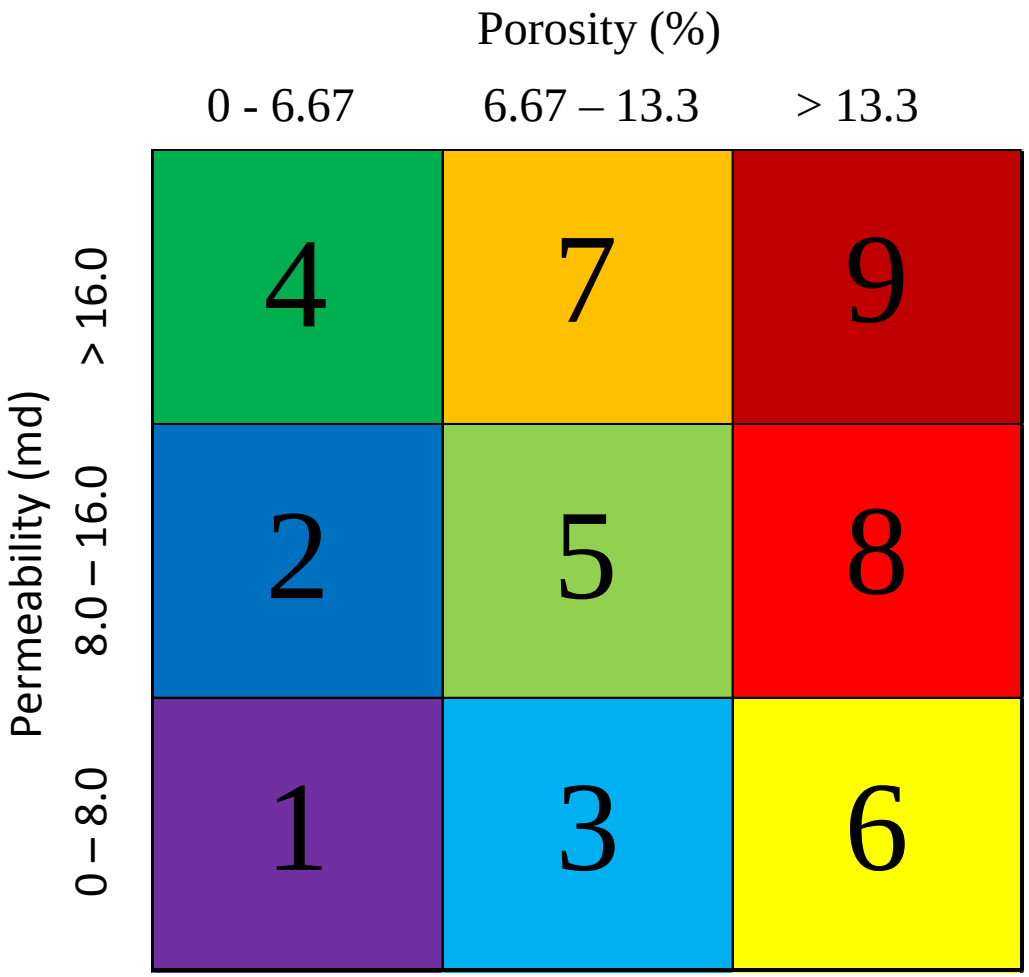

Figure H.34: Definition of flow units (poroperm brackets).

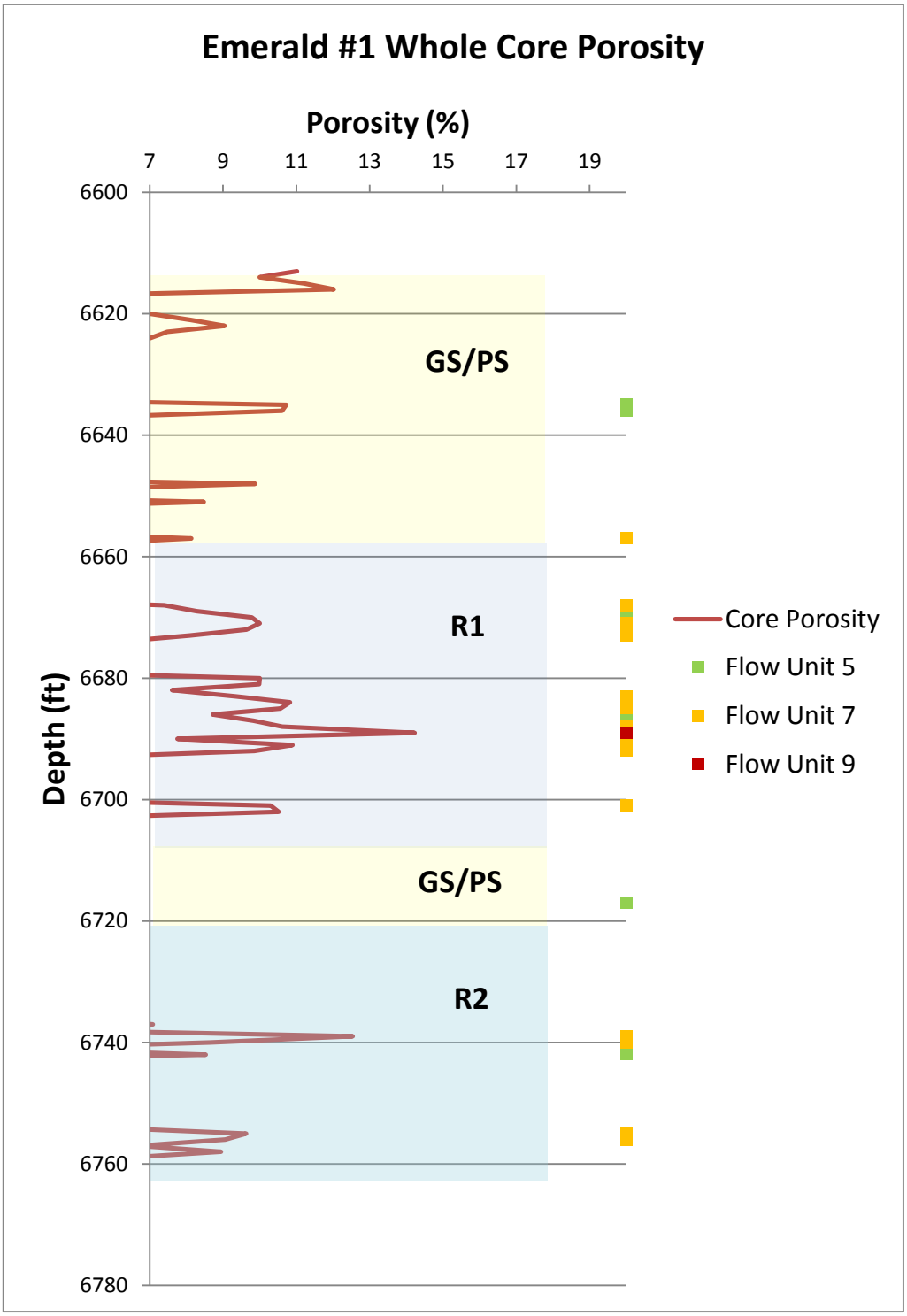

Figure H.35: Emerald #1 core analysis porosity and calculated log porosity with 7% cut off. Flow unit brackets and depositional lithofacies also shown.

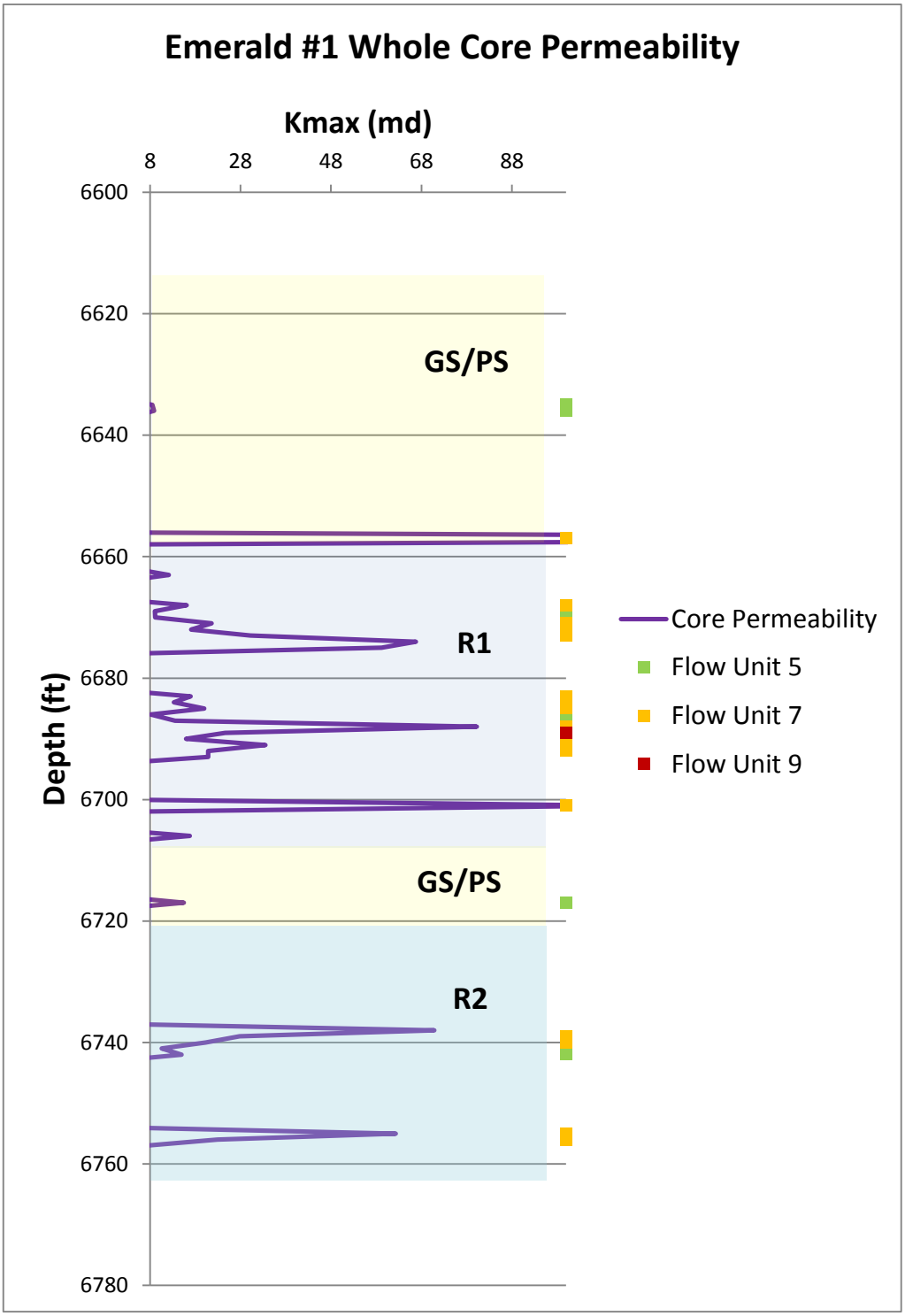

Figure H.36: Emerald #1 core analysis permeability (Kmax) with 8 md cut off. Flow unit brackets and depositional lithofacies also shown.

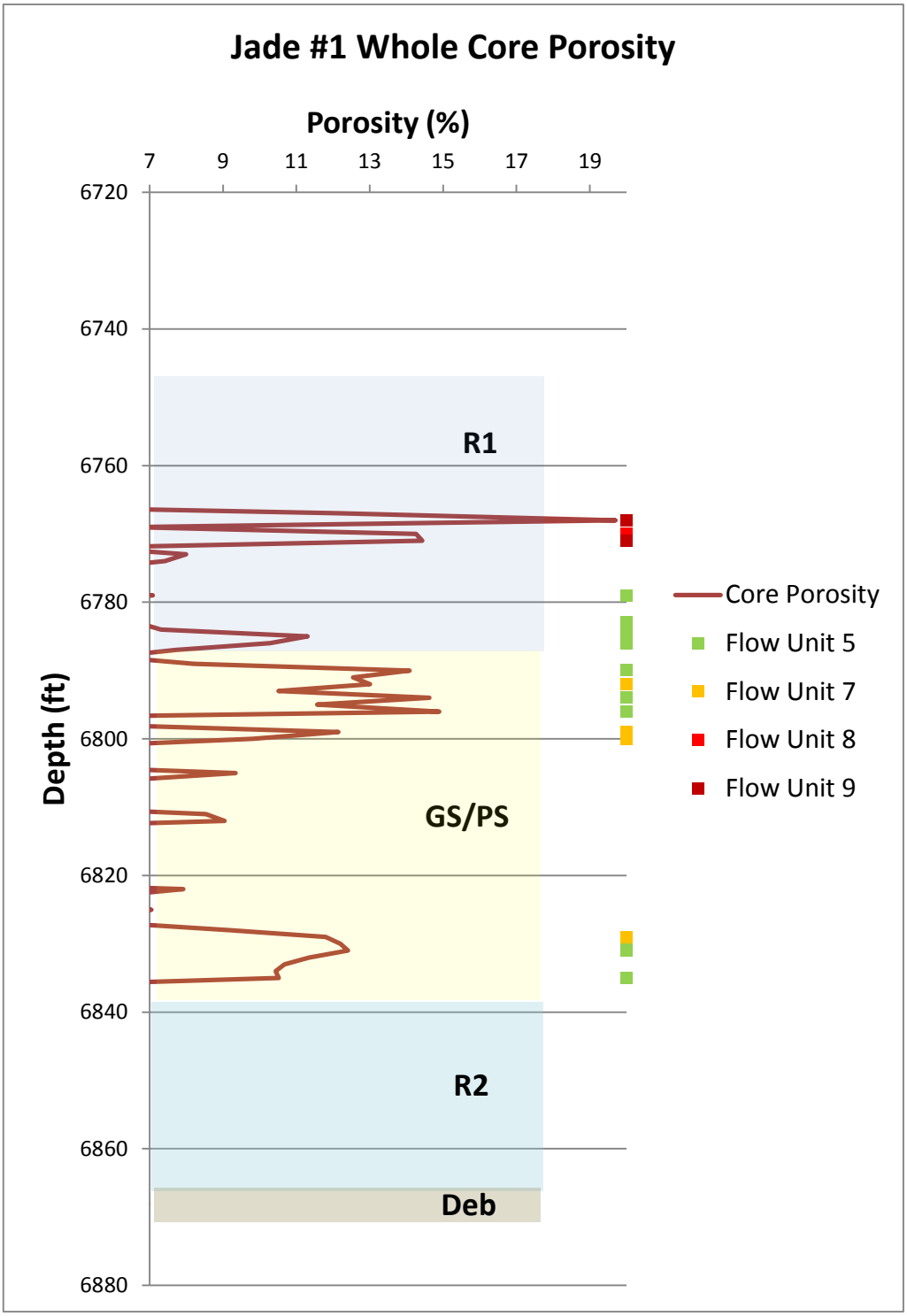

Figure H.37: Jade #1 core analysis porosity and calculated log porosity with 7% cut off. Flow unit brackets and depositional lithofacies also shown.

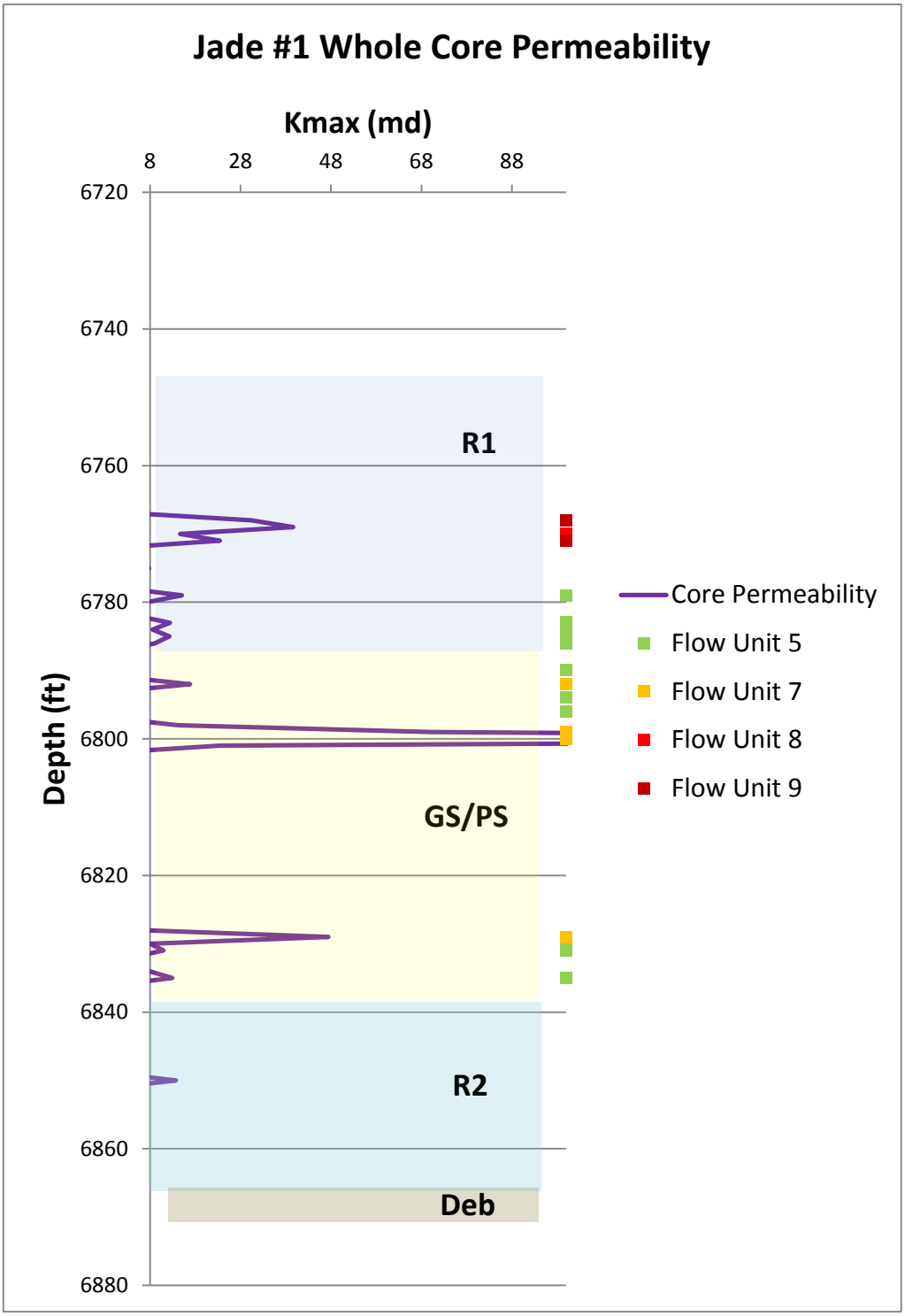

Figure H.38: Jade #1 core analysis permeability (Kmax) with 8 md cut off. Flow unit brackets and depositional lithofacies also shown.

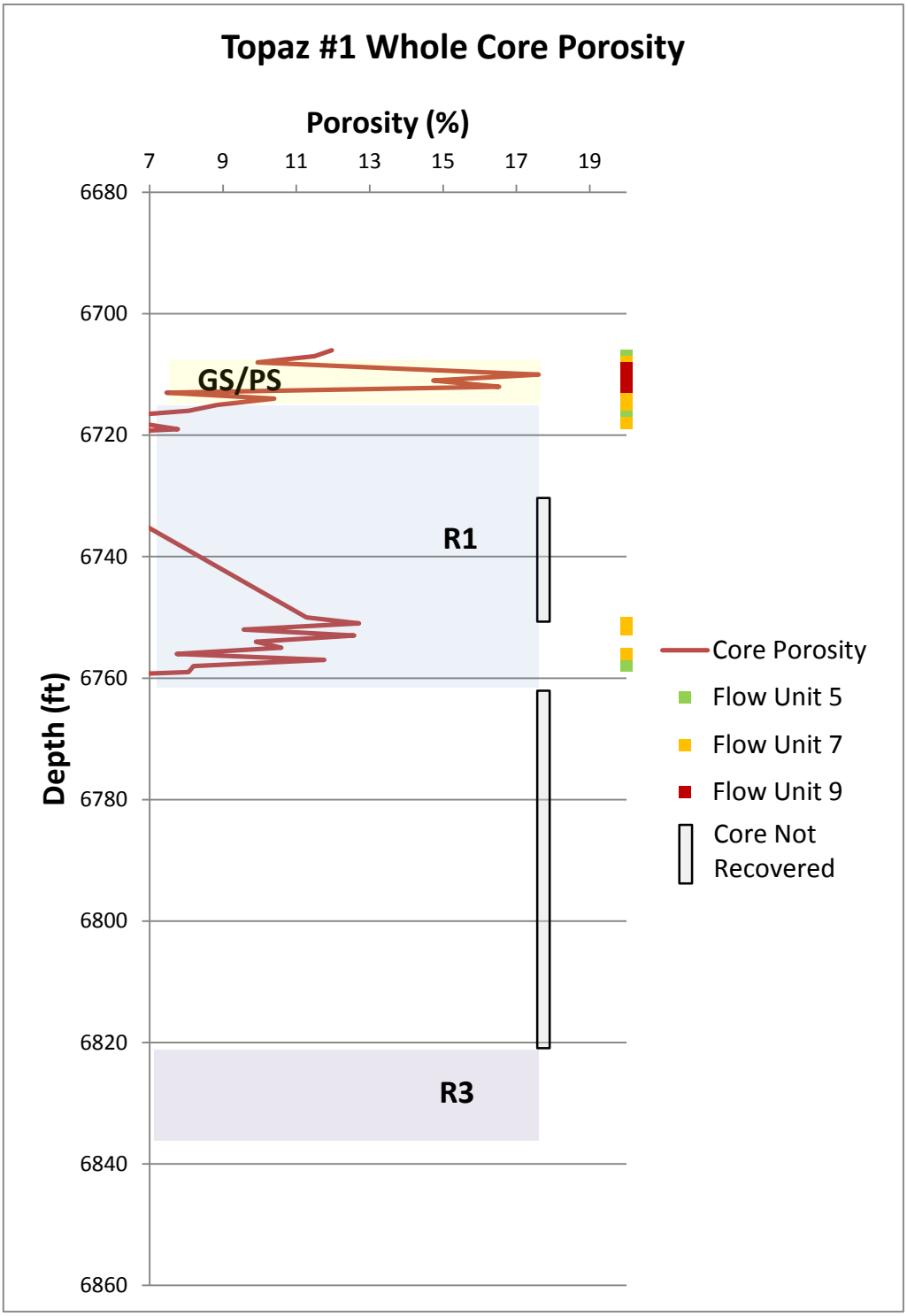

Figure H.39: Topaz #1 core analysis porosity and calculated log porosity with 7% cut off. Flow unit brackets and depositional lithofacies also shown.

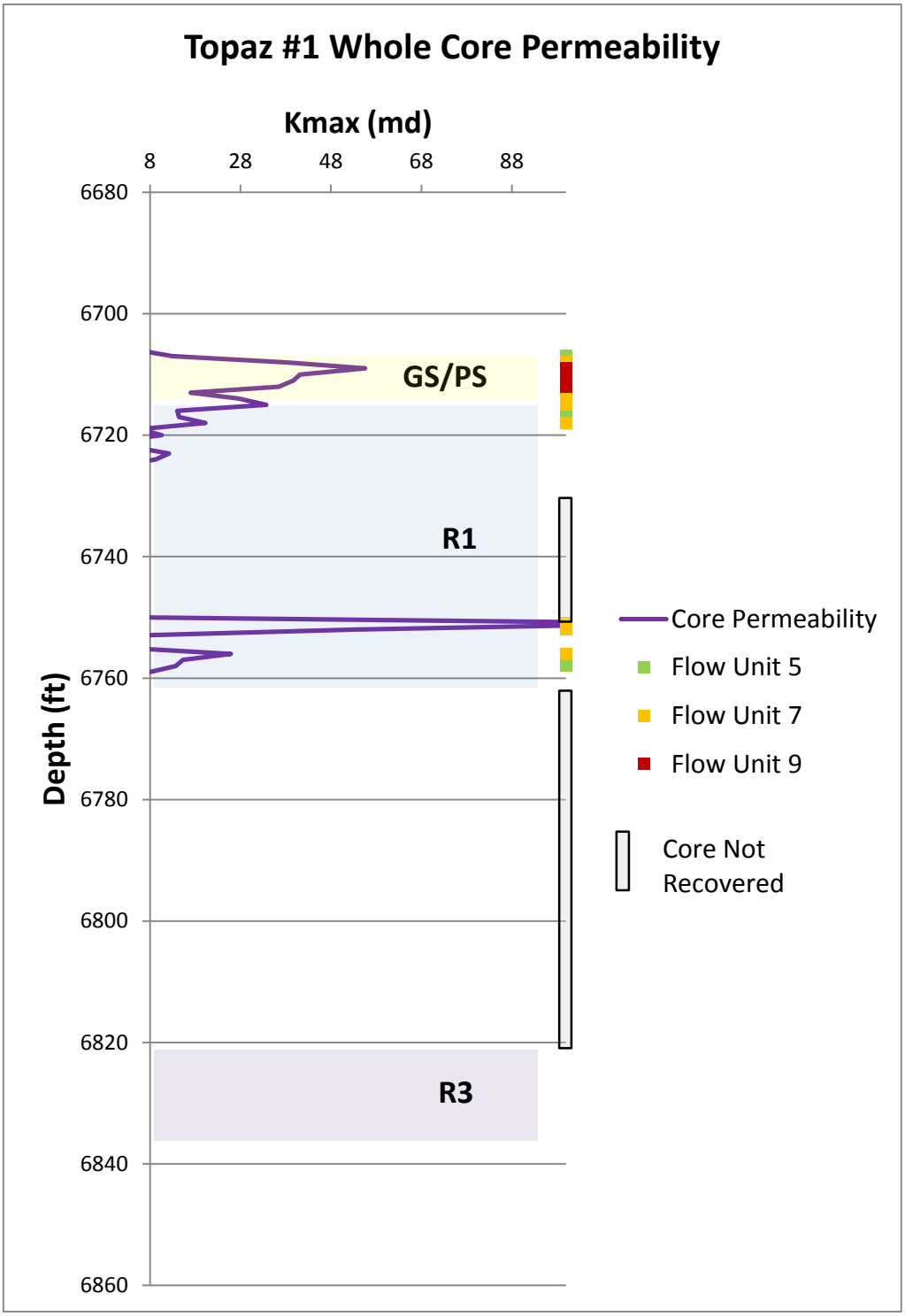

Figure H.40: Topaz #1 core analysis permeability (Kmax) with 8 md cut off. Flow unit brackets and depositional lithofacies also shown.

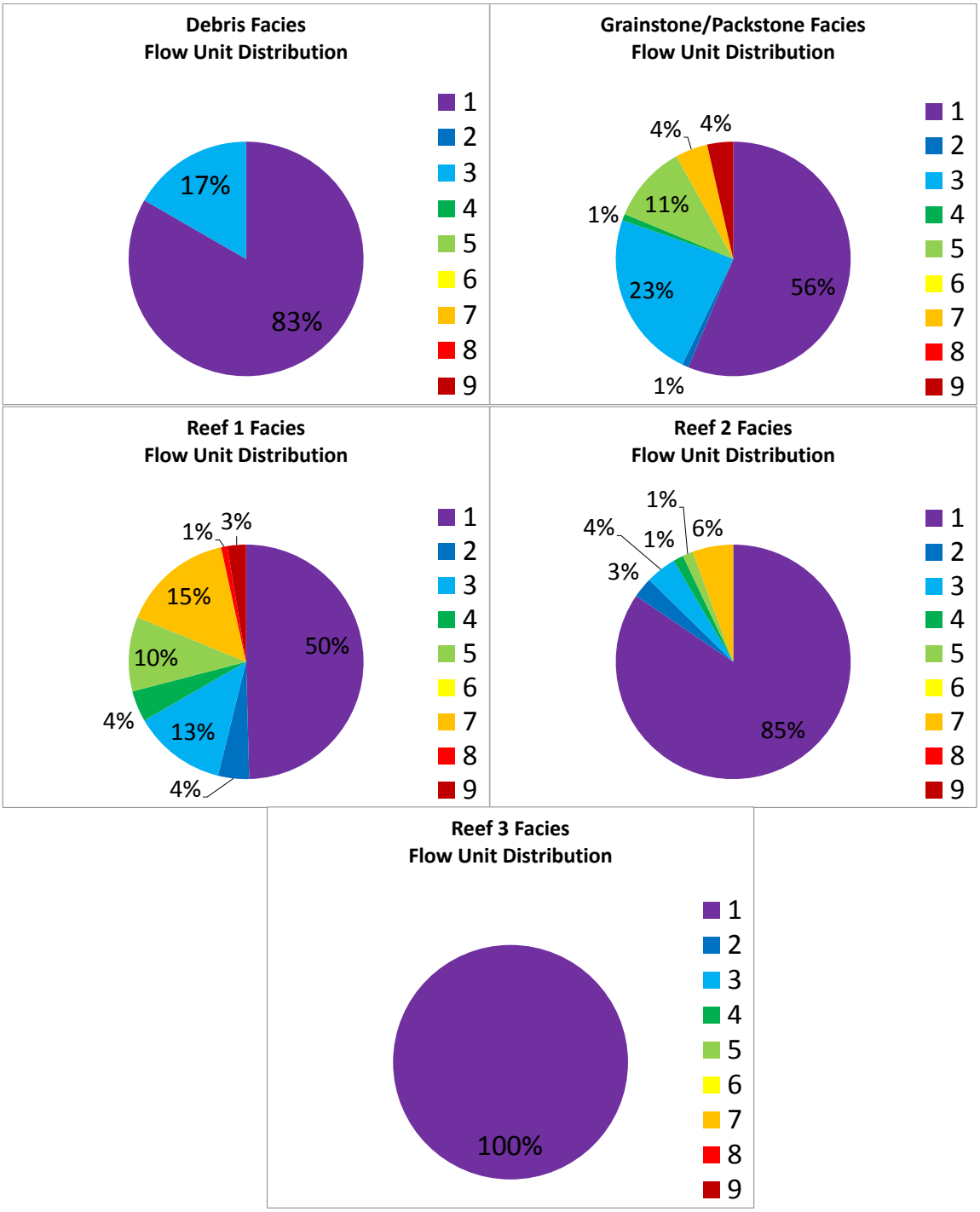

Figure H.41: Distribution of flow units for the depositional facies.

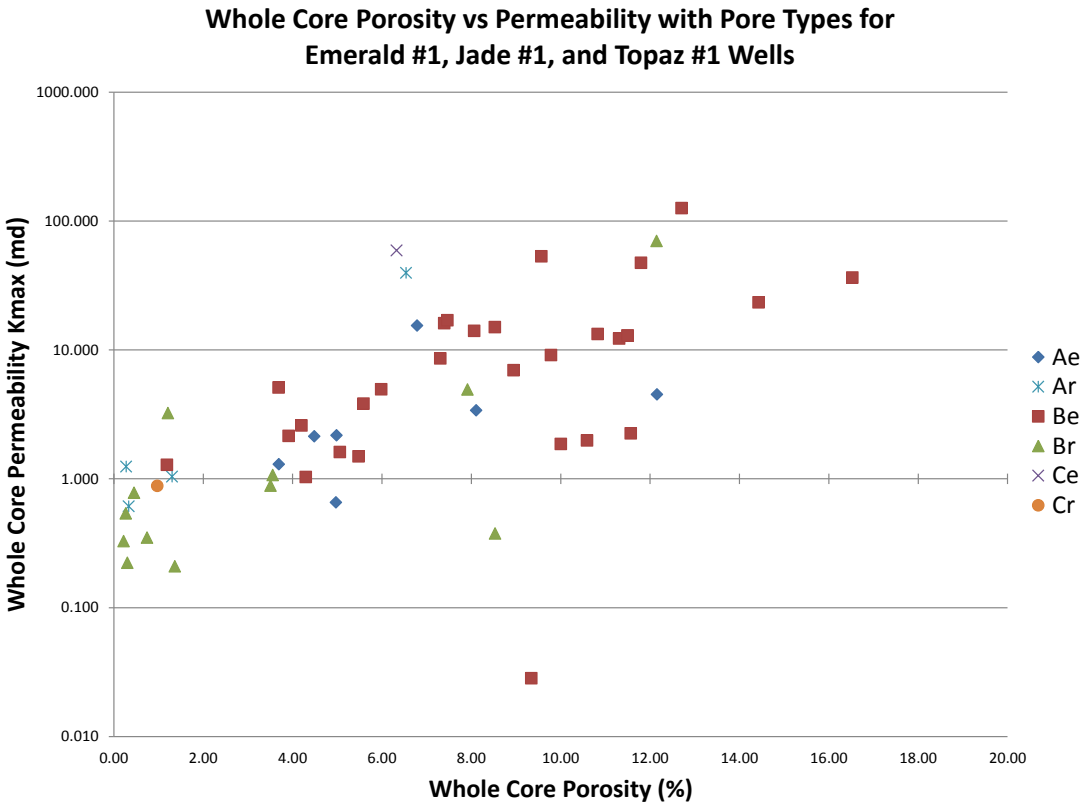

Figure H.42: Core analysis porosity and permeability with pore types.

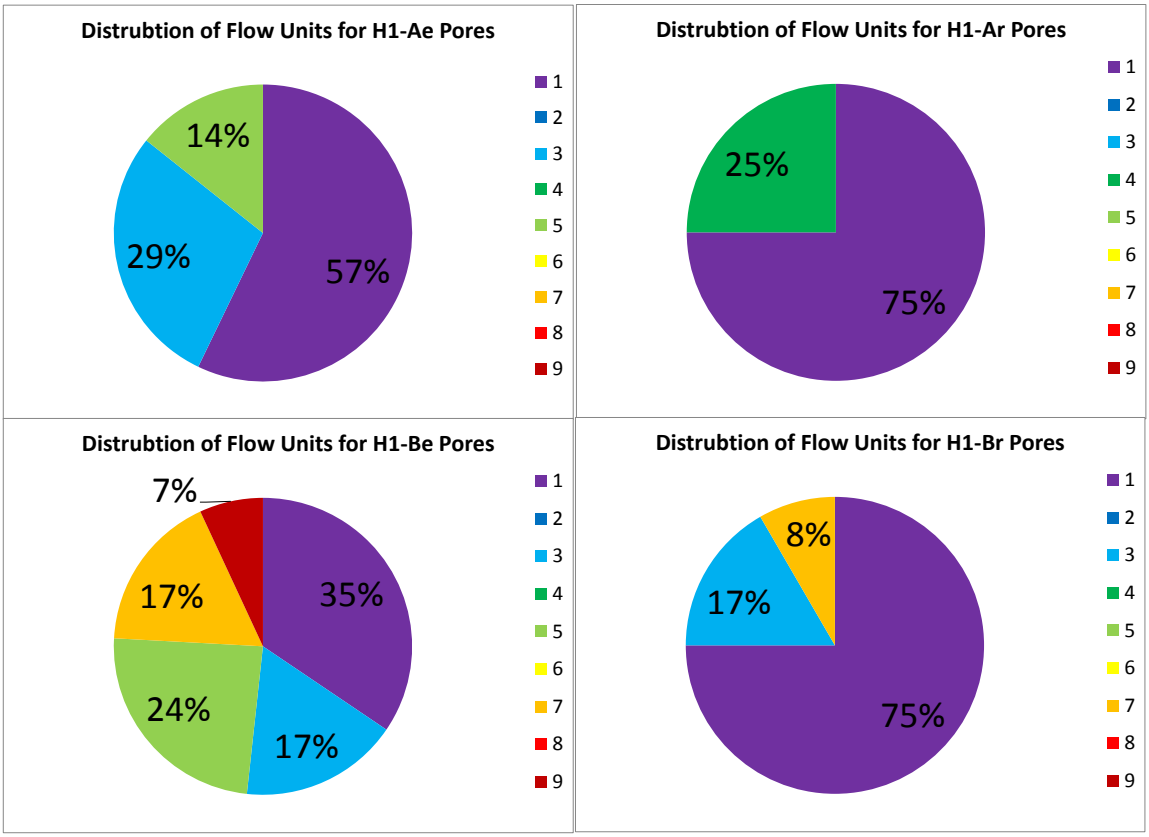

Figure H.43: Distribution of flow units by genetic pore type in thin sections. H1-C pores omitted since only one instance of each is observed in thin section.

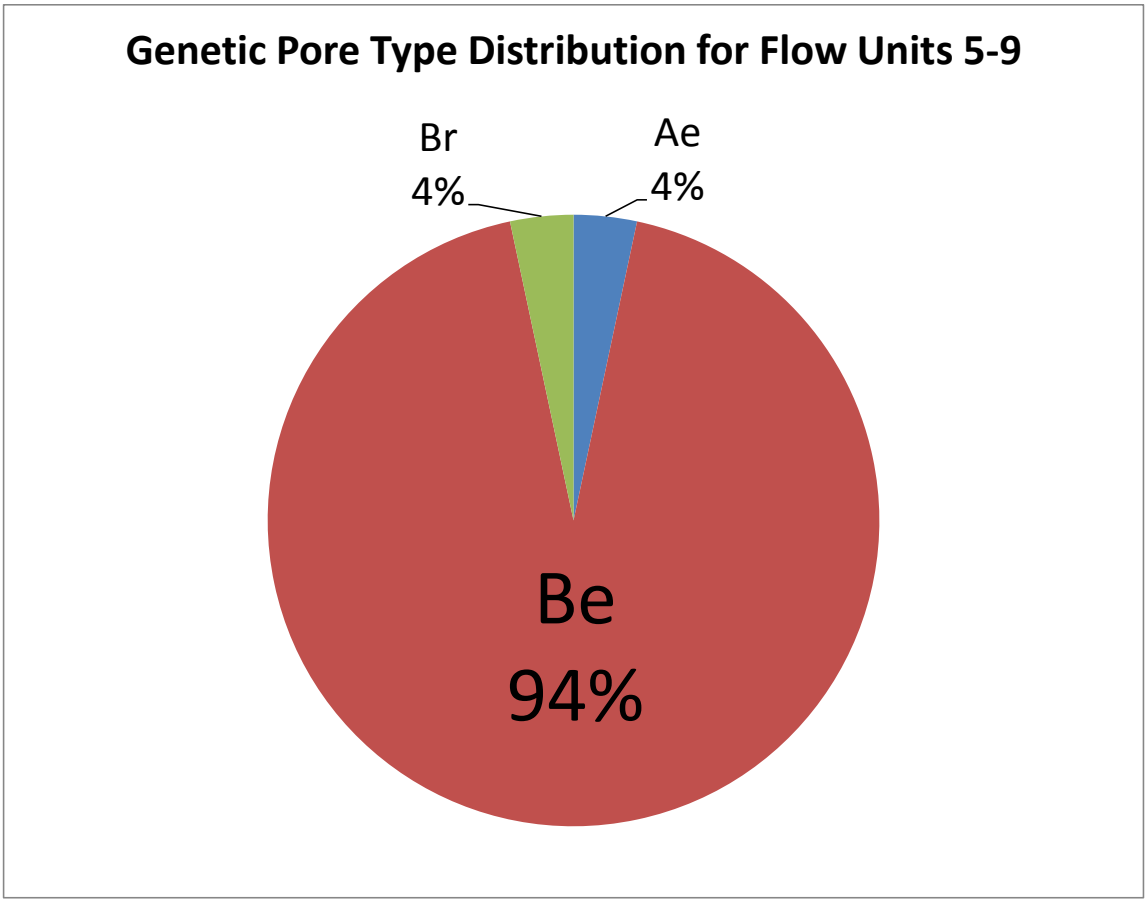

Figure H.44: Genetic pore type distribution for flow units 5-9.

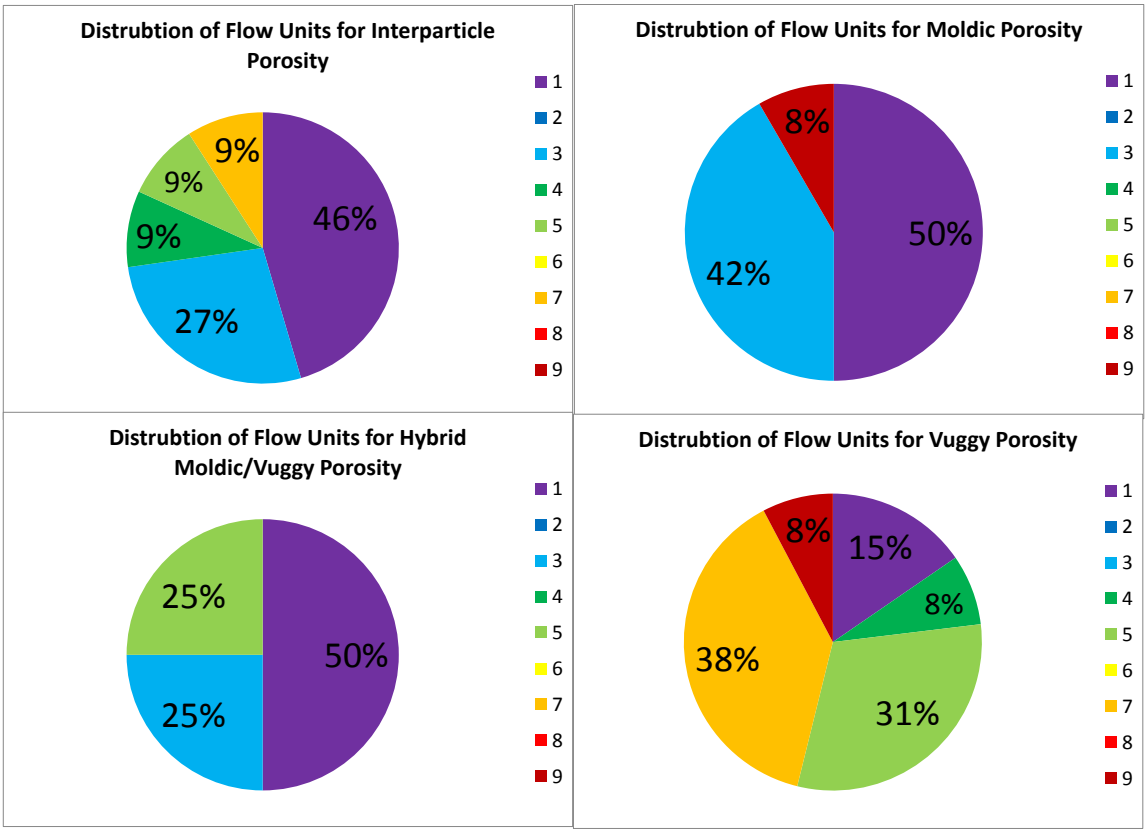

Figure H.45: Flow unit distribution by dominant porosity type.

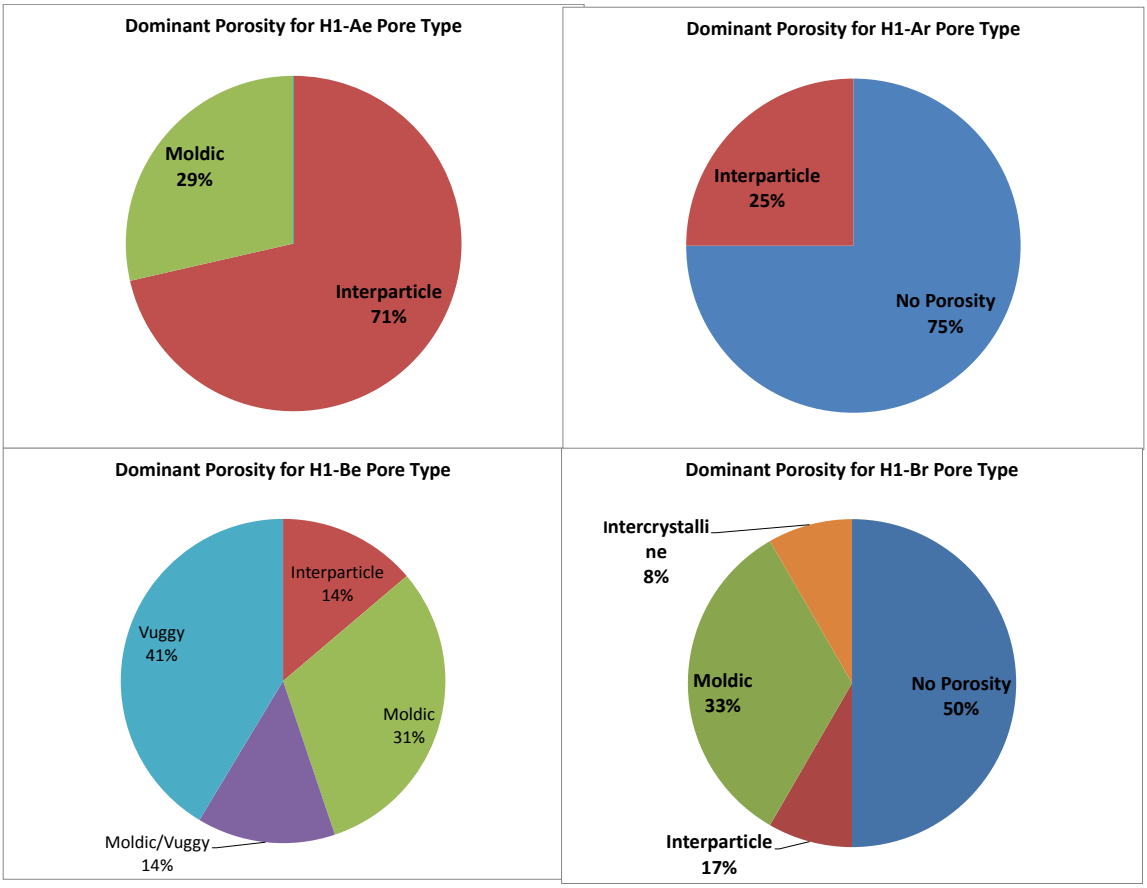

Figure H.46: Dominant porosity for each genetic pore type.

VITA

Name:	Travis James Barry
Address:	Department of Geology and Geophysics, MS 3115, Texas A&M University, College Station, Texas 77843-3115
Email Address:	barr4860@tamu.edu
Education:	B.S., Geology, University of Louisiana Lafayette, 2007 M.S., Geology, Texas A&M University, 2011
Professional Affilations:	American Association of Petroleum Geologists Geological Soceity of America Gulf Coast Association of Geological Socieities Society for Sedimentary Geology
Professional Experience:	Chevron, Midland, TX – Earth Science Intern Schlumberger, Houston, TX – Geomechanics Intern Schlumberger, Houston, TX – Geology Intern Petsec Energy, Lafayette, LA – Geology Intern